THE UNIVERSITY OF CALGARY

Theoretical Considerations on the Modelling of Skeletal Muscle

by

Mario Alberto Forcinito

A DISSERTATION

SUBMITTED TO THE FACULTY OF GRADUATE STUDIES

IN PARTIAL FULFILLMENT OF THE REQUIREMENTS FOR THE

DEGREE OF DOCTOR OF PHILOSOPHY

DEPARTMENT OF MECHANICAL ENGINEERING

CALGARY, ALBERTA

NOVEMBER, 1997

"No existen problemas agotados, solo hay hombres agotados por los problemas."

Comment to the press by Luis Federico Leloir, 1970 Nobel Prize in chemistry.

Abstract

The relatively recent experimental findings of the significant compliance of the thin (actin) and thick (myosin) filaments has brought into question a number of conclusions based on the assumption of perfect myofilament rigidity.

A discrete model of the interaction between individual myofilaments was developed to study the stiffness of a sarcomere for the case in which filament compliance is not negligible. The results of this model are discussed and compared to the predictions given by the previously published model by Ford et al.(1981). Although it can be shown that both models give identical results for an infinite number of links, for partial overlap our model consistently predicts a stiffer sarcomere than the continuous model. An explanation for the discrepancies between models is presented together with a way to correct the continuous model to approximate discrete model results. Additionally, our model is able to provide the stiffness for cases in which few cross-bridges are attached, or when the distribution of attached cross-bridges is not uniform. Our results confirm previous indications that it might be impossible to calculate the number of attached cross-bridges using only stiffness measurements in quick stretch (or release) experiments.

Also, a new phenomenological model of activated muscle is presented. The model is based on a combination of a contractile element, an elastic element that engages upon activation, a linear dashpot and a linear spring. Analytical solutions for a few selected experiments are provided. This model is able to reproduce the response of cat soleus muscle to ramp shortening and stretching and, unlike standard Hill-type models,

computations are stable on the descending limb of the force-length relation and force enhancement (depression) following stretching (shortening) is predicted correctly. In its linear version, the model is consistent with a linear force-velocity law, which in this model is a consequence rather than a fundamental characteristic of the material. Results show that the mechanical response of activated muscle can be considered as viscoelastic. Conceptual differences between this model and standard Hill-type models are analyzed and the advantages of the present model are discussed.

The effect of non-commutativity between changes in activation and changes in length on experiments performed on entire muscle are discussed. The results of exploratory experiments are recorded and a possible analytical approach to the problem is presented and discussed.

To conclude the dissertation, the continuum theory of chemically reacting mixtures is presented and its possible application to muscle mechanics is briefly discussed.

Preface

Chapter II of this dissertation is based on the following manuscripts:

Forcinito M, Epstein M, Herzog W, (1997) Theoretical Considerations on Myofibril Stiffness, *Biophys J.*. **72**: 1278-1286.

Forcinito M, Epstein M, Herzog W, (in press) A Numerical Study of the Stiffness of a Sarcomere, *J. of Electromyography and Kinesiology*.

Chapter III is based on the following manuscript:

Forcinito M, Epstein M, Herzog W, Don't Give Up on Rheological Models (submittted to the *Journal of Biomechanics*).

Acknowledgements

During my years in Calgary I had the opportunity to learn from an exceptional teacher whose personal qualities are only match by the immensity of his knowledge, I would like to thanks Marcelo Epstein for his guidance, support and friendship.

As if finding an excellent supervisor were not enough luck, I also have the luxury of meeting Walter Herzog who acted as a co-supervisor and to whom I will always be thankful for his guidance, support and permanent encouragement to work in muscle mechanics.

I would like to thanks to Gerald Pollack, Ron Zernicke and Nigel Shrive for serving in the dissertation defense committee.

My acknowledgments to Tim Leonard and Hoa Nguyen who gathered and prepared the experimental data mentioned in chapter III.

Special thanks to Prof. Roger Woledge of the University College London for having me as a student in his laboratory for four enriching months.

I would like to acknowledge my indebtedness to the University of Calgary and the Natural Sciences and Engineering Research Council of Canada for the financial support during my post-graduate term.

A special thanks to my loving wife Claudia for her helpful, understanding and constant support along so many years.

Dedication

to ***Claudia and Dante***

Table of Contents

Approval Page ii

Abstract iii

Preface v

Acknowledgements vi

Dedication vii

Dedication vii

List of Tables xi

List of Figures xii

I. Introduction 1

1.1 From Molecules to Muscle 3

1.2 From Muscle to Molecules 7

1.3 Plan of the present dissertation 11

1.4 What is New in This Work 12

II. Structural Considerations on Skeletal Muscle Fibre 13

2.1 Sarcomere Structure 15

2.2 Thick and thin filaments 17

2.3 Cross Bridge Theory 19

2.4 Fibre Stiffness 22

2.5 The Discrete Approach to Stiffness Calculation 24

2.5.1 Recursive stiffness algorithm 25

2.5.2 The Ladder Structure with Additional Series Filament 29
2.5.3 Parallel Array of Ladder Structures with Additional Series Filament 32
2.6 Results 33
2.6.1 The 'Ladder' Structure 33
2.6.2 The Continuous Model Revisited 36
2.6.3 Parallel Array of Ladder Structures with Additional Series Filament 43
2.6.4 Comparison with Experimental Results 45
2.7 Discrepancies between the discrete and continuous models 46
2.8 Three-dimensionality 48
2.8.1 Longitudinal and Transversal Movements 51
2.8.1 Topology 52
2.9 Conclusions 56
III. Muscle as an Engineering Material 60
3.1 Pseudo-Rheological Muscle Models 61
3.2 A Phenomenological Model of Muscle 67
3.2.1 Hill-type model 72
3.3 Results 73
3.3.1 Quick change in length 73
3.3.2 Quick change in Force 74
3.3.3 Constant Speed of Shortening or Stretching 76
3.3.4 Comparison with Experimental Results 77
3.4 Critical Analysis of the present model 81
3.5 Discussion 86
3.6 Interaction Between Muscle Stimulation and Movement 88
3.6.1 Non-Commutativity Between Shortening And Stretching 94

IV. Mechanics and Thermodynamics 98

4.1 Continuum Mechanics 99

4.2 Constitutive Equations 105

4.3 Mixture Theory 106

4.4 Mixture of Chemically Reacting Bodies 111

4.5 Comments on the Application of Mixture Theories to Muscle. 116

4.5.1 Non-Equilibrium Thermodynamics. 118

4.5.2 Other Approaches Worth Exploring. 118

V. Conclusions and Recommendations 120

5.1 Conclusions 120

5.2 Recommendations for Future Work 122

Bibliography 124

Appendix A. The equation of Ford et al. (1981) revisited 132

Index 135

List of Tables

Table 2.1: Comparison between the stiffness calculated with the discrete and continuous models for the overlap zone for an increasing number of panels.....45

Table 2.2: Stiffnesses of the open and closed lattices of ladder structures in parallel. 56

Table 3.1: Parameters used for Hill's model. 73

List of Figures

Figure 1.1: Chemical Power as a function of the fraction v/Vmax derived by Hardt (1978).....10

Figure 2.1: Schematic representation of skeletal muscle fibre showing the myofibrils and the sarcomere.....14

Figure 2.2: Schematic representation of a sarcomere (from M-band to M-band).....16

Figure 2.3: 'Ladder' structure definition.....25

Figure 2.4: External degrees of freedom of the ladder structure with i - panels.....26

Figure 2.5: External and internal degrees of freedom when a new panel is added to the structure.....27

Figure 2.6: N-panel ladder structure with series elastic elements.....30

Figure 2.7: Element lengths for different configurations of the ladder structure. 31

Figure 2.8: Stiffness of the ladder structure as a function of the ratio a/b (top) and the number of panels (bottom).....36

Figure 2.9: Percent difference in the stiffness between the continuum and the discrete solutions for the ladder structure. 38

Figure 2.10: Sarcomere stiffness as a function of the sarcomere length for different stiffness ratios of the ladder structure with additional filaments. 39

Figure 2.11: Ratio of total stiffness and stiffness of the overlap zone as a function of sarcomere length for different stiffness ratios. 41

Figure 2.12: Comparison between the stiffness given by the continuous and discrete models. 42
Figure 2.13: Sarcomere length dependence of yo plotted in the same way as Fig 13 in Ford et al. (1981). 43
Figure 2.14: Stiffness per myosin head....45
Figure 2.15: Discrete model overlap zone 46
Figure 2.16: Variation of the Stiffness per Cross bridge with sarcomere length....47
Figure 2.17: Three dimensional rendering of the super-lattice as described by Squire, 1990. 50
Figure 2.18: Three dimensional rendering of the arrangement of thick and thin filaments as described by Pollack, 1990. 50
Figure 2.19: Topology of the Open and Closed Lattices. 54
Figure 2.20: Variation of the Stiffness divided by the number of cross-bridges with the number of cells for the Open and Closed Lattices 58
Figure 3.1: Isotonic and Isometric static curves for muscle 64
Figure 3.2: Hill's two element muscle model. 65
Figure 3.3: Representation of the contractile element. 68
Figure 3.4: Solution of Eq 3.3 for a forcing function consisting of a periodic function with saturation. 69
Figure 3.5: Rack element representation. 71
Figure 3.6: Rheological model representation. 71
Figure 3.7: Characteristic curve for the present model with constant coefficients compared to the characteristic force-velocity curve with 79
Figure 3.8: Shortening at constant speed: comparison between experimental results, the present model and Hill's model. 81

Figure 3.9: Lengthening at constant speed: comparison between experimental results, the present model and Hill's model. 82
Figure 3.10: Effects of pulse doubling in cat soleus force....82
Figure 3.11: Solution of Eq 3.3 for a square (left) and a triangular (right) pulses for different values of the parameter 84
Figure 3.12: Brush Mechanics. Example of a structure with stable but negative slope force-length relation 84
Figure 3.13: Shortening from fully active state and activation from resting state to reach the same F-L point 90
Figure 3.14: Stretching and reduction of stimulus from fully active state compared to reduction of the activation and stretching....91
Figure 3.15: Active Shortening followed by Stretching of in vivo cat soleus. 95
Figure 3.16: Active Stretching followed by Shortening of in vivo cat soleus. 96
Figure 3.17: Active Shortening followed by reduction of the activation and Stretching of in vivo cat soleus. 97
Figure 3.18: Active Stretching followed by redacting of the activation and Shortening of in vivo cat soleus. 98
Figure A.1: Ladder structure with infinite panels. 134
Figure A.2: Coordinate system definition for boundary conditions. 134

I

Introduction

Skeletal muscle has been the subject of intense study for more than a century. To the obvious interest on muscle functioning arising from biology, we should add the interest from mechanical scientists to understand the most ubiquitous natural transducer of chemical energy into mechanical energy. Undoubtedly, the remarkable properties of skeletal muscle are due to its complex structure; from the molecular level to the entire muscle level, everything in muscle seems to spell structure and order.

Over the last half of the century, biologists and physiologist have tried to accomplish the unlikely task of joining two completely different worlds; the molecular approach and the phenomenological approach. It is opportune here to justify the use of the adjective 'unlikely'. Consider a steel bar subjected to the uniaxial stress test. It is an easy exercise for engineering students to predict the force at which the bar will yield by measuring the cross sectional area of the bar and multiplying it by a single, macroscopically measurable quantity: the yield stress. On the other hand it is also well established that the material is mainly formed by iron and carbon atoms[1] arranged conforming one of a small number of possible crystalline structures. Inter atomic and intermolecular forces are also well known and can be precisely calculated. However the prediction of the yielding stress and deformation based on the knowledge of atomic interactions is unlikely to be successful. The reason is that between the atomic realm and the macroscopic world there are several

[1] With modern tunnel electron microscopy techniques it is possible to actually see the atoms.

levels of organization of matter. In the case of the steel bar, the crystals are not always perfect. Also, the crystals are arranged into grains of different shape and random orientation. All these factors result in a yielding force for the bar that is several orders of magnitude lower than the one predicted for perfect crystals by calculating the effects of inter atomic forces and postulating a dislocation pattern.

This example of a 'simple' problem in engineering behaviour of materials, should teach us to proceed with caution and remind us that we are probably too ambitious if we expect to find a universal and simple model able to describe completely the behaviour of complex systems. Returning to our simple example of the steel bar, one might think that for that case there is no need of a sophisticated model; after all, for practical purposes, one needs only to know at most two properties, the elasticity modulus and the yielding stress, to describe the basic behaviour of the material in the range of practical applications. But progress in science rarely goes hand in hand with practicality. In the case of the steel bar, the shape of the functional form of the potential energy vs. the separation between atoms can be used to demonstrate that, for small elongations, the stress must be proportional to the strain. This shows that although the hope to find a simple model that can predict exactly the macroscopic behaviour and at the same time account for microscopic events is dim, knowledge of microscopic events surely helps to develop and validate better macroscopic models.

Although the same line of reasoning can be applied in general to all problems in material science, in the case of muscle there are some factors that must be taken into account. Unlike the case of the steel bar, the lowest significant level of organization in muscle can be taken to be the level of macromolecules. The proteins that constitute the myofilaments[2] have molecular weights of several hundred thousand Daltons, that is 4 to 5

---

[2] The internal structural arrangement of muscle will be described in chapter II.

orders of magnitude the molecular weight of iron and carbon molecules. Another important difference that must be mentioned is the higher degree of order in which the biological molecules arrange themselves in the muscle as compared with the haphazard way in which crystal grains are arranged in steel. As structural order can be associated to predictability, maybe there is more hope to find a model based on molecular interaction, which at the same time can predict global behaviour, for a muscle than for a steel bar. Perhaps this hope is founded upon the relative success that the two cornerstones of twentieth century muscle physiology, Hill's muscle model and Huxley's Cross-bridge theory, have had.

1.1 From Molecules to Muscle

To keep the perspective on the subject, a rough list of what is known and what is unknown about muscle mechanics will be helpful. At the lower end, although the microscopic structure of myofibrils is relatively well known from electron microscopy, X-ray diffraction studies and biochemical analysis, there are still some points for debate. Details such as whether the myosin head rotates or not, or the exact position and number of myosin heads in a thick filament, to name a few, are still far from being firmly established. Those 'details' could be of secondary importance in the context of cross-bridge models that assume the independence of the force generated by different myosin heads, but they can be of central importance to models that assume the cooperativity between myosin molecules.

Using modern techniques such as laser light traps (or optical tweezers), researchers[3] have been able to measure the stiffness of individual myosin molecules. These advancements in experimental techniques should put an end to many years of debate about the amount of force that each cross-bridge can exert and about the length of the force stroke. Unfortunately the results are inconclusive so far, due to the variability exhibited by the forces and lengths measured in different experimental assays[4]. With the increasing availability of experimental results from such sophisticated preparations, it is possible to foresee a complete elucidation of the mechanical aspects of the minute details of myosin-actin interaction; however, as the experiments at the molecular level are performed either *in vitro* or in skinned preparations, usually far from the physiological ranges of operation, there will always be room for speculation on whether the events *in vivo* resemble the ones measured in the laboratory or not. A larger gap in the knowledge of myosin-actin interaction, is the elucidation of whether there exists some cooperativity between neighbouring force generators. Huxley's cross-bridge theory, as well as all similar and derived theories, assume the independence of force generators. Although most of the researchers in the field agree with that idea, there are some authors that dissent with it based on generally accepted experimental evidence[5]. Zhou and Phillips, 1994, presented a theoretical model that implies the cooperativity between neighbouring

---

[3]See for example Nishizaka et al. 1995.

[4]There are some other problems due to the experimental techniques, for example in Nishizaka et al. 1995. the practice of using a piece of actin filament to attach the myosin heads will mask the real value of the stiffness in the myosin head, unless the exact length and stiffness of the filament are known and accounted for when measuring the displacement. The solution to such problems should be relatively easy to address in future experiments.

[5]See Pollack, 1995 and the answers to that article for a detailed discussion on the matter.

molecules on the actin filament and match *in vitro* experimental data. They used a cellular automata model of the thin filament for which the calcium affinity of actin was modeled as a function of the state of neighbouring troponin molecules. If the mechanism implied by Zhou's model is true, and activation of receptive sites in the actin filament does not proceed at random, it can have important implications on the ability to produce force of the myosin molecules and, consequently, some indirect cooperation between neighbouring myosin heads can be present even if we assume that the attachment of myosin molecules to actin does not have such property.

However, the biggest unknown in the putative cycle of cross-bridge attachment and detachment is, in our opinion, the rate at which the ATP (Adenosine Tri-Phosphate) is hydrolyzed by the actomyosin complex. Experimental results are contradictory in this issue. Researchers have measured different rates of ATP consumption for different experimental conditions. This violates one of the fundamental postulates of Huxley's cross-bridge dynamics, that is, that each cross-bridge cycle hydrolyzes a fixed quantity of ATP. Thermodynamics of chemical reactions can be used to find the bounds of this relation, for example, the sum of mechanical work and heat produced cannot be bigger than the difference in free energies before and after the hydrolyzation. However the correct relation between mechanical work and chemical energy change will, in general, depend not only on the present thermomechanical state, but also on the history of the process, because in general thermomechanical processes the amount of dissipation (entropy production) depends on the path followed. There is also the possibility that the mechanical state affects the chemical affinities between components, which is only partially taken into account by the cross-bridge theory[6]. Cooke et al., 1994, published a

---

[6]In Huxley's original theory only sliding velocity and cross-bridge distortion affect the probability of chemical interaction.

cross-bridge model that allows for detachment of myosin heads without hydrolization whenever the free energy of the attached state exceeds the free energy of the detached state. This type of weakly coupled models predict the relation between ATPase activity and contraction velocity at high shortening velocities more accurately than strongly coupled models.

It is always intriguing that cross-bridge models are unable to predict the force for different velocities of contraction, if a set of constants adjusted for a particular contraction velocity is used. As the constants needed to fit experimental results for a given velocity of contraction are related to the rate constants of the chemical reactions supposed to be relevant in the contraction process, the fact that for different velocities one needs different values for the constants probably mean that the rates of reaction depend on global mechanical parameters such as velocity or force. The dependence of rate constants on contraction velocity can also mean that the kinetics of chemical reactions is different from first order. The problems associated with the measured order of a chemical reaction in reduced spaces was addressed by Savageau, 1995. To put Savageau's conclusions in simple words, for enzymatic reactions the spatial distribution of reactants, more specifically the spatial degree of freedom of the molecules participating in a chemical reaction, have a strong influence on the kinetic order of the reaction. This means that the kinetic order of the reaction and the rate constants measured in a situation where all points in a three-dimensional space can be occupied by the reactants, are very different from the ones corresponding to the same reaction proceeding in a situation where the reactants have restricted spatial degrees of freedom. To our knowledge there is no analysis of the consequences that this can have for myofibrils where the reactions between myosin and actin are restricted to a space of a dimension close to 1.

Going a level up from the molecular constituents of muscle, there are some unsolved problems regarding the properties of the structure of the sarcomere. There is experimental

evidence that the actin filament at least, and possibly the myosin filament too, are more compliant than previously thought. As we show in Chapter II this fact has important implications on the stiffness of the sarcomere, which is often used to assess the proportion of attached cross-bridges in experimental settings. We also show that the structural arrangement of cross-bridges has influence on the stiffness value. To date, the exact distribution of cross-bridges is not known. The contributions of other force carrying components such as titin filaments and Z-discs are often neglected in the analysis, although the influence they can have on the total stiffness of the sarcomere is not known.

1.2 From Muscle to Molecules

In his landmark paper of 1938, A. V. Hill established the bases for the most widely used muscle model in biomechanics to date. From his thermal and mechanical measurements, Hill foresaw that there must be a chemical reaction whose activity is able to produce mechanical work and heat on muscle. Although for today's standards the experimental techniques that Hill used were very crude, he predicted the proper connection between the at the time unknown chemical reaction, the mechanical work and the thermal energy dissipated in the contraction process. Regarding the mechanics of the entire muscle, at first sight things look less complex than at the microscopic level. Considering only the operational aspect, an entire muscle can be looked at as a black box with certain properties or transfer functions between mechanical state variables (force, length and contraction velocity) that depend on the value of a controlling variable (usually called activation). Although some aspects of the transfer functions are very well known, to date there is no muscle model that can represent completely its mechanical behaviour. The state of affairs is worse if one is interested in questions such as how much metabolic

energy is needed to complete a prescribed motion. It is common practice in biomechanics to use the product of the force velocity and force length relations derived from experiments to predict the force and length for any motion condition. The resulting model is not a proper constitutive equation for muscle, its range of application is limited to cases in which the shortening speed is constant or zero and cannot account for such phenomena as force depression following shortening or force enhancement following stretching. Such models are purely mechanical as they do not include any thermodynamics. The thermodynamics is provided by an ad hoc function, derived from experimental data or from cross-bridge modeling. One of the problems is that the thermodynamics of muscle is incompletely known. As shown in chapter IV, the thermodynamics of chemically reacting materials is complex, and theories developed from first principles are seldom used as a framework for building muscle models. One of the reasons for this lack of theoretical work could be the complexity of the mechanical theories for chemically reacting mixtures. Even a model with the most simple geometry, that includes all possible interactions between the stoichiometry, the chemical kinetics and the dynamics of deformable bodies, is almost intractable. Moreover, for the case of a mixture of simple, solid and fluid components, it is not clear how to calculate such quantities as the internal energy and the entropy production. The standard practice in thermodynamics of living tissues is to use expressions of internal energy and free energy derived for the case of perfect gases. Assuming that these expressions are also valid for the calculation of very dilute solutions, we still are far from justifying its direct use in the case of muscles.

An interesting approach to the problem of linking the energy liberated by the chemical reactions with the force and velocity of the muscle is that used by Hardt, 1978. In this unjustly ignored work, Hardt used a cross-bridge model previously published by Julian et al., 1974, to derive numerically the necessary constitutive functions that relate dynamic parameters of a sarcomere to its metabolic energy expenditure measured as a

function of the cross-bridge activity. The constitutive relation is then scaled up to the entire muscle and, using a three-dimensional model of the human limbs, related to the forces and displacements occurring during level walking. Although not very precise (in the sense that the numerical solution was not able to match known experimental results by an order of magnitude), the transfer function found by Hardt had desirable features such as a non-zero steady state chemical power for the isometric state and a smaller, but positive, power for eccentric movements, as shown in Fig. 1.1. Those characteristics, although easy to deduce intuitively are much more than most of mechanical models based on kinematics of rigid bodies will ever be able to show.

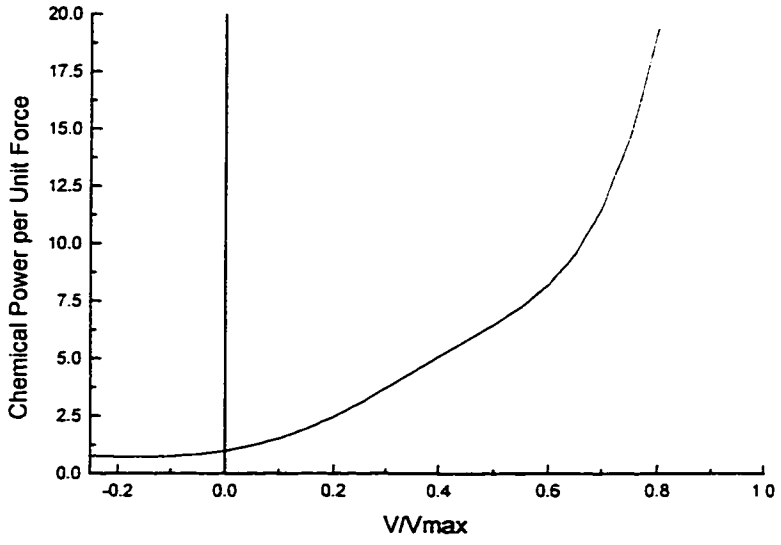

Figure 1.1: Chemical Power as a function of the fraction v/V_{max} derived by Hardt (1978). v is the contraction velocity, positive for concentric contraction and V_{max} is the contraction velocity of the unloaded muscle.

Hardt had worked with the idea of an integrated model in which all the levels from molecular interactions to entire muscular groups are considered as part of the analysis. In his analysis, Hardt uses thermodynamic principles to maintain the consistency. Hardt's main hypothesis was that in any cyclical movement there is a minimization of the global energy expenditure. One can agree or disagree with this hypothesis, which is difficult to prove true or false because criteria based in optimization of energy imply certain order at levels of organization higher than the purely mechanistic level. Nevertheless, the fact that Hardt made use of available models, covering the aspects of molecular interactions, mechanics and thermodynamics, together with an implicit control strategy, is significant in that it points to muscle mechanics as a composition of problems at different levels and shows a possible way to address it.

1.3 Plan of the present dissertation

We have addressed two different problems: the influence of myofilament stiffness at the sarcomeric level, and the force inhibition or enhancement after shortening or lengthening at the entire muscle level. In Chapter II, we present a description of the internal structure of muscle fibers together with a theoretical analysis of the sarcomere stiffness for the case in which the myofilaments are compliant. The analysis is based on a discrete model of the structure representing the interaction between thin and thick filaments. Chapter III describes a simple rheological model of muscle that predicts effects of force depression or enhancement after shortening or lengthening, and some ideas about how the so-called memory effects, in which the activation and the change in length interact, can be mathematically addressed. Chapter IV is a review of modern continuum mechanics and thermodynamics, including a review of the continuum theory of

chemically reacting mixtures. This chapter was included for completeness and to indicate what, in our opinion, is the way for future theoretical developments on muscle mechanics.

1.4 What is New in This Work

Using the model presented in Chapter II to calculate the sarcomere stiffness, it is shown that the number of attachments and the stiffness of an array of intedigitating elastic filaments are not directly related in the range of parameters that are physiologically significant for mammalian skeletal muscle.

Chapter III presents a new rheological model for the entire muscle which is able to account for effects such as the force depression after shortening and the force enhancement after lengthening. The model departs from standard Hill like models in that the force velocity relation is predicted as an explicit consequence of the interaction between the elements appearing in the model, rather than as an intrinsic property of the contractile element. Also, the consequences of the non-commutativity between the application of stimulation and changes in length are discussed and a possible way of addressing the problem is presented at the end of the chapter.

II

Structural Considerations on Skeletal Muscle Fibre

In this part of the dissertation we will restrict our attention to the mechanical events affecting muscular contraction inside skeletal muscle fibres. Skeletal muscles are more or less complex arrangements of fibres of different types, and muscle architecture strongly influences the characteristics of a given muscle; however, since the interaction between fibres in a muscle is supposed to be purely mechanical, we consider the fibre as the minimal unit that exhibits all the essential mechano-chemical interactions that can be found in muscle. For the description of morphological characteristics of fibres, we will follow those given by Woledge et al. 1985, Squire 1981 and Pollack 1990.

A fibre is a multinucleated muscle cell, usually between 20 and 100 μm in diameter and up to 100 mm in length It is surrounded by the cellular membrane, called sarcolemma, which separates the internal media of different fibres. Fibres are chemically and electrically insulated in such a way that they can be stimulated or activated separately by the nervous system. This modularity of the activation function allows the muscle to work over an extended range of forces with the same degree of control. Figure 2.1 shows a schematic drawing of a fibre.

On the inside, the fibre is organized as a bunch of parallel fibres called myofibrils, which are responsible for the contraction. Myofibrils, which are about 1 to 2 μm in diameter and as long as the fibre, retain the striation (with a periodicity of 2 μm at slack length) characteristic of muscular fibres. Each myofibril is surrounded by a network of closed tubules of irregular shape called the sarcoplasmic reticulum, which plays a

fundamental role in the activation process. Upon close examination it can be seen that the myofibril is composed of repeating units of filaments of contracting proteins that run between consecutive structures resembling discs, called Z-discs (or Z- lines).

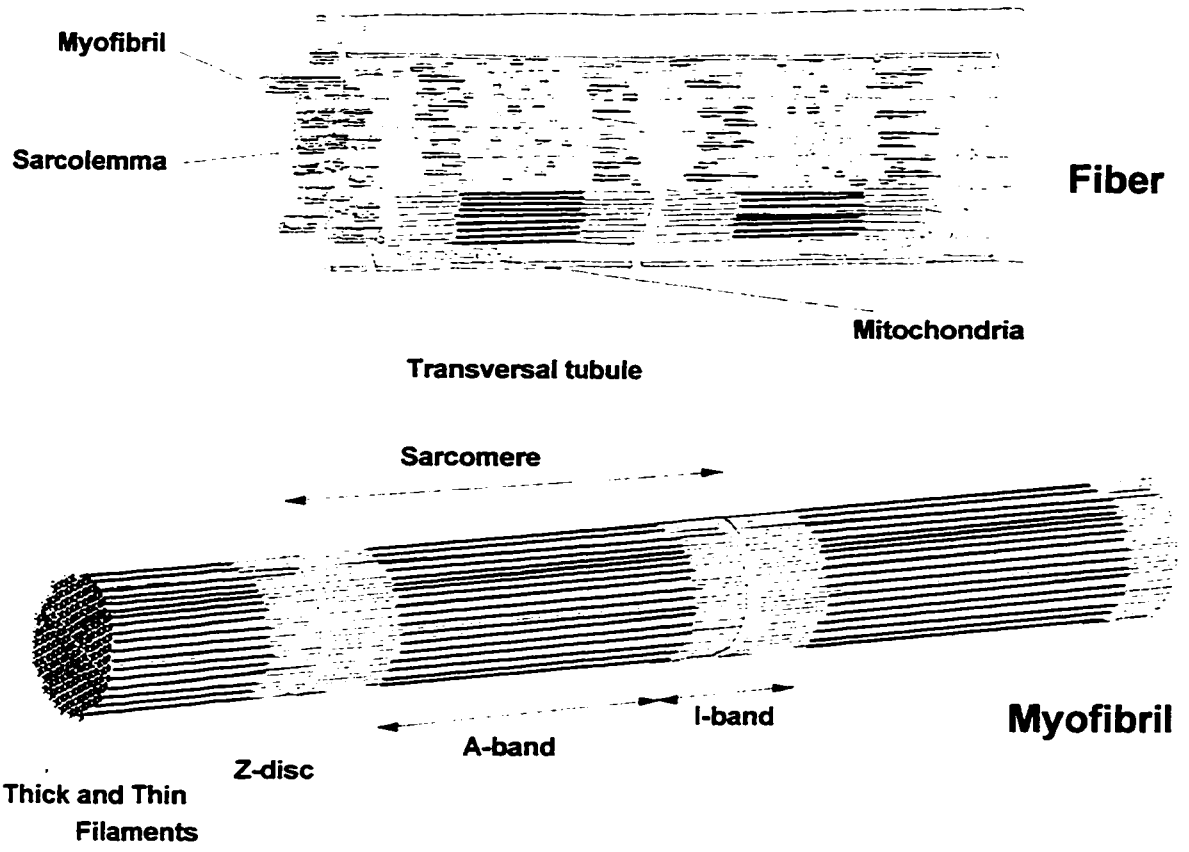

Figure 2.1: Schematic representation of skeletal muscle fibre showing the myofibrils and the sarcomere. (Based on drawings by Woledge, Curtin and Homsher (1985), and Pollack (1990).)

A section of myofibril between two consecutive Z-discs is called a sarcomere. The sarcomere is the minimal structural component of muscle capable of contraction and will be described in some detail in the next section. Other components of the fibre are the system of transversal-tubules (or T-tubules), that provide a shortcut for the electrical

wave of stimulation, and mitochondria which supply energy by means of the oxidative phosphorylation of the adenosine tri-phosphate (ATP).

2.1 Sarcomere Structure

In vertebrate muscle, the separation between consecutive Z-discs, the sarcomere length, may vary between about 2 μm and 4 μm, depending on the degree of stretching of the fibre. Upon contraction, the sarcomere shortens proportionally to the fibre shortening[1]. This proportional shortening is possible thanks to the internal arrangement of sarcomeres which consist mainly of interdigitating filaments of myosin and actin polymers as shown schematically in Fig 2.2. There also exists a connection between the end of each thick filament and the Z-disc through titin filaments, however the prevalent way of thinking is that titin has a passive role of preserving the structural integrity of the sarcomere upon stretching beyond the overlap region of the myofilaments, and that its characteristic of easy foldability does not impose considerable forces upon contraction (Rief et al. 1997, Kellermayer et al. 1997, Erickson 1997).

Thick filaments are cross-linked in their central part by a structure called the M-band which has passive structural functions.

Although there are some objections, like those raised by Pollack (Pollack 1990, Pollack 1995), it is widely accepted that the thick and thin filaments do not change considerably their length when muscle contracts or stretches. This is the base of the sliding filament model first proposed independently by A.F. Huxley and Niedergerke,

---

[1]Although not all sarcomeres shorten by the same amount, on average they shorten proportionally to fiber shortening.

(1954), and by H. E. Huxley and Hanson, (1954). The sliding filament model assumes that thick and thin filaments slide rigidly past each other. The sliding filament model has served as the basis for the cross-bridge theory, the almost unanimously accepted description of muscle contraction, that will be briefly discussed in section 2.3.

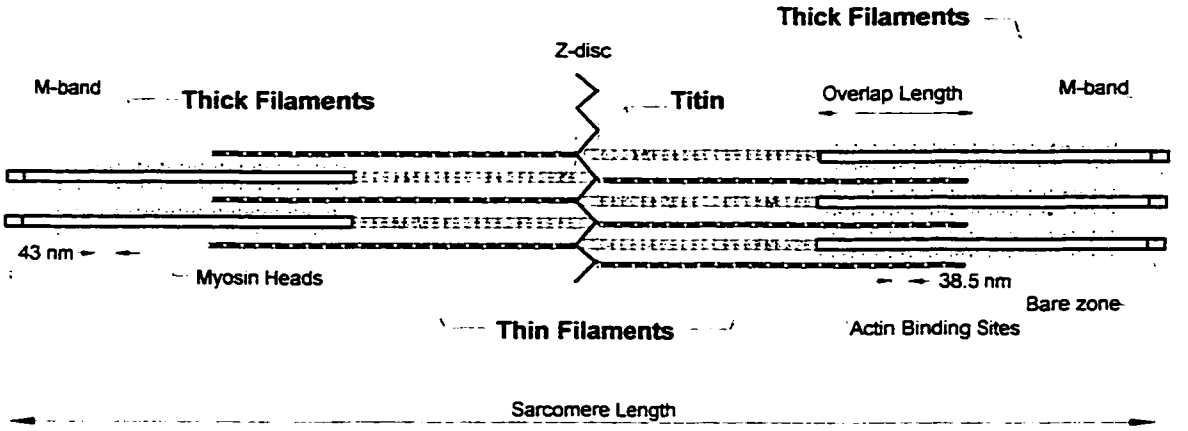

Figure 2.2: Schematic representation of a sarcomere (from M-band to M-band).

2.2 Thick and thin filaments

Thick or myosin filaments are bipolar structures 1600 nm in length, formed by the aggregation of myosin molecules. The length of thick filaments is remarkably constant among different species of vertebrates. Myosin is a large molecule consisting of two identical ellipsoidal heads 20 nm in length connected to a 156 nm long rod which has a flexible hinge at 43 nm from the heads. In the last few years, the myosin molecule has received a great deal of attention by molecular biophysicists, who in 1993 mapped all its

domains in detail and identified the pocket that supposedly binds it to the actin monomer (Rayment et al. 1993, Rayment et al. 1993b). The thick filament is formed by the union of three strands or subfilaments. To form a subfilament, myosin molecules, staggered by 43 nm in the axial direction, slightly twist their tails around each other. The heads projecting out of the filament form three helical tracks separated by 43 nm in the axial direction and a pitch of 86 nm for vertebrate[2] skeletal muscle (Cantino and Squire, 1986). The two halves of the filament on either side of the M-band are of opposite polarity with the tails of the myosin molecules pointing towards the M-band. Because of this arrangement in the centre of the filament, there exists a 150 nm long segment (the bare zone) without myosin heads.

Thin filament length is variable among different vertebrate species, ranging from 950 nm in frogs to 1270 nm in humans. Thin filaments are formed mainly by three proteins: actin, tropomyosin and troponin. Tropomyosin and troponin are believed to play a regulatory role because it has been observed that they change their structure in the presence of calcium ions (Ca++). The thin filament backbone is formed by a two-strand helix of F-actin, with a pitch of 73 nm. F-actin is a polymerized form of actin monomers or G-actin (globular actin), which is a ball-shaped molecule of 5.46 nm in diameter. Actin monomers are believed to provide myosin heads with attachment points, thereby taking part in the formation of cross-bridges. Tropomyosin and troponin lie in the groove of the two F-actin helices. Upon activation, Ca++ binds to specific sites on the troponin molecule which interact with tropomyosin, thereby removing an inhibition imposed by tropomyosin molecules to the formation of acto-myosin connections (cross-bridges).

---

[2]The arrangement of myosin molecules to form the thick filament varies in invertebrates. See Squire 1990 and Pollack 1995 for a detailed description.

When the fibre is in a relaxed state Ca++ is stored in the sarcoplasmic reticulum. Upon activation, Ca++ is released from the sarcoplasmic reticulum and diffuses into the intracellular space to the network of myofilaments. The binding of Ca++ to specific sites in the troponin molecules of thin filaments enhance the affinity of the actin for myosin molecules. Simultaneously, a series of chemical reactions start to restore the free Ca++ to the sarcoplasmic reticulum against the diffusive gradient. The mechanism is known as 'the calcium pump' and it uses a considerable[3] amount of energy generated by the hydrolysis of ATP into adenosine di-phosphate (ADP) and inorganic phosphate (Pi). The calcium pump continues its work even after the contraction is over, restoring a difference in concentration of about three orders of magnitude between the sarcoplasmic reticulum and the intracellular space.

2.3 Cross Bridge Theory

Based on the notion of sliding filaments, A. F. Huxley set forth the cross bridge theory of muscle contraction (Huxley, 1957). The cross-bridge theory assigns the force production of muscles to the interaction between myosin heads and thin filaments. In its original proposal, myosin heads were represented as 'side pieces' sticking out of the thick filament[4]. These side pieces were assumed to be attached to the thick filament by means of a linear elastic spring. It was also assumed that thermal agitation was responsible for making the side pieces oscillate back and forth, and, that the side piece spontaneously attached to actin filaments. In the original proposal Huxley assumed that the farther the

---

[3]Up to 30% of the total energy consumed by the contraction as reported by Woledge et al., 1985.

[4]The detailed structure of the myosin filament was unknown at the time of Huxley's proposal.

side piece is from its equilibrium position, the higher is the probability of attachment to the thin filament. Once the side piece is attached to the thin filament, the cross-bridge cycle can be broken only by a chemical reaction requiring the energy of a molecule of ATP. Probabilities of detachment depend on the strain of the cross-bridge with a high probability of detachment assigned to the case in which the spring is in compression. This simple mechanical model allowed A. F. Huxley to formulate the distribution function of attached cross-bridges in terms of the strain-dependent attachment and detachment constants and the speed of contraction. In 1971 Huxley and Simmons, adopted a slightly different version of the theory in which the side pieces were replaced by a tilting head connected by a spring to the thick filament. The cross-bridge can now be in several states, each with a distinctive potential energy. In this case it is assumed that the myosin head, attached to the thin filament, is able to rotate between states, pulling the tail of the myosin molecule. The model needs the specification of rate constants for transitions between several energy states. Following Huxley's work, a large number of versions of cross-bridge theories arose. In all of them the fundamental mechanisms are mainly the same, except for the number of states and the transition constants between them. Harrington (1979) proposed a different mechanism in which the myosin head attaches rigidly to the actin filament and a helix-coil transition in the tail of the molecule is responsible for the generation of the force. Independently of the detailed mechanism of interaction between thick and thin filaments, all these theories can be grouped as a class; the *independent force generators theories*. The common feature of the independent force generators theories is the assumption that there is a uniform distribution of force generators along the overlap between myosin and actin filaments. As these force generators are assumed to act independent of each other, the total force is proportionally related to the overlap distance

between myofilaments[5]. Representing the proportion of attached cross-bridges by a function $n(x,t)$ of the cross-bridge elongation x and the time t, Huxley's cross-bridge model is described by the following differential equation:

$$-V\frac{\partial n}{\partial x} = f(x) - [f(x) + g(x)] \cdot n \tag{2.1}$$

where V is the (constant) relative sliding velocity between filaments, $f(x)$ and $g(x)$ the attachment and detachment rate functions respectively.

If simple mechanisms involving the interaction between Ca++ and the thin filament are included in the model, Huxley's cross-bridge theory can be expressed by an equation of the form (Zahalak, 1990, Zahalak and Ma, 1990, Zahalak and Motabarzadeh,1997):

$$\frac{\partial n}{\partial t} - v\frac{\partial n}{\partial x} = r([\mathrm{Ca}^{++}]) \cdot f(x) \cdot (\alpha - n) - g(x) \cdot n \tag{2.2}$$

where α the fraction of participating cross-bridges, $v(t)$ the (variable) relative sliding velocity between myosin and actin filaments, and r([Ca++]) a function of the sarcoplasmic free calcium concentration. The force produced by the fibre can be found by integrating the force produced by attached cross-bridges within half a sarcomere as:

$$F = \frac{k}{l}\int_{-\infty}^{\infty} n \cdot x \, dx \tag{2.3}$$

where k is the cross-bridge stiffness in units of force per distance and l is the average separation of attachment sites along the thin filament. Because in this model the detachment of each cross-bridge is driven by a chemical reaction, the total rate of energy liberation is directly related to the energy liberated by the hydrolysis of one ATP molecule, e, by:

---

[5] Note that this proposition is exact if and only if myofilaments are considered rigid.

$$E = \frac{e}{l}\int_{-\infty}^{\infty} f \cdot (\alpha - n)\, dx \qquad (2.4)$$

and the rate of heat liberation can be calculated as $Q = E - PV$.

From the point of view of continuum mechanics, the models implicit in 2.1 and 2.2 are very limited particular cases. For example, if the filaments are considered as linear elastic with a stiffness that is non-negligible[6] with respect to the stiffness of the cross-bridges, then n and v also depend on X, the material coordinate along the sarcomere. Mijailovich et al., 1996, presented a modified Huxley's equation that includes filament stretch, but these equations are only applicable in the limit of small strains, where the material and the spatial derivatives are approximately equal. During an isometric contraction, further simplification of the equations can be obtained because for small displacements the difference between Lagrangian and Eulerian coordinates can be neglected.

The rate constants in Huxley's model depend only on x, the strain of the cross-bridge, there is no allowance for a dependence on the filament global stress. Given that the interaction between macromolecules in the filaments is supposed to be stereospecific, it is plausible to hypothesize that the strain in the filaments, especially in the thin filaments, or the cross-bridges, may modify the affinity of attachments. Cooke et al., 1994, proposed a model in which, under fast isotonic contractions, the detachment of myosin from the thin filament is carried out before the completion of the hydrolysis of ATP, implying that the rate constants are also dependent on the contraction velocity, or that there is a non-strict relation between the number of cross-bridge cycles and the number of ATP molecules hydrolyzed.

---

[6]What constitutes non-negligible stiffnesses of the filaments will become apparent in later sections.

Despite the above mentioned shortcomings and the inability of predicting phenomena often associated with 'memory effects' such as force depression/enhancement, (we will discuss this in more detail in chapter III), the cross-bridge theory can be considered as one of the most successful theories in muscle physiology. It is worth noting that a simple but morphologically plausible mechanical model of the molecular interaction gives a differential equation that can be used to predict the outcome of macroscopic experiments, a feat comparable to that of the kinetic theory of gases in physics.

2.4 Fibre Stiffness

According to the cross-bridge theory (Huxley, 1957; Huxley and Simmons, 1971), force production in skeletal muscle occurs through formation of linkages (cross-bridges) between thick (myosin) and thin (actin) filaments. Furthermore, it is assumed that the thick and thin filaments slide rigidly past one another during contraction: that is, any compliance in the thick-filament—cross-bridge—thin-filament complex is associated with the cross-bridges. Therefore, quick release or quick stretch experiments were used to determine actomyosin stiffness, and from the stiffness values, the number of attached cross-bridges was calculated. For rigid myofilaments, the relation between stiffness and number of attached cross-bridges obtained in this way is linear (Ford et al., 1981).

Recent experimental evidence suggests that actin and myosin filaments are not perfectly rigid but elongate when a muscle goes from a relaxed to a contracted state (Kojima et al., 1994, Huxley et al., 1994, Wakabayashi et al., 1994, Goldman and Huxley, 1994). Although these elongations are only in the order of a fraction of a percent (~ 0.2% for the actin filament, Kojima et al., 1994), the length of the filaments compared to the

length of the cross-bridges is so large that as much as 50% of the fibre compliance has been associated with the myofilaments (Higuchi et al., 1995). Since in the past two decades many conclusions about skeletal muscle mechanics have relied on calculations of the number of attached cross-bridges based on stiffness measurements, these conclusions must be revisited with the new experimental findings in mind.

Ford, Huxley and Simmons (1981) addressed the problem of instantaneous stiffness and its relation to the number of attached cross-bridges. They used a model consisting of linear elastic rods to represent the thick and thin filaments, and a continuous material which transfers force proportionally to the distortion, to represent the cross-bridges. Distortion in their model becomes an internal variable that can be related to the geometry of the sarcomere. Our model proves to be more general than that presented by Ford et al. (1981) and, although simplified in structure, it can be used to draw useful conclusions about the mechanical properties of sarcomeres.

It is widely accepted that in a contracting skeletal muscle, the link between thick and thin filaments is physically realized through millions of myosin molecules attaching to specific actin sites. Because of the huge number of links, a continuous model of force transfer between representative filaments seems appropriate. However, consider the myosin filament: its total length is about 1600 nm. It has a central bare zone of approximately 160 nm, which leaves 720 nm for the myosin heads on each side of the centre. The separation between successive cross-bridges facing a given thin filament is about 43 nm: that is, only 17 cross-bridges can be formed between a given pair of thick and thin filaments at maximum overlap length. For less than optimum overlap or for submaximal activation, therefore, the validity of the continuum assumption may be questionable.

The purpose of this study was to develop a structural model of actomyosin interaction which allows the calculation of muscle (sarcomere) stiffness for any stiffness of the actin and myosin filaments, as well as the cross-bridges. Assuming that the entire sarcomere behaves like the composition of many individual filaments acting in parallel, we decided to base our model on a discrete description of the interaction between single thick and thin filaments.

2.5 The Discrete Approach to Stiffness Calculation

Let us start by analyzing the static behaviour of a structure formed by elastic links, as shown in Fig 2.3, which we call a "ladder" structure. In particular, we are interested in calculating the total stiffness of such a structure if the stiffness of the links is known. The ladder is one-dimensional, that is, points 0,1,2,..,2N+1 can move only in the horizontal direction.

Each sub-structure formed by four springs arranged in a closed circuit is referred to as a "panel". For example, points 0-2-3-1-0 enclose a panel. Panels are numbered from 1 to N. The stiffness (in units of force per unit length) of each elastic link is denoted by a_i, b_i and m_i for the links corresponding to the actin filament, the cross-bridges, and the myosin filament, respectively.

The stiffness of a structure (measured in units of force per unit length) with N+1 panels is obtained as the composition of the stiffness of the N-panel structure and the contribution of the three new spring elements that must be added to close a new panel.

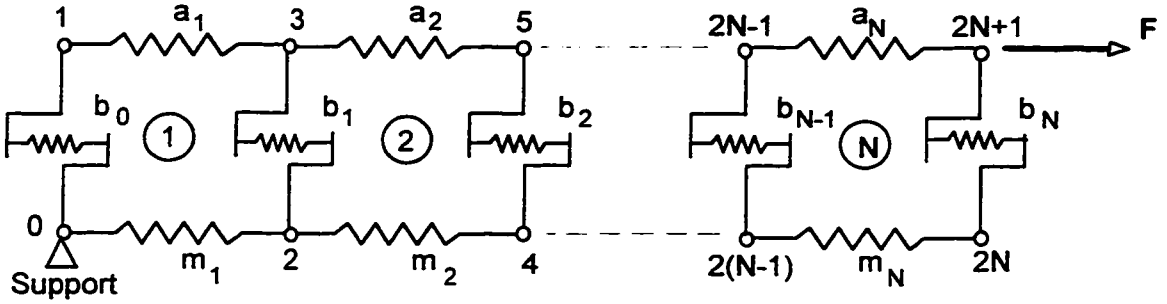

Figure 2.3: "Ladder" structure definition. Panel numbers are circled. Joints are numbered from 0 to 2N+1. Joints can move in the horizontal direction only. Joint 0 is fixed. a, b and m, are the stiffnesses, defined as force per unit length of deformation, of the links in the actin, cross-bridges and myosin filaments, respectively.

2.5.1 Recursive stiffness algorithm.

Given the one-dimensional spring ladder shown (Fig. 2.3), we wish to calculate the stiffness relative to a displacement of point 2N+1.

We will do this inductively. Consider the case of i panels and assume that its stiffness matrix (relative to the degrees of freedom shown in Fig. 2.4) is known:

Therefore:

$$\mathbf{F}' = \mathbf{K}' \cdot \mathbf{X}' \tag{2.5}$$

where the forces are given by

$$\mathbf{F}' = \begin{Bmatrix} F_1' \\ F_2' \end{Bmatrix} \tag{2.6}$$

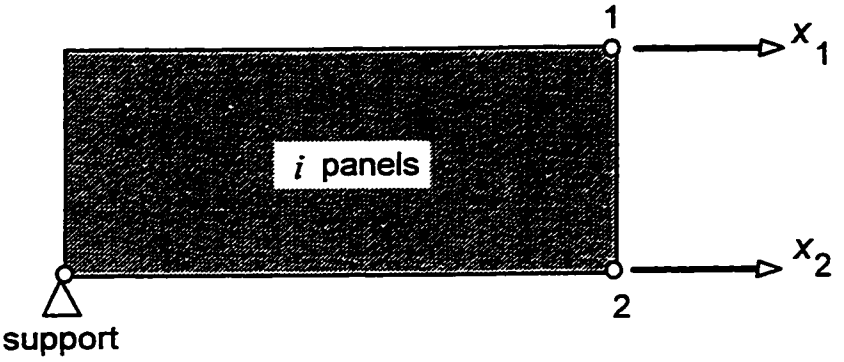

Figure 2.4: External degrees of freedom of the ladder structure with i - panels..

the displacements by:

$$\mathbf{X}^{i} = \begin{Bmatrix} X_1^{i} \\ X_2^{i} \end{Bmatrix} \tag{2.7}$$

and the stiffness matrix by:

$$\left[\mathbf{K}^{i}\right] = \begin{bmatrix} k_{11}^{i} & k_{12}^{i} \\ k_{21}^{i} & k_{22}^{i} \end{bmatrix} \tag{2.8}$$

The $i+1$ - panel case will have a 4 x 4 stiffness matrix (with respect to the degrees of freedom shown in Fig 2.5) which can be calculated as:

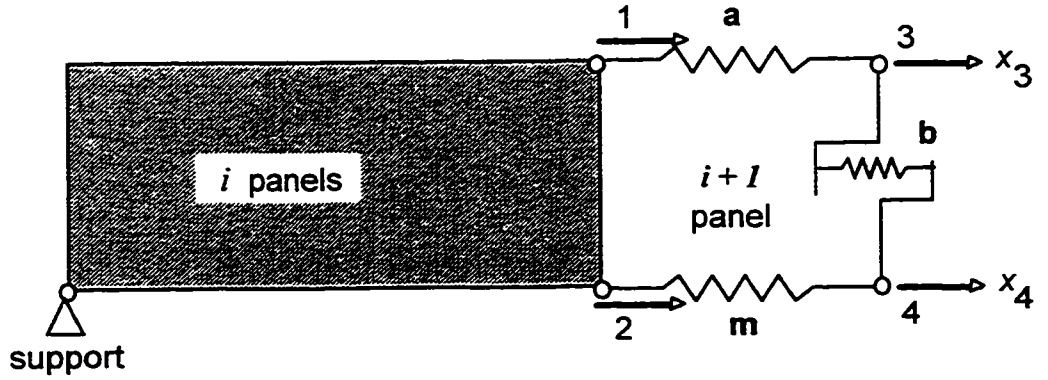

Figure 2.5: External and internal degrees of freedom when a new panel is added to the structure.

$$\left[\mathbf{K}^{i,j-1}\right]=\begin{bmatrix} k'_{11}+\mathsf{a} & k'_{12} & -\mathsf{a} & 0 \\ k'_{21} & k'_{22}+\mathsf{m} & 0 & -\mathsf{m} \\ -\mathsf{a} & 0 & \mathsf{a}+\mathsf{b} & -\mathsf{b} \\ 0 & -\mathsf{m} & -\mathsf{b} & \mathsf{b}+\mathsf{m} \end{bmatrix} \tag{2.9}$$

Since there will be no forces applied at points 1 or 2, those degrees of freedom can be eliminated algebraically, by subdividing the 4 x 4 matrix into four 2 x 2 blocks, as follows:

$$\left[\begin{array}{cc|cc} k'_{11}+\mathsf{a} & k'_{12} & -\mathsf{a} & 0 \\ k'_{21} & k'_{22}+\mathsf{m} & 0 & -\mathsf{m} \\ \hline -\mathsf{a} & 0 & \mathsf{a}+\mathsf{b} & -\mathsf{b} \\ 0 & -\mathsf{m} & -\mathsf{b} & \mathsf{b}+\mathsf{m} \end{array}\right] \cdot \left\{\begin{array}{c} x_1 \\ x_2 \\ \hline x_3 \\ x_4 \end{array}\right\} = \left\{\begin{array}{c} 0 \\ 0 \\ \hline F_3 \\ F_4 \end{array}\right\} \tag{2.10}$$

After the elimination is carried out, the 4 x 4 stiffness matrix reduces to a 2 x 2 matrix according to the following scheme:

$$\underset{4\text{x}4}{\left[\begin{array}{c|c} \mathbf{A} & \mathbf{B} \\ \hline \mathbf{B}^{\mathrm{T}} & \mathbf{C} \end{array}\right]} \longrightarrow \underset{2\text{x}2}{\left[\mathbf{C}-\mathbf{B}^{\mathrm{T}}\mathbf{A}^{-1}\mathbf{B}\right]} \tag{2.11}$$

In our case:

$$\left[\mathbf{A}^{-1}\right]=\frac{1}{\Delta'}\begin{bmatrix} k'_{22}+\mathsf{m} & -k'_{21} \\ -k'_{12} & k'_{11}+\mathsf{a} \end{bmatrix} \tag{2.12}$$

with:

$$\Delta' = \left(k'_{11}+\mathsf{a}\right)\left(k'_{22}+\mathsf{m}\right)-\left(k'_{12}\right)^2 \tag{2.13}$$

$$\left[\mathbf{B}\right]=\left[\mathbf{B}^{\mathrm{T}}\right]=\begin{bmatrix} -\mathsf{a} & 0 \\ 0 & -\mathsf{m} \end{bmatrix} \tag{2.14}$$

$$\left[\mathbf{C}\right]=\begin{bmatrix} \mathsf{a}+\mathsf{b} & -\mathsf{b} \\ -\mathsf{b} & \mathsf{b}+\mathsf{m} \end{bmatrix} \tag{2.15}$$

Thus, the components of the stiffness matrix corresponding to i+1 panels are obtained as:

$$k_{11}^{i+1} = a + b - \frac{a^2}{\Delta^i} \cdot \left(k_{22}^i + m\right) \tag{2.16}$$

$$k_{12}^{i+1} = k_{21}^{i+1} = -b + \frac{a \cdot m}{\Delta^i} \cdot k_{12}^i \tag{2.17}$$

$$k_{22}^{i+1} = b + m - \frac{m^2}{\Delta^i} \cdot \left(k_{11}^i + a\right) \tag{2.18}$$

To get a complete formulation we need an explicit expression for $[\mathbf{K}^1]$ which is obtained as:

$$[\mathbf{K}^1] = \begin{bmatrix} \frac{a \cdot b}{a+b} + b & -b \\ -b & b+m \end{bmatrix} \tag{2.19}$$

Finally, once $[\mathbf{K}^n]$ has been obtained, the stiffness relative to a displacement at 2N+1 can again be obtained as before, because the force associated with the degree of freedom number 2 is zero:

$$K_{lad}^n = k_{11}^n - \frac{\left(k_{12}^n\right)^2}{k_{22}^n} \tag{2.20}$$

2.5.2 The Ladder Structure with Additional Series Filament.

The ladder structure represents the overlap zone between filaments well. However, if filament compliance is evenly distributed along the filament, sarcomere properties at lengths exceeding optimal sarcomere length may be governed by the compliance of the

filaments in the non-overlap zone. Even a small compliance of the filaments must be taken into account in the calculation of the stiffness of the total structure.

The next step in the analysis is, therefore, to calculate the stiffness for the ladder structure with two elastic links on each side (Fig 2.6). The total stiffness of the structure can be calculated using the formula for springs in series, i.e.,

$$1/K_{tot} = 1/\alpha + 1/K_{lad}^{N} + 1/\beta \qquad (2.21)$$

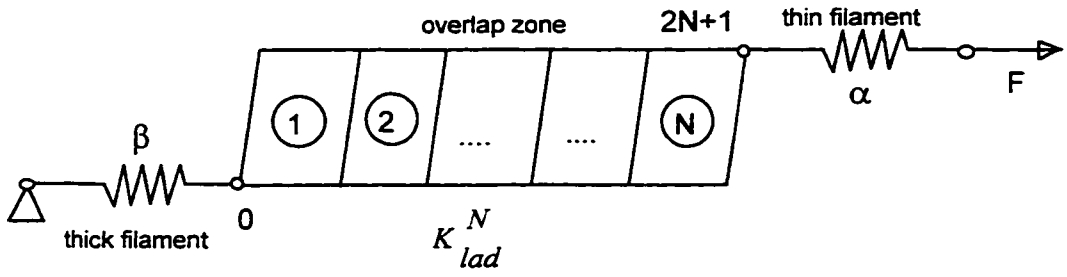

Figure 2.6: N-panel ladder structure with series elastic elements. α and β are the stiffnesses of the portion of thin and thick filaments, respectively.

where K_{tot} is the stiffness of the complete structure, and K_{lad}^{N} is the stiffness corresponding to a ladder structure having N panels. α, β represent the stiffness of the portions of thin and thick filaments beyond the overlap zone. Consequently, α and β are functions of the stiffness per unit length and the length of the filaments beyond the overlap zone.

In order to represent the approximate geometry of a vertebrate muscle sarcomere, it was assumed that each panel has a length δ = 40 nm. This length was taken to approximate the repeat distance of the cross-bridges on the thick filament. The exact value for the cross-bridge repeat is not required for estimating sarcomere stiffness;

maintaining approximate ratios of the cross-bridge repeat and the myofilament length is sufficient for adequate estimation of the sarcomere stiffness.

In order to simplify the calculations, it was assumed that filament lengths were similar to those of rabbit skeletal muscle and that they were integer multiples of δ. Let L_a = 1120 nm, the length of the actin filament; L_m = 800 nm, the length of half the thick filament; and L_o = 720 nm, the length of the portion of the thick filament containing cross-bridges. The number of panels for maximum overlap is then N_{max}=18. Fig 2.7 shows a half sarcomere for three relevant configurations.

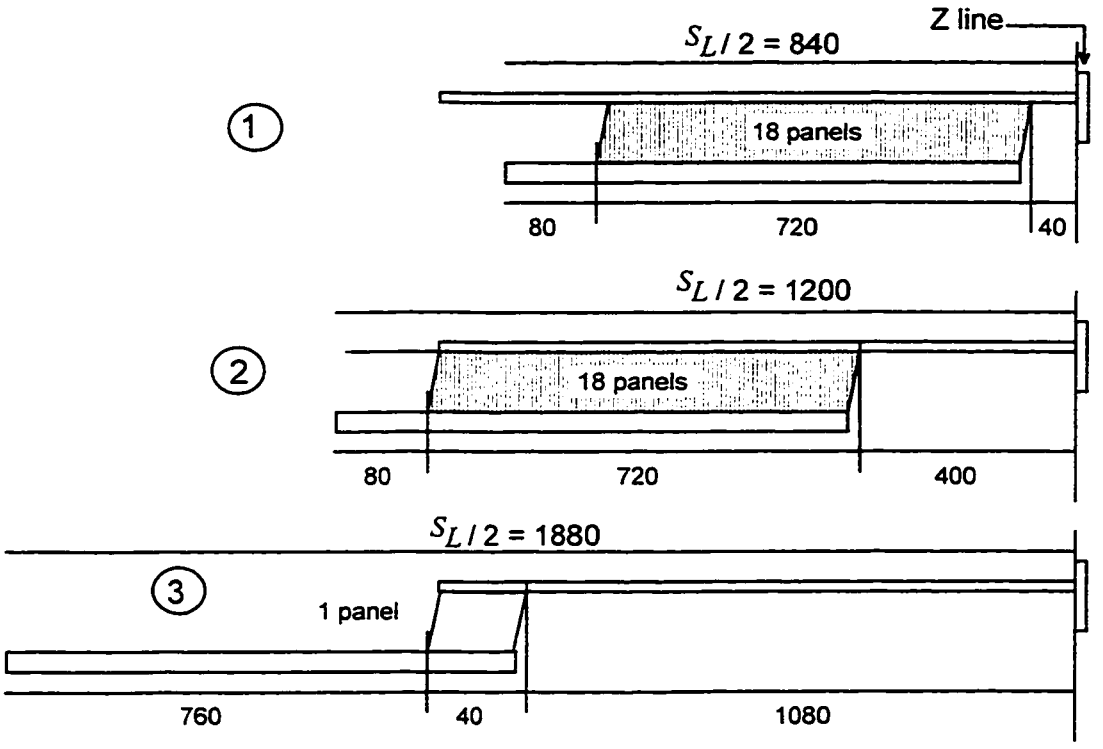

Figure 2.7: Element lengths for different configurations of the ladder structure. Lengths [nm] relate the structure to the approximate sarcomere geometry of rabbit skeletal muscle.

With the dimensions defined, the sarcomere length S_L and the number of panels N_p of the ladder structure are related by:

$$\text{maximum}\left\{0, \text{minimum}\left[\left(L_a + L_m - S_L/2\right)/\delta, 18\right]\right\} = N_p \qquad (2.22)$$

where [x] denotes the integer part of x.

2.5.3 Parallel Array of Ladder Structures with Additional Series Filament.

If we consider a sarcomere as an array of n filaments in parallel, the total stiffness of such a system can be calculated as:

$$K_S = \sum_{i=1}^{n} K_{tot_i} \qquad (2.23)$$

This formula assumes that there is no mechanical interaction between neighbouring filaments, which is an approximation considering the experimental evidence reviewed in, for example, Squire (1990) and Pollack (1990).

Of course, if all ladder structures are identical, the stiffness of the array of ladders will be a multiple of the stiffness of each ladder. The array of ladder structures can be used to investigate the influence of the proportion of attached cross-bridges with respect to the total number of cross-bridges available for interaction: for each cross-bridge in each panel, the cross-bridge is attached to the thin filament if, and only if, $x_R \leq P_{att}$, where x_R is a random number in the interval [0,1], and P_{att} is the constant probability of attachment. Recall that the analysis is done for a quasi-static case or, more properly, within an infinitesimal time period, in which it can be assumed that the structure does not

change its configuration. In this case, although the overlap region for each pair of filaments has the same length, the number of panels in each unit may be different because of the random process used to generate the ladder structures. Consequently, the stiffness, K_{tot_i}, of each unit may also be different. Two ladder structures can have the same length but a different number of panels. In the case of missing cross-links, our model takes care of the void by combining the stiffnesses of the corresponding myofilament portions, therefore, panels can have different lengths as required[7].

The total stiffness of the structure reflects the stiffness of the average structure, and a large number of filament pairs has the effect of reducing the dispersion of the total stiffness value with respect to the average. To calculate the average stiffness per myosin head, s, the total stiffness K_S is divided by the maximum number of cross-bridges available for interaction at the corresponding overlap and attachment proportion, $N_{CB\max} = n \cdot P_{att} \cdot (N_p + 1)$.

2.6 Results.

2.6.1 The "Ladder" Structure.

We first consider the ladder structure with an increasing number of equal panels; this corresponds to the sarcomere overlap region gradually increasing with all the cross-

---

[7] The recursive formulas should be modified by replacing a, b and m with a_{i+1}, b_{i+1} and m_{i+1}.

bridges attached at intervals of 40 nm. Calculations of the total stiffness were performed starting from one panel with the minimum overlap possible, and going up to a hypothetical maximum of 30 panels for the case in which $a_1 = a_2 = ... = a_N = a$; $m_1 = m_2 = ... = m_N = m$ and $b_0 = b_1 = ... = b_N = b$ where a is the stiffness of a portion of the thin filament between two successive attachment sites, m is the stiffness of a portion of the thick filament between two myosin heads, and b is the stiffness of an individual cross-bridge. These conditions imply that the cross-bridges have the same elastic properties and that the distribution of attachment sites is uniform along the thin filament.

In general, the thick and thin filaments can have different elastic properties. If we write $a = \rho m$, a particular configuration can be defined by knowing the stiffness of a cross-bridge, b, and the parameters a/b and ρ.

Intuitively, it is easy to see that for a fixed value of ρ, the total stiffness of the structure will be a linear function of the number of panels when the ratio a/b tends towards ∞, i.e. when the filaments become rigid. However, it is difficult to predict a priori how large the ratio a/b must be for the structure to behave as if the filaments were rigid.

Fig. 2.8a shows the variations in stiffness of the ladder structure versus the ratio a/b for specific numbers of panels (5,10,...,30 panels) when $\rho = 1$. Experimental evidence indicates that the filaments are much stiffer than the cross-bridges, therefore attention will be given to the cases in which the stiffness of the horizontal links (filaments) is much greater than the stiffness of the 'vertical' links (cross-bridges).

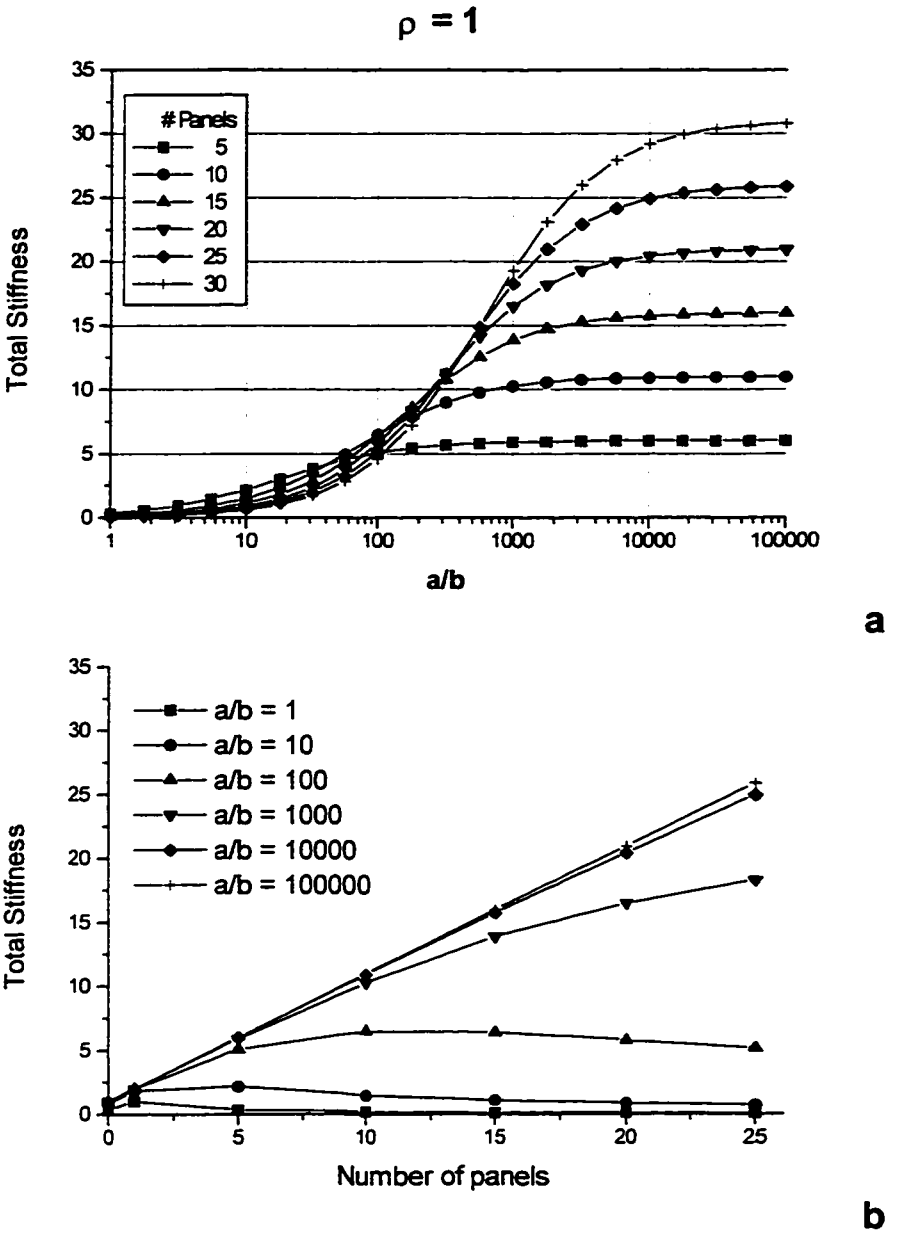

Figure 2.8: Stiffness of the ladder structure as a function of the ratio a/b (top) and the number of panels (bottom). The ratio m/a was 1 in all cases shown. The structure behaves as if the filaments were effectively rigid for a/b ratios of 10^5 or larger, as indicated by the flat part of the curves on the top, or the straight lines on the bottom.

Fig. 2.8b demonstrates that the total stiffness is not a linear function of the number of panels for a/b less than 10^5. This result means that even though the horizontal links (filaments) are much more rigid than the vertical links (cross-bridges), the behaviour of the structure is not equivalent to that of the same structure having rigid filaments. Therefore, the proposition that the stiffness is directly proportional to the number of vertical links (i.e. attached cross-bridges) is not valid for a wide range of a/b ratios. Qualitatively, the behaviour of the system does not change if filaments are given different stiffnesses (within the same order of magnitude), i.e. for values of ρ other than 1.

As the number of panels increases (i.e. more myofilament overlap), cross-bridges in parallel add to the total stiffness, while increasing the length of the filaments in series with the ladder structure adds to the total compliance. The total compliance of an N-panel ladder can be approximated by $\frac{1}{b(N+1)}+\frac{N}{a}$ which has a minimum for $N=\sqrt{a/b}-1$. Note that the stiffness curves in figure 2.8b have a maximum when the number of panels is $\approx\sqrt{a/b}$.

The conclusions extracted from the solution of the ladder structure can be applied readily to the overlap region between thin and thick filaments in one half of a sarcomere, assuming a uniform distribution of the cross-bridges.

2.6.2 The Continuous Model Revisited.

The discrete model presented here should be able to reproduce the limiting case in which the number of equal panels goes to infinity while the stiffness properties are kept unaltered,(i.e. the width of the panel goes to zero). This process of going to the limit of the discrete model is one way of constructing a continuous model in which the stiffness of

the filaments and the cross-bridges are given as properties per unit length. The process is described fully in Appendix A. Here, we will reproduce the result for the case in which the stiffness per unit length is the same in both filaments:

$$k_{cl} = \frac{\sigma}{\left(L/2 + \coth(\gamma L/2)/\gamma\right)} \tag{2.24}$$

$$\gamma = (2\eta/\sigma)^{1/2} \tag{2.25}$$

where: k_{cl} is the stiffness of the overlap region, L is the overlap length, σ is the characteristic stiffness per unit length of the filaments, and η is the characteristic stiffness per unit length of the cross-bridges. Taking the term representing the overlap zone in equation A 9 of Ford et al., (1981) for the case in which the compliances per unit length of both filaments are equal ($c_A = c_M$ following the notation therein), we obtain:

$$C_f = 1/k_{cl} = \frac{c_A}{2}\zeta + \frac{c_A}{\mu}\coth(\mu\zeta/2) \tag{2.26}$$

which, after applying the definitions given by Ford et al. (1981), is exactly the same as 2.24.

How does 2.24 (or 2.26) compare with the results given by the discrete model? Answering this question is the same as calculating how many panels a ladder structure should have to be well represented by the continuum approximation. Fig 2.9 shows the difference between the discrete (finite number of panels) and the continuum (infinite number of panels) solutions for the overlap region between two similar filaments. Values in Fig 2.9 were obtained by calculating the percent difference between the stiffness of the ladder structure, K_{lad}^{N}, and the stiffness calculated using Eq. 2.24, k_{cl}, for the continuum structure of identical length and elastic properties. For the same number of panels, the

difference is independent of the panel length and varies only slightly with the ratio between filament and cross-bridge stiffness.

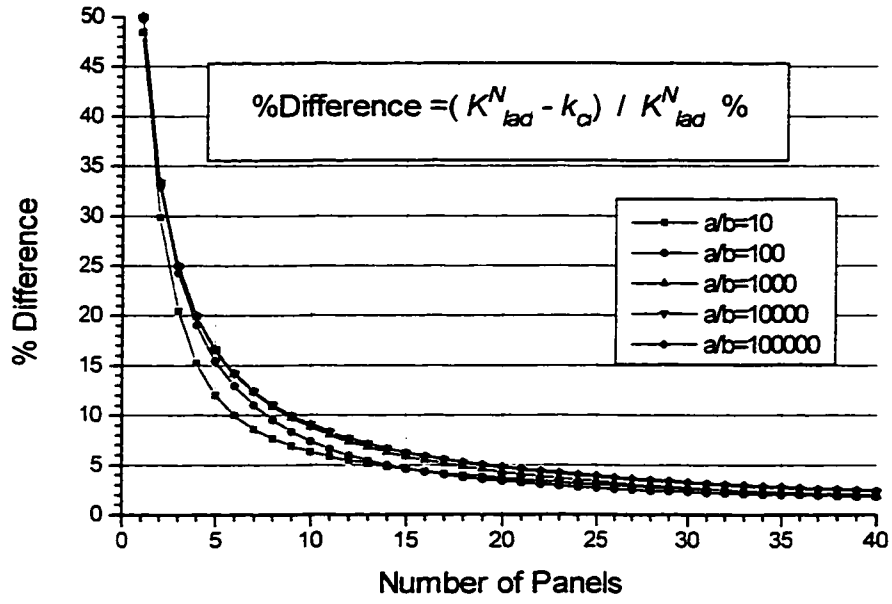

Figure 2.9: Percent difference in the stiffness between the continuum and the discrete solutions for the ladder structure. Even for 20 panels, the continuum solution gives a stiffness that is about 5% lower than the discrete solution.

Assuming that all the available myosin heads are attached simultaneously to the thin filament, only about 20 cross-bridges can be formed between a thin and a thick filament at maximum overlap (for example in the rigor state). The number of attached cross-bridges during a tetanic contraction is likely only a fraction of those attached in rigor, implying that the continuum approach is not appropriate for representing the actin-myosin interaction (Fig. 2.9). Therefore, the differences in stiffness between the discrete and the continuous model cannot be neglected in cases of partial activation or in cases of small

overlap between thick and thin filaments. For a/b ratios greater than 1000, the term representing the stiffness of the overlap zone (second term on the left hand side of Eq. 2.21) is dominant; therefore, a change in the value of this second term will give about the same change in total stiffness. The dominance of this term increases for increasing stiffness of the filaments.

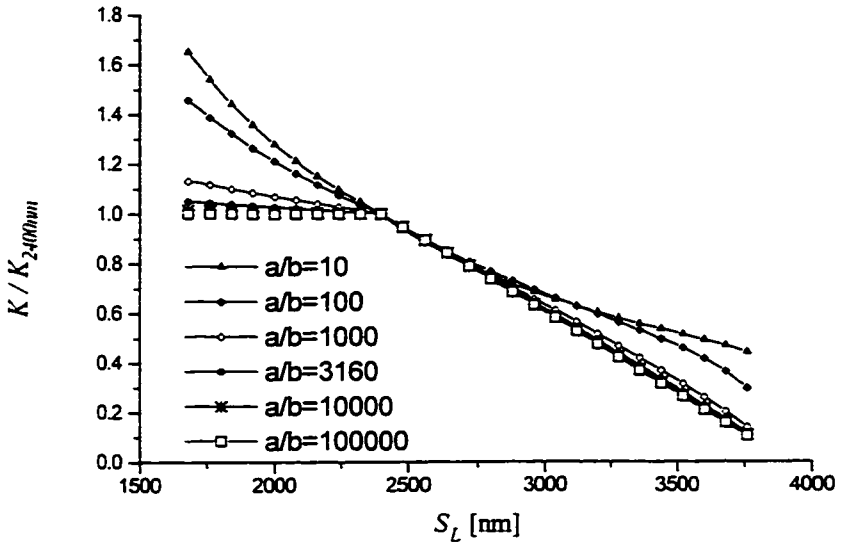

Figure 2.10: Sarcomere stiffness as a function of the sarcomere length for different stiffness ratios of the ladder structure with additional filaments. Stiffness values are plotted relative to the stiffness at 2400 nm, corresponding to configuration 2 in Fig 2.7

Although the continuum solution can be derived as a particular case of the discrete ladder structure, some of the properties of the discrete structure with a few panels are lost in the continuum solution. For a low number of panels the continuum solution underestimates the stiffness because the implicit, continuously varied deformation gradient is different from the piecewise constant deformation gradient of each elastic link in the discrete model. In other words, the continuous model allows the transfer of forces

and deformations between two consecutively attached cross-bridges while the discrete model does not. This situation is the exact counterpart of the well-known rigidization effect of finite-difference solutions in continuous structures. Because of the discrete nature of the system under study, the discrete model is deemed as a better approximation than the continuous model.

Using the solution of the ladder structure and the sarcomere geometry given in Fig 2.7, stiffness as a function of sarcomere length can be calculated using Eq. 2.21. The resultant stiffness of half a sarcomere is shown in Fig 2.10. Clearly, as the filaments become more rigid with respect to the cross-bridges, the total stiffness approximates a direct linear relation with the number of panels (attached cross-bridges).

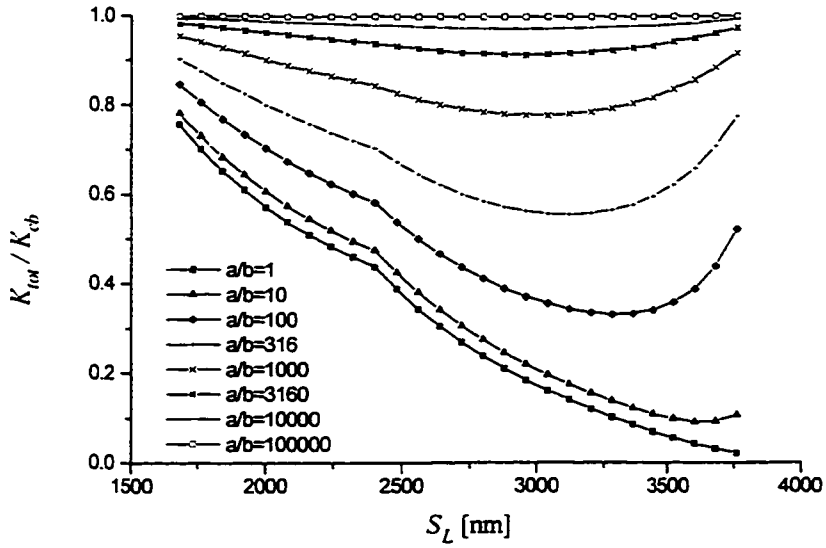

Figure 2.11: Ratio of total stiffness and stiffness of the overlap zone as a function of sarcomere length for different stiffness ratios. Ladder structure with additional filaments.

In Fig 2.10, the stiffness was normalized with respect to the stiffness calculated at a sarcomere length of 2400 nm, the length at which myofilament overlap is maximum and

no portion of the thin filament is unstressed. Fig 2.11 shows the ratio between the stiffness of the entire structure and the stiffness corresponding to the overlap zone as a function of sarcomere length. The graph clearly shows that the more rigid the filaments are, the closer is the stiffness of the complete structure to that of the overlap zone (ladder structure) alone.

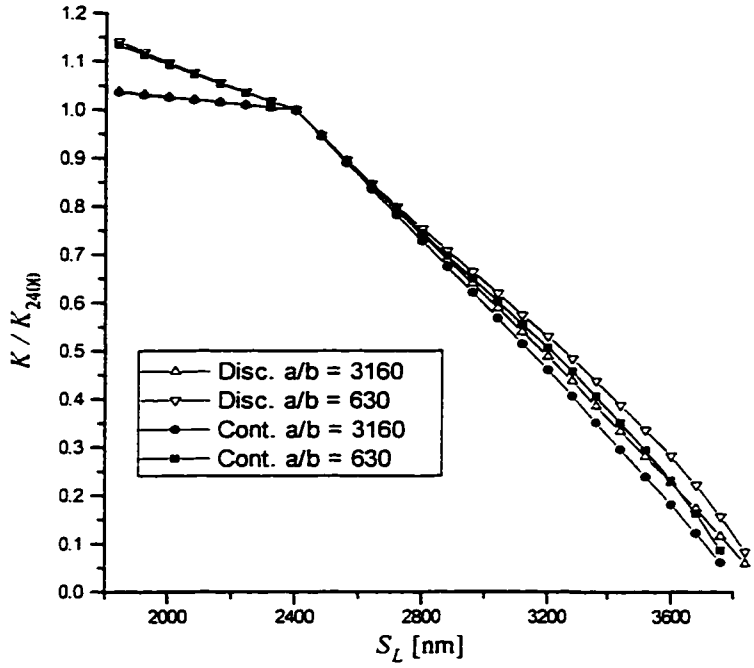

Figure 2.12: Comparison between the stiffness given by the continuous and discrete models. Stiffness values are plotted relative to the stiffness at 2400 nm, corresponding to the optimum overlap. a/b=3160 and a/b=630 correspond to μ = 0.61 μm^{-1} and μ = 1.4 μm^{-1}.

Comparison between the present, discrete model and the continuous model of Ford et al. (1981) is shown in Figs 2.12 and 2.13. Fig 2.12 shows the stiffness normalized relative to the stiffness at optimum overlap for both models with two biologically relevant values of the parameter a/b. In Fig 2.13, the value of y_o, the amount of shortening that would

bring the tension to zero, is normalized in the same way as Fig 13 in the work by Ford et al. (1981). The values 90% and 50% correspond to the cases in which the cross-bridges contribute 90% and 50% of the compliance at optimum length respectively. The difference between the continuous and the discrete model indicates that the discrete model becomes relatively stiffer than the continuous model with increasing sarcomere lengths.

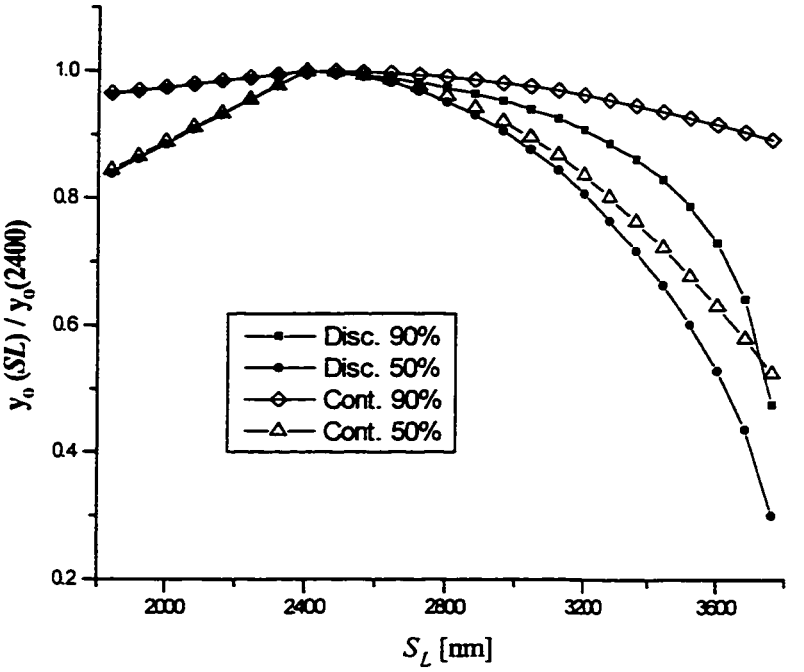

Figure 2.13: Sarcomere length dependence of y_0 plotted in the same way as Fig 13 in Ford et al. (1981). y_0 was taken to be proportional to compliance times overlap. Comparison between discrete and continuous models: curves indicate that the longer the sarcomere the stiffer the discrete model is with respect to the continuous model with the same parameters.

2.6.3 Parallel Array of Ladder Structures with Additional Series Filament.

Figure 2.14 shows the total stiffness K_S and the stiffness per myosin head s, calculated for a parallel array of filaments interacting in pairs. The results for a ratio a/b = 3160 are shown together with the corresponding results of Ford et al. (1981) for the same proportion of active cross-bridges. For a fixed overlap, variations of the stiffness per cross-bridge as a function of the proportion of attached cross-bridges, are not the same for the continuous and discrete models. This result can be relevant in the study of the influence of activation.

When normalized with respect to the stiffness at a sarcomere length of 2400 nm, the total stiffness values are all nearly the same regardless of the number of filament pairs or the probabilities of cross-bridge formation. When the total stiffness is divided by the maximum number of possible cross-bridge attachments, $N_{CB\max}$, the measure of stiffness per cross-bridge depends on the proportion of attached cross-bridges and is independent of the total number of filament pairs. This result implies that if the total stiffness of the system is measured, the stiffness of an individual cross-bridge cannot be calculated without measuring, in an independent way, the proportion of attached cross bridges. This conclusion holds for both the continuous and the discrete model. However, in the discrete model, even if the proportion of attached cross bridges is known, the number of attached cross-bridges cannot be calculated uniquely from the overall stiffness measurement, because for the discrete model the stiffness is also a function of the distribution of

attachments, unlike the continuous model which was formulated for a uniform distribution of attachments. This difference between discrete and continuous models, although irrelevant in many experimental situations, could be important for *in vitro* assays in which very few cross-bridge links are present.

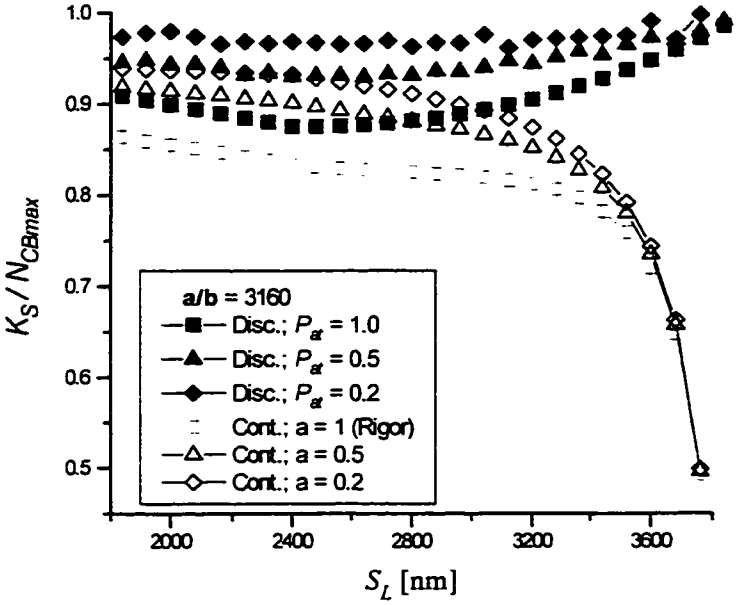

Figure 2.14: Stiffness per myosin head. Results corresponding to a parallel array of 10000 filament pairs with additional series filament shown with filled symbols for three different values of P_{at}, the probability of attachment of individual cross-bridges. Results corresponding to the continuous model are shown with hollow symbols for three different values of a, the proportion of attached cross-bridges. The ratio a/b (corresponding to rigor state) was set to 3160.

2.6.4 Comparison with Experimental Results.

Higuchi et al. (1995) measured the stiffness of the thin filament to be in the range of 45 - 67 pN/nm for a 1 μm long filament. Taking a value of 65 pN/nm per 1000 nm, the stiffness of a 40 nm long portion is $a = 1625$ pN/nm. For a single cross bridge, Nishizaka et al. (1995) reported a value for $b \approx 0.6$ pN/nm. These numbers put the ratio a/b in the order of 3000; a region in which our calculations indicate that the stiffness is not linearly related to the number of attached cross-bridges.

A comparison between our numerical results and an absolute measure of stiffness, although tempting, is premature. Other factors, such as the possibility of interaction of one thick filament with several thin filaments and the effects of the distribution of attached cross-bridges on stiffness, must be addressed. A similar approach to the one presented here can be used to study a system comprised of a myosin filament interacting with six surrounding actin filaments. Also, interactions beyond those in the immediate neighbourhood can be considered. If the distribution of cross-bridge attachments along the actin filament is not uniform, the problem still can be addressed using the approach presented here.

2.7 Discrepancies between the discrete and continuous models.

In order to show some further discrepancies between the continuous (Ford et al. 1981) and discrete models, Table 2.1 presents comparative results for the total stiffness of the overlap zone. The values shown in the table correspond to the stiffness ratios $a/c = 1$, $a/b = 3000$. This last value is likely to be physiologically relevant, as suggested by the

latest experiments by Kojima et al., 1994 and Huxley et al, 1994. The last column shows the linear variation corresponding to the limiting case $a/b \rightarrow \infty$. The values in Table 2.1 show a more or less constant difference between the discrete model stiffness for the overlap zone and that calculated using Eq. 2.24. Moreover, the continuous values seem to 'lag' the stiffness of the discrete structure by one panel.

number of panels	K_{ladder}/b discrete	K/b Ford et al 1981	K/b rigid filaments
1	2.00	1.00	2.0
2	3.00	1.99	3.0
3	3.99	2.99	4.0
4	4.98	3.98	5.0
5	5.96	4.97	6.0
6	6.94	5.95	7.0
7	7.91	6.92	8.0
8	8.87	7.88	9.0
9	9.81	8.84	10.0
10	10.75	9.78	11.0
11	11.67	10.71	12.0
12	12.58	11.62	13.0
13	13.47	12.52	14.0
14	14.35	13.41	15.0
15	15.21	14.28	16.0
16	16.06	15.14	17.0
17	16.88	15.97	18.0
18	17.69	16.79	19.0
19	18.48	17.59	20.0
20	19.25	18.37	21.0
21	20.00	19.12	22.0
22	20.72	19.86	23.0
23	21.43	20.58	24.0
24	22.12	21.28	25.0

Table 2.1: Comparison between the stiffness calculated with the discrete and continuous models for the overlap zone for an increasing number of panels (cross bridge attachments). The values shown in the table correspond to the stiffness ratios $a/c = 1$, $a/b = 3000$. The column on the right shows the values of the stiffness in the case of rigid filaments which is directly proportional to the number of cross bridges attached.

To understand this particular property of the difference, suppose for a moment that the connection between both filaments actually consists of a uniform "jelly", represented by the shaded area in Figure 2.15. If we want to model the transfer of force between filaments by the finite element method, the usual procedure is to subdivide the continuum into a number n of elements of width h, replacing the distributed stiffness of each element by one discrete spring in the middle of the element in question, shown as thick black lines in Figure 2.15. This procedure will result in a discretized structure that is shorter than the continuous one by a distance h. In our case, the discrete structure is considered to be the exact representation of the biological system; therefore, in order to have a continuum equivalent with the same stiffness, it should be longer by a distance $\approx h$, the characteristic length of a panel.

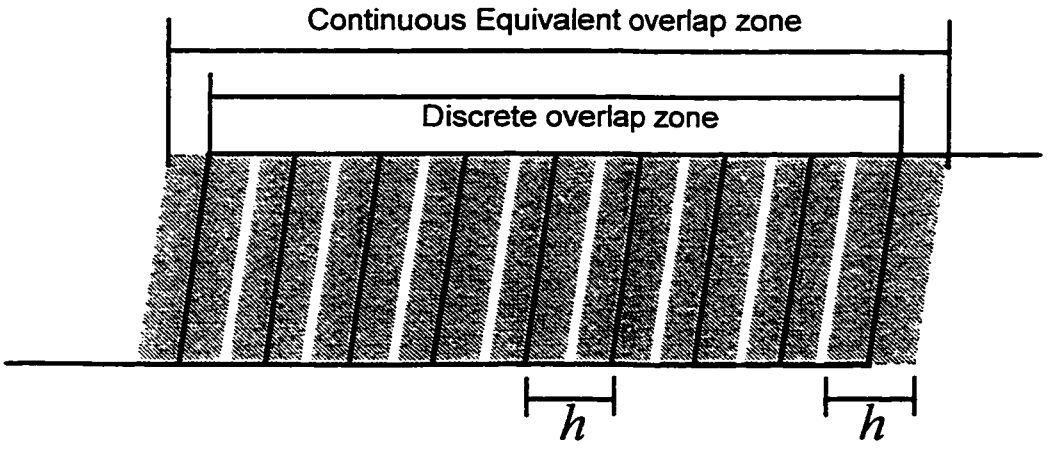

Figure 2.15: Discrete model overlap zone (thick black lines) and the continuous overlap zone of an equivalent continuous model (shaded area).

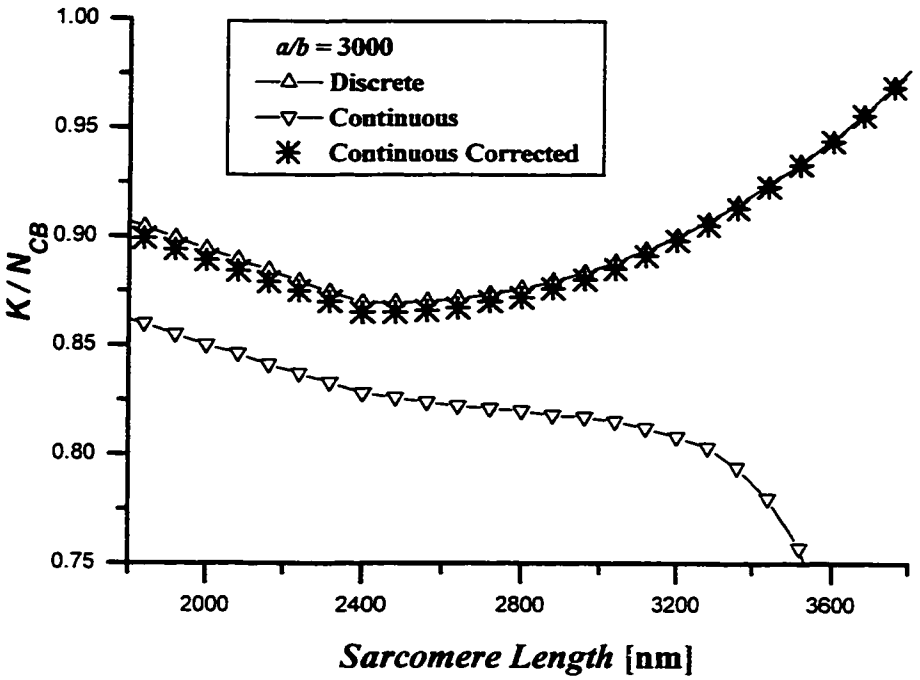

Figure 2.16: Variation of the Stiffness per Cross bridge with sarcomere length. Comparison between discrete and continuous model and 'corrected' continuous model. Parameters for the calculations are taken as: characteristic spacing between cross-bridges, h = 40 nm, length of the actin filament, L_a = 1120 nm, length of half the thick filament; L_m = 800 nm, length of the portion of half the thick filament containing cross-bridges, L_o = 720 nm, number of panels for maximum overlap, N_{max}=18, ratio a/c = 1 and ratio a/b = 3000.

In order to calculate sarcomere stiffness, we combine the stiffness of the portions of myosin and actin filaments beyond the overlap zone with the stiffness of the ladder structure using the formula for springs arranged in series. In this way, the variation of a half sarcomere stiffness with the length of the sarcomere can be calculated. Figure 2.16

shows the results of such calculations for the following parameters, chosen to approximate those of rabbit skeletal muscle: h = 40 nm, the approximate characteristic spacing between cross-bridges, L_a = 1120 nm, the length of the actin filament; L_m = 800 nm, the length of half the thick filament; and L_o = 720 nm, the length of the portion of half the thick filament containing cross-bridges. The number of panels for maximum overlap is then N_{max}=18, that is, all possible cross bridges are assumed to be attached. Ratios *a/c* and *a/b* are taken as 1 and 3000 respectively. Fig. 2.16 shows values of stiffness per cross-bridge, that is, the total stiffness of half a sarcomere divided by the number of attached cross bridges for the corresponding overlap length. Also the stiffnesses calculated by using the continuous model and the continuous model with the correction previously discussed are shown in the same graph. It must be noted that while the correction in length is applied to the overlap zone, this extra length is not deducted from the length of the filaments out of the overlap zone.

2.8 Three-dimensionality.

So far we have introduced in our model the structure of a sarcomere in a limited sense. When we consider the interaction between myofilaments, only structural effects on the longitudinal directions were accounted for. In a sarcomere, myofilaments are interconnected in a more complex way than that so far assumed by our model. Squire, 1990, and Cantino and Squire, 1986, describe the transversal arrangement of thick and thin filaments in vertebrate skeletal fibers as reducible to a repetition of a super-lattice formed by three thick filaments and six thin filaments with an orientation such that the myosin heads of each thick filament can interact with the six surrounding thin filaments.

Figure 2.17 is a three-dimensional rendering of the super-lattice described by Squire, 1990.

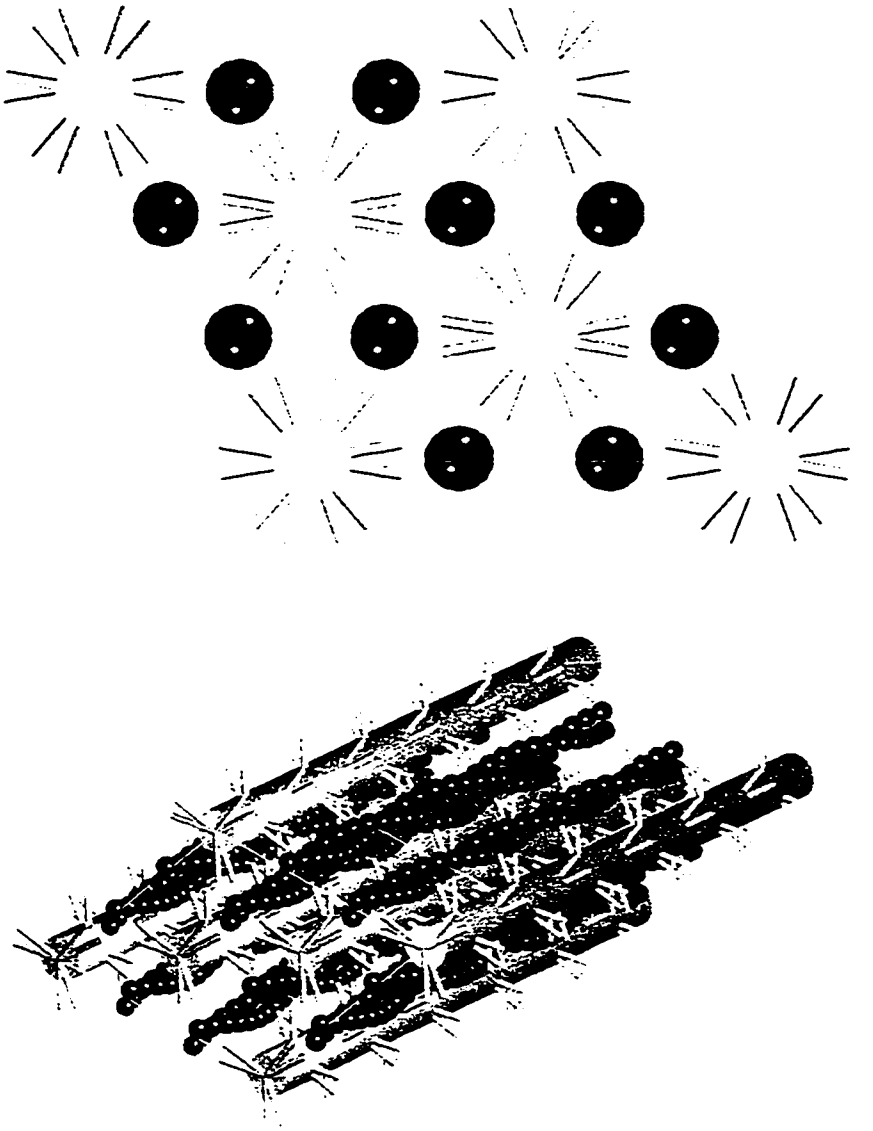

Figure 2.17: Three dimensional rendering of the super-lattice as described by Squire, 1990.

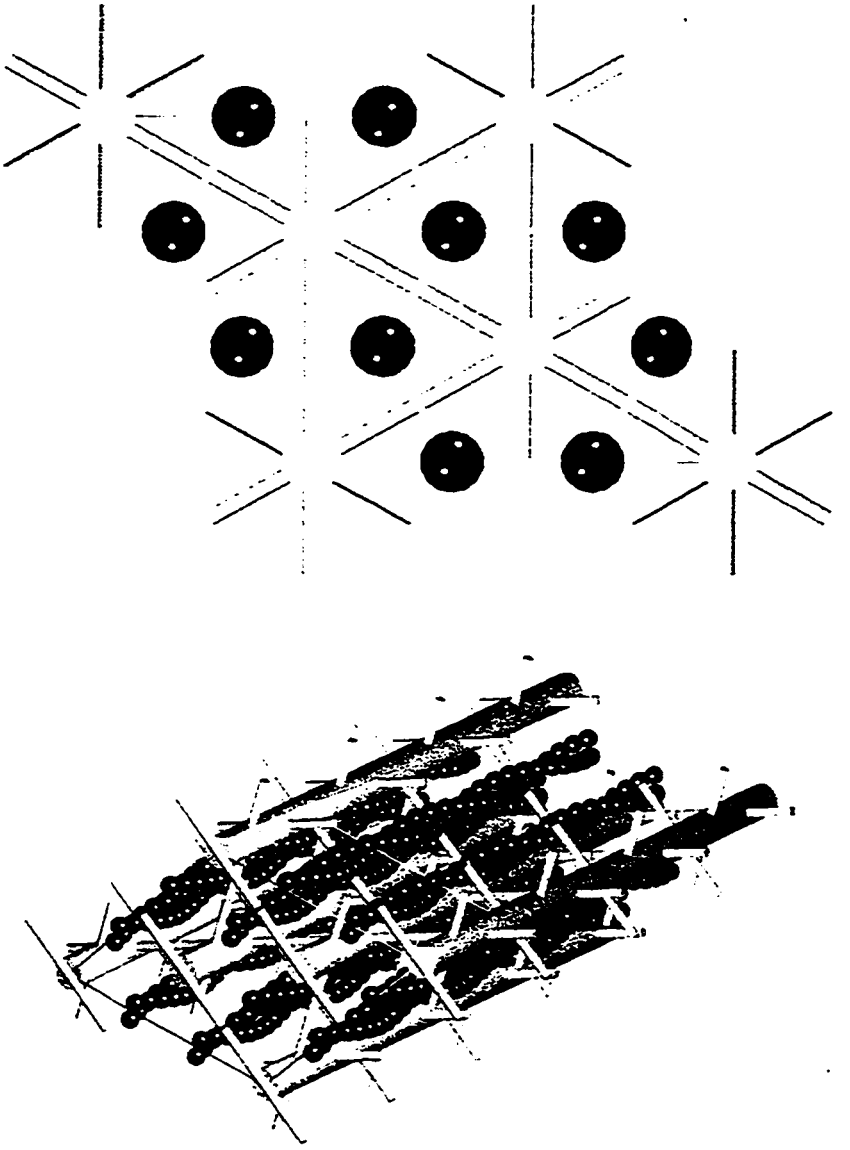

Figure 2.18: Three dimensional rendering of the arrangement of thick and thin filaments as described by Pollack, 1990.

Squire's interpretation is not the only possible interpretation that can be drawn from the existing body of experimental evidence. Pollack, 1990, has a different interpretation based on a similar pool of experimental data. A rendering of the arrangement proposed by

Pollack, 1990 is shown in Fig. 2.18. The lattice assumed by Pollack makes the functional model different from Huxley's model, in that in the former cross-bridges form between neighbouring thick filaments instead of between thick and thin filaments, the thin filaments being caged in a framework of cross-bridges and thick filaments. In Pollack's model, it is the crawling action of thin filaments against the myosin-myosin cage that brings about the contraction.

The fact that the array of thick and thin filaments form a three-dimensional structure brings two issues that were not taken into account so far: first, the stiffness in the longitudinal direction is the result of the combined movement of points in the longitudinal and radial directions, and second, the topology of the connections between filaments would have an effect on the longitudinal stiffness. In the next two sections we analyze how both issues affect stiffness calculations.

2.8.1 Longitudinal and Transversal Movements.

In the calculation of the stiffness of the ladder structure, points in either filament are restricted to move only in the longitudinal direction. In the sarcomere there is no physical structure that can impose such a restriction on the movement of filaments. If we allow the connection points of the ladder structure to displace without restriction in the transversal direction, the ladder structure will collapse to a line upon the application of any force. Some sort of restriction of the transversal movement is needed for the filaments not to collapse into the line of application of the force. In the sarcomere, the necessary transversal restriction can be provided by constraints such as the preservation of volume in the myofibril or the strain of other elastic structures, able to carry compressive loads,

associated with the filaments. The character and stiffness of the transversal restraint, will of course influence the value of the longitudinal stiffness.

Experiments conducted on skinned fibers by Xu et al., 1993 and Kawai et al., 1993 show that, upon attachment of cross-bridges, the radial spacing between filaments decreases, and the radial stiffness is not directly proportional to the axial stiffness. Note, that the cross-bridge theory predicts the proportionality between radial and axial stiffness because if the filaments are rigid, the two stiffnesses are directly proportional to the number of attached cross-bridges. The distinctive behaviour of both radial and axial stiffness is supposed to arise from structural differences in the attached states of myosin heads. To assess how the structural difference can influence the measure of stiffness, an exact model of the structure is needed. Unfortunately the required structural data are not available.

2.8.2 Topology.

The structural models presented here to calculate the stiffness rely on the assumption that one can lump the elastic properties of thick and thin filaments into two representative filaments. However X-ray diffraction and electron microscopy studies support a model in which one thick filament is connected to the six surrounding thin filaments, which in turn are connected to other thick filaments. Trying to model the complex lattice of interconnections through a discrete model accurately is a formidable task in terms of the computational resources involved. The fact that there still are unknowns and

controversies about the exact arrangement of the interconnections[8], makes the task of modelling a three dimensional lattice an futile exercise. Instead a comparatively simple model of the influence that such interconnection between filaments may have on stiffness is presented here.

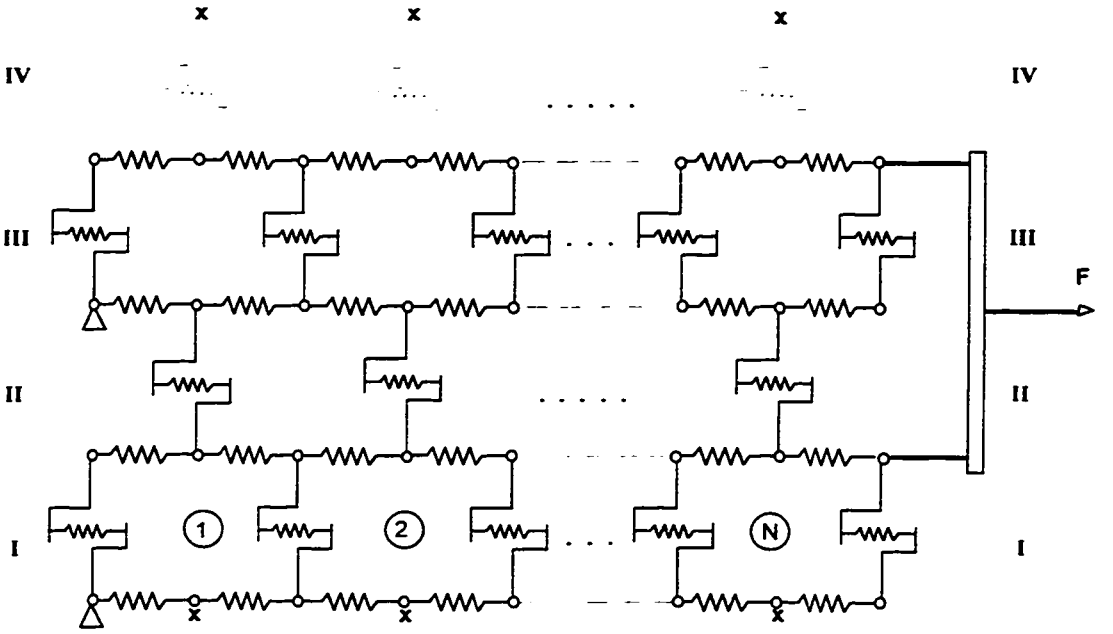

Figure 2.19: Topology of the Open and Closed Lattices. The Closed Lattice structure is obtained by adding a row of cross-links such as row IV (dashed) and connecting the points marked as 'x'

[8] For example, the model of thick filament presented in Pollack, 1990, and the one presented in Squire, 1990, differ in the number of myosin molecules by 2/3, although they are drawn from almost the same raw data.

Consider the structure represented in Fig 2.19. In it, two sets of elastic filaments, those attached to fixed points on the left and those attached to the load on the right, are interconnected by linear elastic, uni-dimensional links as shown. We considered two topologies, the 'open lattice', in which only the links in rows I, II and III exist, and the 'closed lattice', which also includes the links (shown in dotted lines) denoted as row IV which close the lattice joining the point marked by an X. Our objective was to compare the stiffness of the two lattices with respect to each other and with respect to the simple ladder structure, and to assess the effect of the connections with neighbouring filaments on the stiffness. More specifically we wanted to investigate whether or not the connection with parallel filaments will 'spread' the force sharing among filaments in such a way that the stiffness of the discrete structure will resemble more closely the stiffness of the continuum model.

The two lattices were modelled, and the corresponding stiffnesses calculated, using a standard finite element code (ANSYS) with the results shown in table 2.2 and Fig 2.20. In the table, the column '# of cells' refers to the number of cells on odd numbered rows (see figure 2.20). The numbers in this column are a measure of the overlap between the two sets of filaments. The column named '# of pairs' refers to the number of rows on the closed lattice divided by two. Notice that for open lattices with the same overlap, increasing the number of pairs has a very small influence on the stiffness per cross-bridge. Although not shown in the table, the same is true for closed lattices. It becomes apparent from the results that the cross-linking between non-consecutive filaments does not influence considerably the results obtained with the ladder structure alone for small overlaps. It is also evident that the way in which the filaments are interconnected influences the measure of stiffness, that is, the stiffness of a model with a different

number of interconnections or a different distribution of links between filaments would, in general, have a different behaviour.

2.9 Conclusions.

Based on the commonly accepted idea that interactions between actin and myosin filaments occur through cross-bridges, and the fact that only a few links can be formed between pairs of myofilaments, we developed a discrete model to calculate the stiffness of a sarcomere. The model retains the characteristic static behaviour of a sarcomere.

		Open		Closed	
# of Cells	# of pairs	K_{tot}	K/N_{cb}	K_{tot}	K/N_{cb}
1	8	23.00	1.00	24.00	1.00
4	8	67.56	0.99	71.51	0.99
7	8	110.67	0.97	117.44	0.97
11	4	77.14	0.95	—	—
11	8	164.38	0.95	174.52	0.94
11	12	251.50	0.94	—	—
14	8	200.93	0.92	213.24	0.91
17	8	233.76	0.88	247.87	0.88
20	4	123.57	0.85	139.13	0.84
23	4	135.44	0.82	152.09	0.80

Table 2.2: Stiffnesses of the open and closed lattices of ladder structures in parallel. The values shown in the table correspond to the stiffness ratios $a/c = 1$, $a/b = 3000$.

In this study, we were only concerned with calculating the order of magnitude of sarcomere stiffness. We refrained from trying to fit numerical predictions to experimental

results such as those found by Higuchi et al. (1995) and Nishizaka et al. (1995) because, as was shown here, stiffness is very sensitive to the exact configuration of the system. Unfortunately, the exact geometry of the attached cross-bridges and their connections between the myofilaments is not clearly understood at the moment. If stiffness properties of actin and myosin filaments and the cross-bridges were known through *in-vitro* experiments, a discrete model, such as the one presented here, could be used to investigate different geometries which would match the total stiffness values.

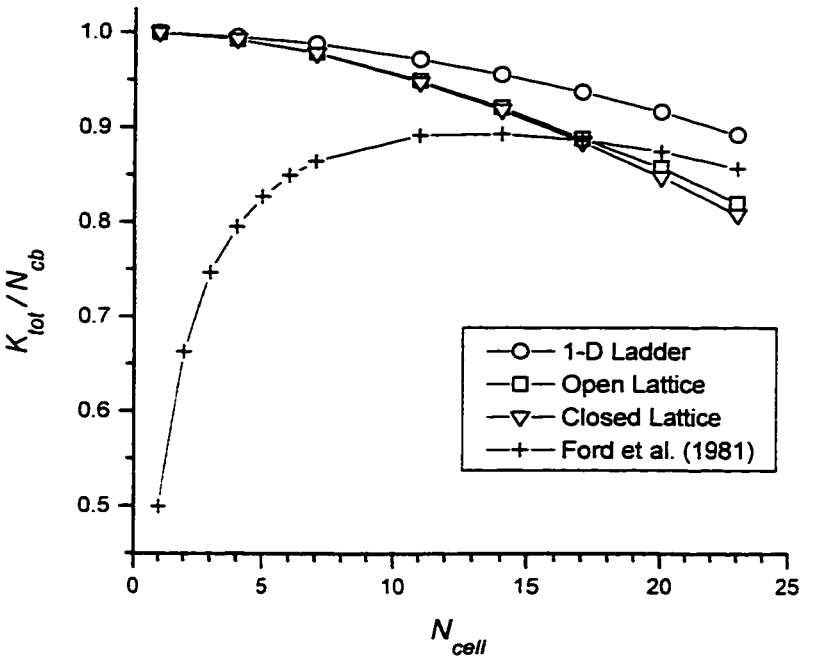

Figure 2.20: Variation of the Stiffness divided by the number of cross-bridges with the number of cells for the Open and Closed Lattices. The curve labeled '1-D Ladder' correspond to the ladder structure of Figure 2.3 and the curve labeled 'Ford et al.' correspond to the continuous solution without the correction discussed in section 2.8. .

We compared our discrete model to the continuum model developed by Ford et al. (1981). Our main conclusion was that the continuum model is not able to represent a system formed by a few links adequately. The difficulty in calculating the stiffness attributable to an individual cross-bridge without knowing the exact number of attached cross-bridges emerges, in our model, as a consequence of its sensitivity to the exact geometry of the attached cross-bridges.

Considering that, in the case of mammalian skeletal muscle, for maximum overlap only about 18 cross bridges can be formed between any given thin-thick filament pair, it follows from Table 2.1 that, for less than maximum overlap, or in the case of partial activation, the validity of the continuum hypothesis is questionable, unless the model parameters are corrected to take into account the discrete nature of the problem. Other factors which may influence the overall sarcomere stiffness are: attachment irregularities (i.e., vacancies) as well as slight differences in distances between contiguous attachment sites. A discrete model, such as the one presented here, could be used to investigate the relative importance of these factors. We have shown that the continuous model presented by Ford et al. (1981) can be used to approximate the discrete structure provided that the overlap length is corrected.

The experimental finding that actin, and possibly myosin, filaments are more compliant than first thought, is intriguing from a mechanistic point of view. Typically, it has been assumed that stiffness of tetanized, single, intact muscle fibers is nearly proportional to filament overlap (Ford et al., 1981, Huxley and Simmons, 1972) suggesting that filament compliance is negligible and that stiffness measurements can be used to determine the number of attached cross-bridges directly. However, there are instances when force (which is presumably proportional to the number of attached cross-bridges) and stiffness are not proportionally related. One such example occurs during the

onset of a tetanus when stiffness precedes force (i.e., the fibre is stiff but shows no external force), and so produces a variable relationship between stiffness and force in the early phase of muscle activation. Although it has been proposed that this observation is associated with different cross-bridge attachment states; a first state which contributes to stiffness alone and a second state which contributes to stiffness and force, this observation may possibly be explained by a nonlinear relationship between stiffness and force as proposed in the literature (Bagni et al., 1988). The non-linearity could possibly be related to the effect produced by myofilament compliance.

If myofilaments contribute to sarcomere compliance by as much as 50% (Kojima et al., 1994), cross-bridge stiffness, by necessity, would have to be much higher than assumed up to date. Recent evidence of the force produced by individual cross-bridges (~5 pN Finer et al. 1994), and the release distance which brings the force of a fully activated fibre to zero (4 to 6 nm per half sarcomere, Ford et al., 1977) suggests that cross-bridge stiffness is approximately 1.0 pN/nm. However, this stiffness value for the cross-bridge is about 2-5 times larger than those proposed in the literature which account for the kinetics of early force recovery following a quick release or stretch (Huxley and Simmons, 1971, Lombardi and Piazzesi, 1990). These larger values for cross-bridge stiffness obtained from work on isolated cross-bridges compared to the corresponding stiffness values obtained indirectly from experiment on fibres could possibly be explained by the compliance of the myofilaments.

However, apart from the mechanistic implications of force production in skeletal muscle associated with the idea of compliant myofilaments, one must ask the question how such compliance affects the whole muscle behaviour and the modelling of whole muscle. This is a difficult question, and at the moment, cannot be answered conclusively. To relate myofilament compliance to the two most frequent models of muscle, i.e., the

Hill model and the cross-bridge model, several factors should be considered. For example, one of the drawbacks of any Hill-type model aimed at representing the actual structures of skeletal muscle (that is, a contractile element associated with the sarcomere and a series elastic element associated with the tendon) is that the length changes and force distribution among the rheological elements of the model are hard to obtain. Myofilament compliance is yet another elastic element arranged in series with the force-producing cross-bridges, and therefore will make interpretations derived from Hill-type muscle models even more difficult than they are when assuming rigid myofilaments.

For cross-bridge models, myofilament compliance has one very direct modelling implication. So far, with the exception of one cross-bridge model by Mijailovich et al., 1996, it has always been assumed that the relative speed of fixed points on the thick and thin myofilament are linearly related to the shortening speed of the sarcomere. With the myofilaments being compliant, this strict relationship between sarcomere shortening speed and the relative speed of fixed points on the myofilaments does not exist anymore.

Summarizing, the recently discovered compliant properties of myofilaments have important implications for interpreting muscle mechanical tests on the sarcomere or fibre level. Furthermore, myofilament compliance should be considered in cross-bridge models and should be accounted for in the series elasticity of Hill-type models. Stiffness testing with the aim of deriving the number of attached cross-bridges must be made by accounting for myofilament compliance.

We have shown that it is possible to construct a model which can account for variables such as the elasticity of myofilaments and individual cross-bridges. On such a basis, and counting on the increasing sophistication in performing *in vitro* experiments on individual molecules, future discrete models of sarcomeres are a viable tool to help in the understanding of muscle function.

III

Muscle as an Engineering Material

As we saw in the previous chapter, skeletal muscle has a very complex structure at any level of description. This structural complexity results in a mechanical behaviour that is far more complex than the usual behaviour exhibited by standard engineering materials.

We mentioned in chapter II that the available structural knowledge on muscle is, to say the least, incomplete. This uncertainty in structural arrangements prevents us from formulating a theory that, based on a model of molecular events, can be used to predict the outcome of experiments on the macroscopic level. In studying the dynamics of animal movement, the mechanical characteristics of entire muscles or groups of muscles are needed in order to predict the forces acting on the body segments. At that level of description, it is sufficient to have a global model of muscle function that, given the position of its ends and the activation state[1], is capable of predicting the force and the energy expenditure. Such models have existed for a long time and are often used in biomechanics. In this chapter we will discuss critically the most widely used type of model, that is, Hill type models, and present an alternative model developed to address certain aspects of muscle behaviour, such as force enhancement and force depression, that are presently ignored by Hill type models. Other problems such as the non-commutativity of the response to activation, will be briefly discussed towards the end of the chapter.

[1]In the sense of an internal parameter related in some way to the myoelectric activity or control signal sent by the nervous system.

3.1 Pseudo-Rheological Muscle Models

Systematic measurements of the mechanical characteristics of entire muscles and fibers are being conducted since the last decades of the XIX-th century. In 1938, from thermal and mechanical measurements, A. V. Hill concluded that the relation between isotonic force and shortening velocity for a tetanized muscle has the form (Hill, 1938):

$$(F+a)(v+b)=constant \tag{3.1}$$

where F is the force, v the shortening velocity and a and b the characteristic muscle constants. By the time A.V. Hill set forth this famous hyperbolic force-velocity relation, it was already well known that "the force exerted by a muscle decreases as the speed of shortening increases" (Gasser and Hill, 1924), however Hill also showed that it is possible to derive the correct force-velocity relation from thermodynamical arguments. From there, it was possible to infer that the energy of a chemical reaction was being used to drive contraction years before the discovery of the hydrolysis of ATP as the energy source for muscle contraction. The real value of Hill's equation lies in that its shape was verified experimentally by many researchers in many different experiments and, since its discovery, equation 3.1 has been used as the paradigmatic constitutive equation for shortening muscle. It is worth mentioning here that Eq. 3.1 is not a proper constitutive relation for muscle dynamics. To see why, let us analyze how the experimental data were obtained. Hill's experiments proceed as follows: a muscle is tetanized and held isometrically until it develops the maximal force. Then a lever instantaneously switches the load holding the muscle to a lower than isometric load, and the 'steady state' shortening speed is measured from length vs. time records. This procedure is repeated several times for different loads. Each experiment is plotted as a point in the load-shortening speed plane, resulting in the hyperbola 3.1. Confirmation of the results

obtained by Hill in 1938, obtained by using an electromagnetic puller, was reported by Edman, 1979. To measure the maximum speed of shortening, that is the shortening speed of the unloaded muscle, Edman performed experiments in which the muscle was held isometrically and suddenly shortened by a controlled distance. The time that the muscle takes to recover the slack was recorded and the maximum speed of shortening was calculated as the shortened distance divided by the time. The maximum speed of shortening measured in this way fits remarkably well with the value extrapolated (using Hill's hyperbola) from points obtained by clamping the load with the puller. Later in 1986, Edman, used a puller to confirm the hyperbolic shape of the force-velocity curve, although this time he found that the best fit was obtained using two different hyperbolic functions; one covering the range from 0 to 78% of the maximal isometric force, another covering the range from 78% to the maximal isometric force.

Despite the different techniques, and the marginally different results, all force-velocity curves were obtained 'statically'. Static refers to the idea that each point on the curve was obtained from a particular experiment in which a steady state situation was attained. Therefore, a muscle that is shortening at a varying velocity will not follow a path on the static force-velocity relationship.

Similarly, the force-length relation found by Gordon et al., 1966 can be thought of as a static relation. In this case the curve is obtained by plotting the isometric force obtained when a muscle is maximally activated at a constrained length. Figure 3.1 schematically shows the resulting curves for both, isotonic and isometric experiments. The axes in which the isotonic curve was plotted is such that stretching velocities are positive and shortening velocities are negative. Note that the stretching branch of the curve is not a continuation of the shortening hyperbola. In this region it is very difficult to obtain experimental values because the muscle yields and it is very difficult to measure the force accurately.

The isometric force-length curve exhibits a flat region called 'plateau' in which the force is the same for different lengths within a narrow zone around the relaxed, or slack length of the muscle. The curve labeled 'Active' in Fig 3.1 is obtained by subtracting the passive force, that is, the resistance provided by elastic structures formed by connective tissue, from the total force, labeled 'Active + Passive' in the figure. Active force is the force provided by the contractile machinery and the decreasing, linear relationship agrees well with the predictions based on the cross-bridge theory (Gordon et al., 1966).

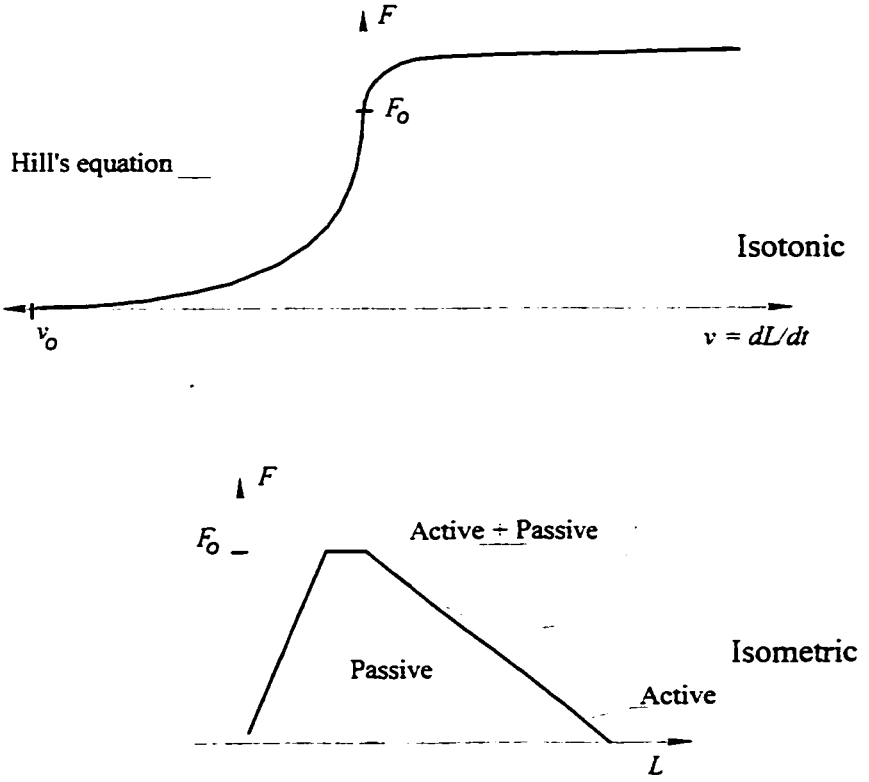

Figure 3.1: Isotonic and Isometric static curves for muscle

In his 1938 classic paper, A. V. Hill stated that muscle behaves as if it were composed of a contractile element that shortens upon activation, arranged in series with an elastic element. In Hill's model, the contractile element is endowed with the

characteristic equation derived from isotonic release experiments. The simplest way to construct a model of muscle based in the above mentioned static curves, is to attach a spring (*SEE*), to a contractile element (*CE*) endowed with the characteristic force-velocity and active force-length relation. Figure 3.2 shows a representation of such a model. The lengths L_{CE} and L_{SEE} have no obvious physical meaning except that they are constrained by the relation $L_{CE} + L_{SEE} = L_{MT}$, where L_{MT} is the total length of the muscle. The initial length of the series elastic element can be determined form the initial condition and the static equilibrium given by $F = F_{CE} = F_{SEE}$. Note, that the series elastic element is not related to the passive force curve depicted in Figure 3.1. The passive force is associated with an elastic element in parallel with the contractile element. The model described in Figure 3.2, which does not have a parallel elastic element, works because the length L_{CE} is an internal variable[2] that compensates for the lack of the parallel element.

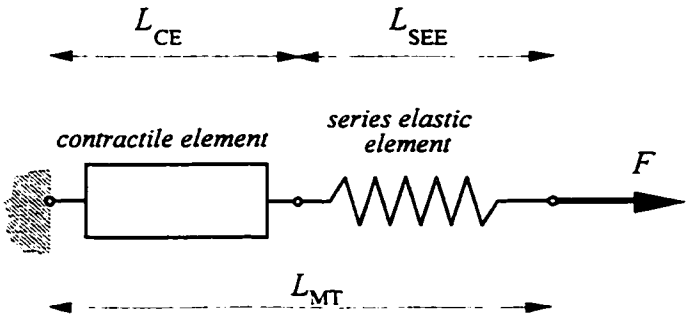

Figure 3.2: Hill's two element muscle model.

It is common practice to assume the constitutive equation for the force exerted by the contractile element as:

$$F_{CE}(L_{CE}, v_{CE}) = F_O \cdot \hat{M}(L_{CE}) \cdot \hat{T}(v_{CE}) \tag{3.2}$$

[2] This is the reason why we called this type of models 'pseudo-rheological'.

where $\hat{M}(\cdot),\hat{T}(\cdot)$ are respectively the dimensionless forms of the isometric and isotonic functions given by the curves in fig 3.1, and Fo is the maximal isometric force. $\hat{M}(\cdot),\hat{T}(\cdot)$ are dependent on two parameters that carry information on how the values of static curves change for different muscles. $v_{CE} = \frac{d}{dt} L_{CE}$ is the contraction velocity of the contractile element. As the functions $\hat{M}$ and $\hat{T}$ are usually measured under maximal activation conditions, 3.2 is multiplied by a coefficient between 0 and 1 to account for partial activation.

Over the years, this simple model was modified by adding linear elastic or viscous elements in parallel or in series with the contractile element and by using non-linear elastic elements to accommodate experimental findings into the phenomenological theory. None of these models, however, can account for what are called memory-dependent phenomena, such as force depression following shortening or force enhancement following stretch. Also, Hill-type models are not good at simulating single twitches. Furthermore, when Hill's model is used together with the force-length relation for sarcomere lengths beyond the optimal length, the simulation becomes numerically unstable because of the negative slope of the force-length relation in this range. Despite these shortcomings, Hill's model has dominated the field of muscle biomechanics because it is simple and readily applicable to many situations.

Our intention here is to formulate a phenomenological model which, on the one hand, is able to represent the so-called memory-dependent phenomena and, on the other hand, remains tractable. The formulation of such a model offers a simpler alternative to phenomenological models based on the concept of fading memory (Fung, 1993). In general, we consider phenomenological models as workable alternatives to those based on biophysical explanations of muscle contraction (Huxley, 1957, Huxley and Simmons, 1971, Mijailovich et al., 1996), and those that are mathematical approximations of

biophysical models (Zahalak, 1990, Zahalak and Ma, 1990 Zahalak and Motabarzadeh 1997), which are computationally much more complex than Hill's model.

Gasser and Hill (1924) characterized the mechanical response of activated muscle as that of a viscoelastic material. Later, in his 1938 manuscript, Hill disregarded the 1924 viscoelastic model on the basis of thermal measurements. He reasoned that a viscous component (if any was present) should release approximately the same amount of heat during shortening as during lengthening, contrary to the experimental evidence coming from his own heat measurements. Hill deduced that a chemical reaction must be responsible for most of the heat and mechanical work produced by the contracting muscle, as was later shown by biochemical experiments (see chapter 4 of Woledge et al. 1985 for an overview of the relevant experiments). However, a system undergoing chemical reactions with rate constants that vary with muscle length and speed of shortening may exhibit a behaviour similar to a non-linear viscoelastic material. This viscoelastic behaviour is a product of the chemical reactions between filaments, the characteristics of the internal structure, and the material properties of myofilaments which are not included in the model but are represented by a combination of dashpots and springs.

3.2 A Phenomenological Model of Muscle

Our starting point in the construction of a phenomenological model is the reinterpretation of the two basic experiments: isometric and isotonic contractions. It is obvious that the force-length relation established by Gordon, Huxley and Julian (1966) cannot be directly related to the dynamical behaviour of muscle, as has been assumed in many phenomenological muscle models. In force-length experiments, the isometric force

for a given length will be reached *if and only if* the muscle is held at a constant length throughout the entire contraction. If a length change is imposed once the muscle has been activated, the force will not follow the force-length relation. Moreover, if after a change in length the original length is restored, the isometric force following the length change will not be the same as the force obtained during an entirely isometric contraction at the original length. Therefore, we will consider the isometric force-length relation as a fundamental, static characteristic of muscle, while requiring that the isotonic force-velocity relation arise as a consequence of the model instead of being introduced as a characteristic of the contractile element. It should be pointed out here that this specific consideration is in direct contrast with typical Hill-type models in which the force-velocity relationship is introduced as part of the behaviour of the contractile element.

The model presented here is built around a contractile element and an elastic rack with the following properties:

Contractile element: Upon activation, the contractile element, represented in Fig. 3.3, will provide a force f. Let the dependence of f with time be governed by the equation:

$$f + \beta \cdot \dot{f} = g(t) \tag{3.3}$$

where β is a material coefficient, and $g(t)$ is a forcing function that we will loosely call activation. This activation function can be associated in some way to the intracellular concentration of Ca^{++} (Fig. 3.4). We assume that the force develops from zero to its saturation value $f(L_o)$ which depends only on the muscle length, L_o. For the sake of simplicity, saturation time may be set to zero, so that the free force development is instantaneous and the saturation force remains at $f(L_o)$ until the activation is reduced or stopped. This thinking is tantamount to assuming that $\beta = 0$ in Eq. 3.3. The function $f(L_o)$ can be identified with the isometric, fully activated force-length relation. Note that this is

the simplest possible model of force generation; a more realistic contractile element would include some dependence of the force on the instantaneous length.

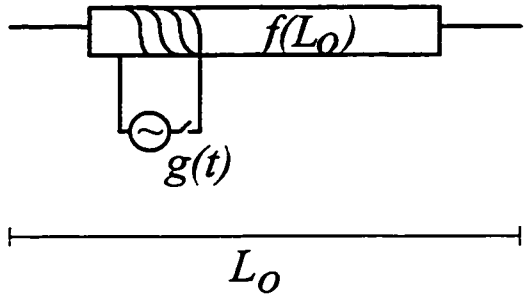

Figure 3.3: Representation of the contractile element.

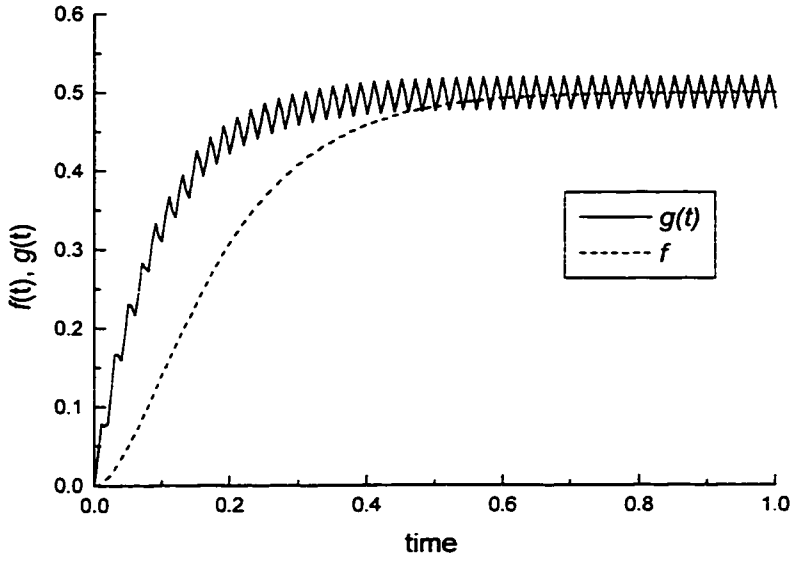

Figure 3.4: Solution of Eq 3.3 for a forcing function consisting of a periodic function with saturation.

Elastic rack: Experiment on force depression following shortening contractions (Granzier and Pollack, 1989, Sugi and Tsuchiya, 1988, Abbott and Aubert, 1952, Maréchal and Plaghki, 1979, Herzog and Leonard, 1997) suggest that the force

depression is approximately proportional to the amount of shortening experienced by the muscle, as if an elastic element were acting in parallel with the contractile element. This parallel elastic element seems to be 'recruited' (Edman and Tsuchiya, 1996) only when muscle is activated. This property of activated muscle can be modeled using an 'elastic rack', shown schematically in Fig. 3.5. When the muscle is activated, a relay engages the elastic rack. Thus, the effective stiffness of the muscle is increased upon activation. If a linear elastic material is assumed for the rack, the stiffness of the rack decreases linearly with increasing initial length L_o. Indeed, if A denotes the cross-sectional area of the rack and E stands for the modulus of elasticity, the effective stiffness of the rack is EA/L_o. It is, of course, possible to conceive a rack whose stiffness increases with L_o or remains constant; however, the cross-bridge theory indicates that stiffness must decrease with increasing length, at least for sarcomere lengths greater than optimal (Ford et al., 1981, Forcinito et al., 1997a). Although the experimental evidence indicates that force enhancement upon stretching is a phenomenon of a somewhat different nature, here we will use the same rack element to model stretches as well. In a general model, the elasticity need not be linear and the strength of the engagement need not be infinite. Depending on the net force acting on the rack and the direction of its force (tension or compression), the engagement between rack and "muscle" could be broken allowing the free relative movement of the end pieces.

Fig. 3.6 shows the proposed model consisting of a combination of the contractile element, the elastic rack and a dashpot and spring arranged in parallel to the contractile element. The motion of such a system is governed by the following system of ordinary differential equations:

$$F = f(t, L_o) + \frac{EA}{L_o} x + (1+\frac{EA}{kL_o})\, c\dot{x} \qquad (3.4)$$

$$L = L_o + x + \frac{c}{k}\dot{x} \tag{3.5}$$

where c is the dashpot constant, k the spring elastic constant, and a superimposed dot denotes the first time derivative. The physical meaning of x is the elongation of the dashpot from its rest position (the length L_o, before the activation is applied).

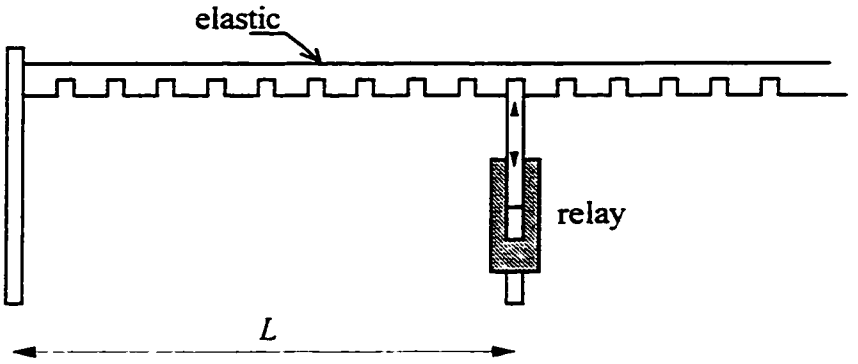

Figure 3.5: Rack element representation.

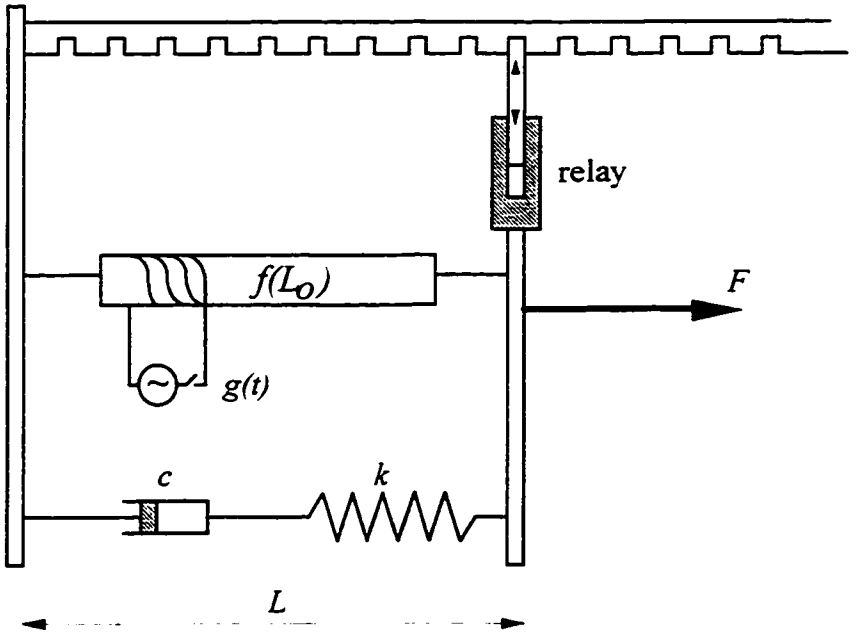

Figure 3.6: Rheological model representation.

3.2.1 Hill-type model

For the purpose of comparison, we will use the standard Hill-type model as depicted in Fig. 3.2, which consists of a contractile element that follows a single-state equation $\dot{L}_{CE} = h[L_{CE}(t), L_{MT}(t)]$ and a series elastic element. In this model the force is given by:

$$F_{CE} = F_{SEE} = \frac{F_{MAX}}{(U_{MAX} L_{SLACK})^2}(L_{SEE} - L_{SLACK})^2 \tag{3.6}$$

where F_{MAX} is the maximal isometric force, L_{SLACK} and U_{MAX} are the resting length and the strain at maximal isometric force of the series elastic element and $L_{SEE} = L_{MT} - L_{CE}$. Here, shortening of the contractile element is governed by Hill's (1938) characteristic equation, and lengthening is defined in the same way as used by Cole et al. (1996). Therefore:

$$h = \begin{cases} -\dfrac{b(F_{LEN} - F_{CE}/F_{MAX})}{(F_{CE}/F_{MAX} + a/F_{MAX})} & \text{if } \dot{L}_{MT} \le 0 \\ -L_{CE(OPT)}\left[\dfrac{c_1}{F_{CE}/F_{MAX} + c_2} + c_3\right] & \text{if } \dot{L}_{MT} > 0 \end{cases} \tag{3.7}$$

where a and b are the characteristic muscle constants, and, as defined by Cole et al. (1996), $c_1 = \dfrac{B_{REL} F_{LEN}^2 (1 - F_{ASYMP})^2}{SF(F_{LEN} + A_{REL})}$, $c_2 = -F_{LEN} F_{ASYMP}$, $c_3 = -\dfrac{B_{REL} F_{LEN}(1 - F_{ASYMP})}{SF(F_{LEN} + A_{REL})}$. The ratio of the isometric force at a given length to the maximal isometric force, F_{LEN} is a function of the contractile element length and the optimal contractile element length $L_{CE(OPT)}$. The shape of this function was adapted from Fig. 2(b) in Herzog et al. (1992). For concentric contractions, it was assumed that $a / F_{MAX} = b / V_0 = 0.25$. For cat soleus,

the maximal shortening velocity V_0 is taken to be 180 mm/s. Table 3.1 shows the numerical values of all parameters used in the calculations.

$L_{CE(OPT)}$ [m]	F_{ASYMP} *	SF *	A_{REL} *	B_{REL} *	U_{MAX} *	L_{SLACK} [m]	b [m/s]
0.03257	2.3	1.5	0.23	1.65	0.055	0.041	0.045

* Dimensionless

Table 3.1: Parameters used for Hill's model.

3.3 Results.

The response of the proposed model was analyzed using different conditions which are often encountered in experiments. In the next section the results are compared to experimental results and the standard Hill-type model presented in the previous section (Cole et al., 1996).

3.3.1 Quick change in length

When the length of an isometrically contracting muscle is quickly changed, the force exerted by the muscle also changes quickly, and then recovers slowly to a value different from that of the isometric force of the muscle at the final length. A lengthening will produce, after a short transient response, a steady-state force higher than the isometric force obtained at the final length (force enhancement). On the other hand, a shortening

will produce a steady-state force lower than the corresponding isometric force at the final length (force depression). In order to obtain the response of the model to a quick length change in the muscle, we impose an instantaneous length change from L_o to L_f at time $t = 0$. Solving Eq 3.5 for L, x is obtained (with zero initial conditions) as:

$$x = L_f - L_O - \left(L_f - L_O\right) \cdot e^{-\frac{k}{c}t} \tag{3.8}$$

Upon substitution into Eq 3.4, one obtains:

$$F = f(L_O) + \frac{EA}{L_O}\left(L_f - L_O\right)\left(1 - e^{-\frac{k}{c}t}\right) + \left(1 + \frac{EA}{kL_O}\right)\left(L_f - L_O\right) \cdot e^{-\frac{k}{c}t} \tag{3.9}$$

which corresponds to an exponential decay of the force to a force different from the original isometric force. For large values of time, t, Eq. 3.9 gives a steady-state force:

$$F_\infty = f(L_O) + \frac{EA}{L_O}\left(L_f - L_O\right) \tag{3.10}$$

that is, the change in force is a function of the total length change.

3.3.2 Quick change in Force

If the force of an isometrically contracting muscle is quickly changed to a lower value than the isometric force, the muscle will shorten isotonically. Substituting the force step into Eq 3.4 and solving for the internal variable x, one obtains:

$$x = \left(F_f - f(L_O)\right)\frac{L_O}{EA}\left(1 - e^{-\frac{EA}{c\left(L_O - EA/k\right)}t}\right) \tag{3.11}$$

after substitution of Eq 3.11 into Eq 3.5, one obtains:

$$L = L_O + \left(F_f - f(L_O)\right)\frac{L_O}{EA}\left(1 - \frac{e^{\frac{EA}{c\left(L_O - EA/k\right)}t}}{1 + \frac{EA}{kL_O}}\right) \tag{3.12}$$

$$\dot{L} = \frac{F_f - f(L_O)}{c\cdot\left(1 + \frac{EA}{kL_O}\right)^2} e^{\frac{EA}{c\left(L_O - EA/k\right)}t} \tag{3.13}$$

$$\left.\frac{dL}{dt}\right|_{0^+} = \frac{F_f - f(L_O)}{c\cdot\left(1 + \frac{EA}{kL_O}\right)^2} \tag{3.14}$$

Equation 3.14 represents a "linear" force-velocity relation. In order to fit the experimental results, one would have to introduce a material non-linearity in the constitutive behaviour of one or more of the four elements which make up the muscle model. Note, that the denominator in equation 3.14 represents a viscosity coefficient relating the *excess* force to the velocity. Here, the velocity is defined positive for stretching and negative for shortening.

Finally, after a very long time, the steady-state length, L_∞, becomes :

$$L_\infty = L_O\left(\frac{F_f - f(L_O)}{EA}\right) \tag{3.15}$$

$$\left.\frac{dL}{dt}\right|_\infty = 0 \tag{3.16}$$

In this model (with linear springs and a dashpot) Hill's (1938) force-velocity relationship will be satisfied (qualitatively, at least) between the (isotonic) force and the initial velocity upon release. If, however, the rack element is disengaged during the isotonic experiment, the velocity will remain constant in time. As suggested by

experimental evidence, (Granzier and Pollack, 1989) an isotonically contracting muscle will shorten at a constant speed or with a decreasing speed depending on the length step and the length of the muscle upon release.

For short length steps, experimental evidence suggests that the speed of contraction is constant (Hill 1938, Granzier and Pollack 1989, Edman and Tsuchiya, 1996). A constant speed of contraction for a short period after release can be well matched by an exponential function. In the present model, a constant speed of contraction can be achieved by temporarily disconnecting the rack element.

The conceptual difference between the present model and that developed by Hill (1938) is that the force-velocity characteristic is a consequence of the elements in the model while Hill (1938) assigned the force-velocity characteristic to the contractile element.

3.3.3 Constant Speed of Shortening or Stretching

When an isometrically contracting muscle is shortened (or stretched) at a constant velocity, α, during a period of time, τ, and held isometrically at some final length, the force exerted by the muscle decreases (increases), reaches a minimum (maximum) value and stabilizes at a lower (higher) force than the corresponding isometric value at the final length. This phenomenon is known as force depression or force enhancement following shortening or lengthening, respectively (Abbott and Aubert, 1952, Maréchal and Plaghki, 1979, Granzier and Pollack, 1989, Herzog, and Leonard, 1997, Edman and Tsuchiya, 1996). A Hill-type model is not able to predict these force depressions or force enhancements, because when the speed of contraction is zero, the force in the contractile element will be dictated by the force-length relation exclusively which is derived from

isometric experiments alone. If the final length of a contraction is on the descending limb of the force-length relation, Hill-type models will become unstable because of the negative slope of the associated force-length curve.

For the case of a constant speed of contraction, the length is a known function of time, *L(t)*, and the force predicted by the present model can be calculated by inserting *L(t)* as the left member of Eq 3.5. It is useful, in order to simplify the resulting expressions, to introduce a 'step' function defined by:

$$u_a(t) = \begin{cases} 0 \; if \; t < a \\ 1 \; if \; t \geq a \end{cases} \tag{3.17}$$

Using the definition given by equation 3.16, the muscle length corresponding to shortening at a constant speed, α, starting at t = 0 and finishing at $t = \tau$, can be described by: $L(t) = L_O + \alpha[t - (t-\tau)\cdot u_\tau(t)]$. Substituting *L(t)* into 3.5 and solving for x, one obtains:

$$x = \alpha\left[\frac{c}{k}(u_\tau - 1) + t(1-u_\tau) + \frac{c}{k}\left(1 - u_\tau \cdot e^{\frac{k}{c}\tau}\right)e^{-\frac{k}{c}t} + \tau \cdot u_\tau\right] \tag{3.18}$$

$$\dot{x} = \alpha\left[(1-u_\tau) - \left(1 - u_\tau \cdot e^{\frac{k}{c}\tau}\right)e^{-\frac{k}{c}t}\right] \tag{3.19}$$

which can be inserted in Eq 3.4, to obtain the corresponding force as a function of time.

3.3.4 Comparison with Experimental Results.

In order to test the predictive ability of the present model, the results of the model were compared with selected experimental results.

Quick force release: The present model predicts that the velocity of shortening is an exponentially decaying function in time and that the muscle will eventually stop shortening. These predictions seem to contradict what is known as one of the principal characteristics of shortening muscle under constant load: the constancy of the shortening speed. We have not found convincing experimental evidence of constancy of speed of shortening during isotonic contractions. At any rate, it is physically obvious that the shortening speed cannot remain constant for a long period of time. Consider the experiments performed by Granzier and Pollack (1989). In Fig 3, 4 and 5 of their paper, records of fiber length and force as a function of time for different shortening distances are shown. In all cases, there is a noticeable decrease of the shortening velocity in time. However, this behaviour was not observed at the sarcomere level. Edman and Reggiani (1983) showed that small sections of muscle can lengthen while the entire muscle is shortening. These differences in length change observed on the entire muscle and on the sarcomere level indicate that the behaviour of the entire muscle could be a product of the structural arrangement between fibers and the non-uniformity of sarcomere lengths rather than a characteristic of the contractile machinery.

In their 1966 paper, Gordon Huxley and Julian show records of an isotonic contraction that goes towards a steady length (Fig. 8B in their paper). Podolsky (1960) carefully measured the transient fiber length changes after a muscle was released isotonically. The length records exhibited an almost perfectly constant slope after the transient phase of shortening, but they only showed the first 10-20 ms following release. If the time constant of the exponential is large enough, the behaviour of a model in which the speed of contraction decreases exponentially can look as if it had a constant velocity of shortening when followed for only a few milliseconds. Nonetheless, it is generally accepted that isotonic force and shortening velocity follow Hill's (1938) characteristic

equation. The characteristic equation for the present model with constant parameters *EA*. *k* and *c* is a straight line given by Eq. 3.14 (Fig 3.7).

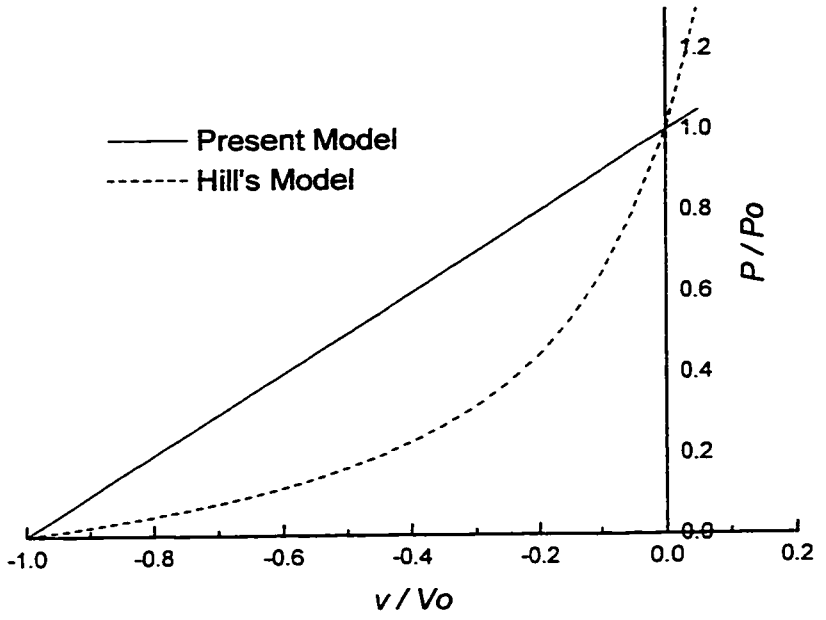

Figure 3.7: Characteristic curve for the present model with constant coefficients compared to the characteristic force-velocity curve $(P+a)(v+b) = constant$ **with** $a / P_0 = b / V_0 = 0.25.$

Active shortening at constant speed: The present model was used to match experimental data from an *in situ* preparation of cat soleus muscle (Herzog and Leonard, 1997). In these experiments, soleus muscle and tendon were surgically exposed and the distal end of the tendon was cut from its insertion with a remnant piece of bone. The hind limb of the cat was fixed rigidly in a stereotaxic frame and the end of the tendon was attached to a muscle puller. An electrode implanted on the tibial nerve was used to stimulate the muscle. The muscle was passively stretched to the initial length, activated supramaximally until the isometric force was fully developed, then the muscle was

allowed to shorten 4 mm at a constant speed, and subsequently was held isometrically at this final length while the activation was maintained. In order to fit the experimental results, it was necessary to determine the three constants EA, k and c. First EA was determined using Eq. 3.10 as the asymptotic solution after the shortening was completed, then k and c were adjusted to match the peak value of the force (at the end of shortening), and the force corresponding to the point at which half the total shortening was performed. Fig 3.8 shows the resulting fit for shortening speeds of -8 mm/s and -20 mm/s. The constants were obtained for the -8 mm/s trial and were used for both, the -8 mm/s and the -20 mm/s trials.

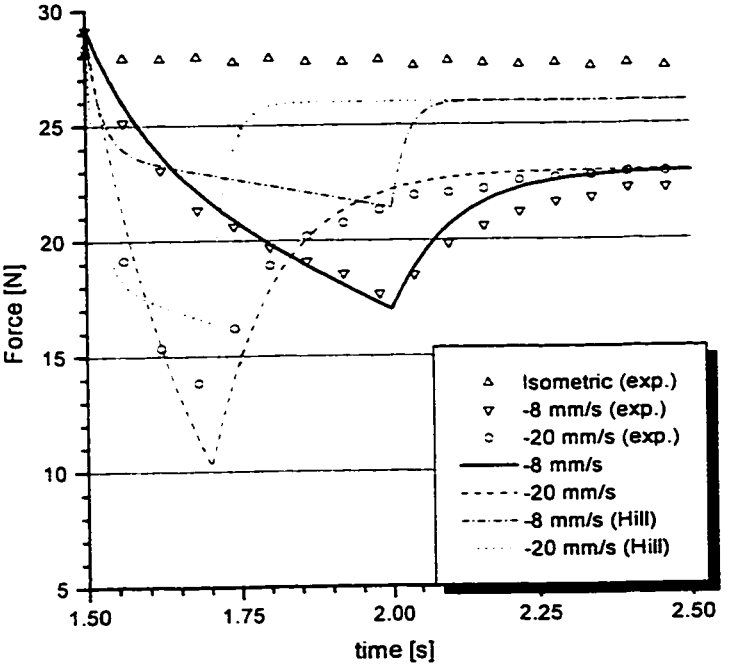

Figure 3.8: Shortening at constant speed: comparison between experimental results, the present model and Hill's model. The points labeled isometric correspond to the isometric force at final length. The values of the constant used (adjusted for -8mm/s) were $EA = 1.575 \cdot L_O$ N, $k = 7.0$ N/mm and $c = 0.757$ N·s/mm. Hill's model parameters were those listed in Table 3.1.

Using the same constants, the maximal speed of shortening was determined to be $V_0 = 90.7$ mm/s.

Active lengthening at constant speed: The same procedure as applied to the shortening contractions was used to fit the lengthening contractions. The results are shown in Fig 3.9. For lengthening, a different value for the constant EA was used because the magnitude of force enhancement following active lengthening is different from that of the force depression following active shortening. Fig. 3.9 also shows the force-time history calculated using Hill's (1938) model as described by Cole et al. (1996).

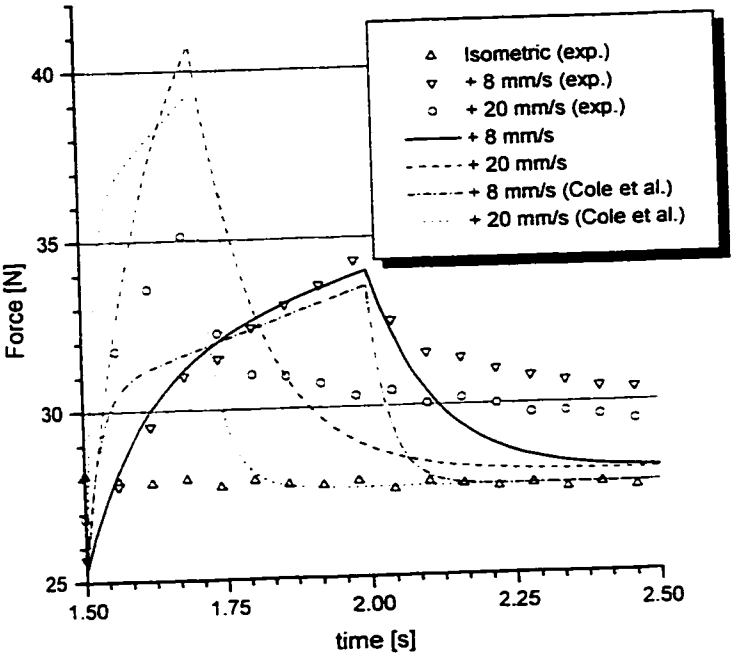

Figure 3.9: Lengthening at constant speed: comparison between experimental results, the present model and Hill's model. The points labeled isometric correspond to the isometric force at the final length. The values of the constants used (adjusted for +8mm/s) were $EA = 0.675 \cdot L_0$ N, $k = 7.0$ N/mm and $c = 0.757$ N·s/mm. Hill's model parameters were those listed in Table 3.1.

3.3 Critical Analysis of the present model.

Contractile element: A linear model of the contractile element, such as the one represented by 3.3, will not be adequate to represent the experimental force response of a muscle if the signal *g(t)* is associated with an electrical stimulation because Equation 3.3 implies the linear sum of effects. Experimental evidence shows that when two electrical pulses are given to a muscle with a short inter-pulse interval, the response is more than two times larger than that of a single pulse (figure 3.10). In a simple model presented by Bobet and Stein, 1996, a static non-linearity is needed in the transfer function between stimulation and force to represent the potentiation effect of a double electric pulse adequately. Looking at the response of this simple equation to a square pulse or a triangular pulse (Figure 3.11 left and right, respectively) we can see that the solutions do not correspond with the response of a muscle to a single stimulation pulse (twitch). A twitch starts with zero slope and positive curvature, has an inflexion point and then reaches the maximum before a second change in curvature. It is easy to show that the solution of equation 3.3, for the case in which *g(t)* is a triangular function is not exactly as the twitch. Therefore *g(t)* was associated with some measure of [Ca++] in the intracellular space rather than with the electrical stimulation. In some sense we are 'dumping' the non-linearity into the transfer function between the stimulus and the calcium concentration.

Elastic rack: A fixed elastic rack has a limited range of application. In a prolonged contraction, the elastic rack should be able to slip and change its reference (unloaded) length without significant change in force, in a similar way to a yielding material. Epstein, 1994 and Allinger, 1995 have proposed a mechanical device that exhibits such behaviour. The device can be described as two brushes that are placed opposite to each other so that

their bristles interpenetrate as shown in Figure 3.12. The force-length relation of such a device exhibits a global negative slope although, locally, the stiffness is always positive. If one of the brushes has an infinite number of bristles, the device would exhibit a force-length relation similar to an elasto-plastic material except for the small scale saw-tooth shape. There are alternative devices which are able to represent yielding behaviour, such as the one based on snap-springs presented by Müller and Villaggio, 1977. For a more general treatment of stability of materials with non-convex energy potential the reader can turn to Truskinosvsky and Zanzotto, 1996.

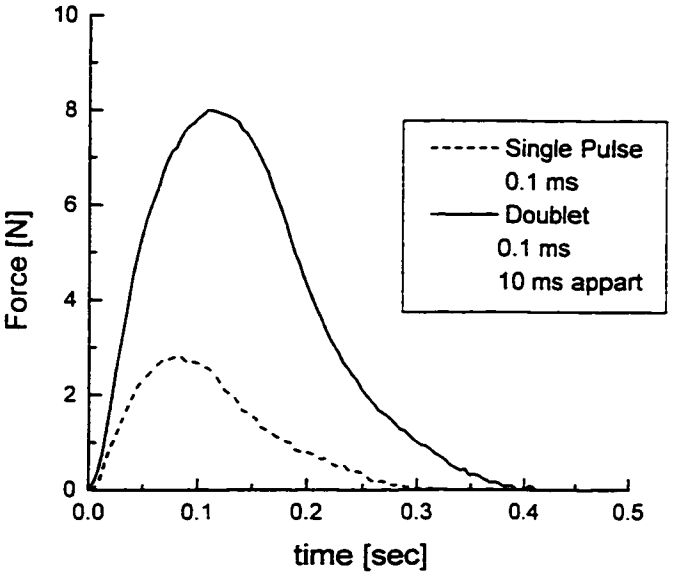

Figure 3.10: Effects of pulse doubling in cat soleus force (from *in-vivo* experimental data gathered by Herzog and Leonard, 1997b).

Linear Force-velocity relation: A chief idea underlying the development of the present model was that the force-velocity relation should arise as a consequence, rather than an inherent property, of the interplay between the elements explicit on the model.

Equation 3.14, which gives the contraction velocity immediately after a force step, shows that the velocity is a linear function of the force step, instead of a hyperbolic function as the experiments by Hill and others indicate.

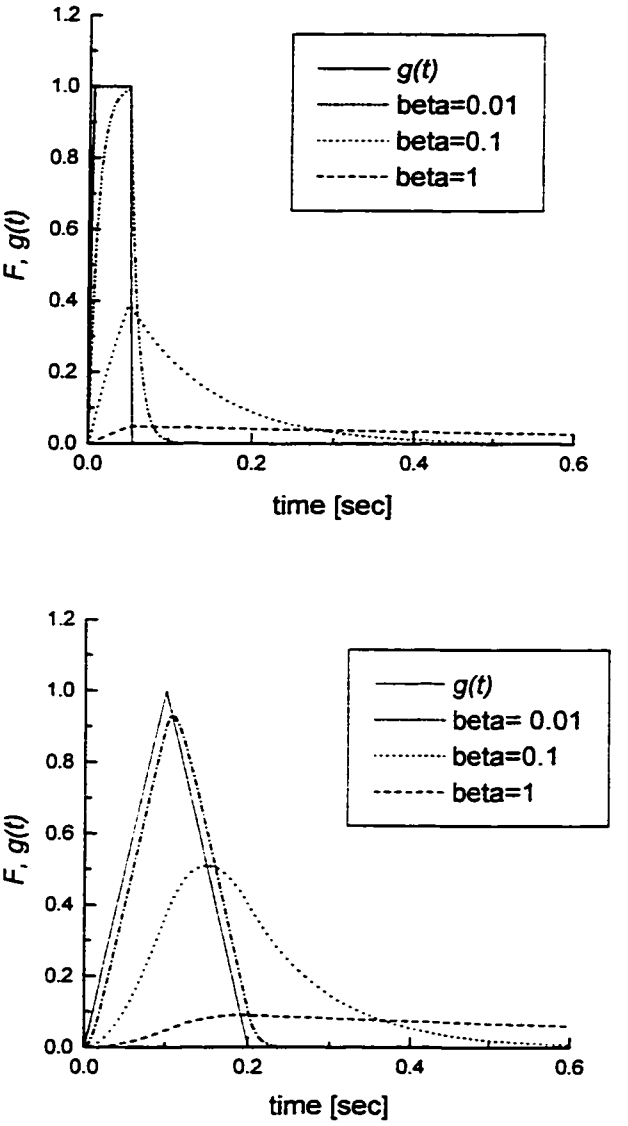

Figure 3.11: Solution of 3.3 for a square (left) and a triangular (right) pulses for different values of the parameter β.

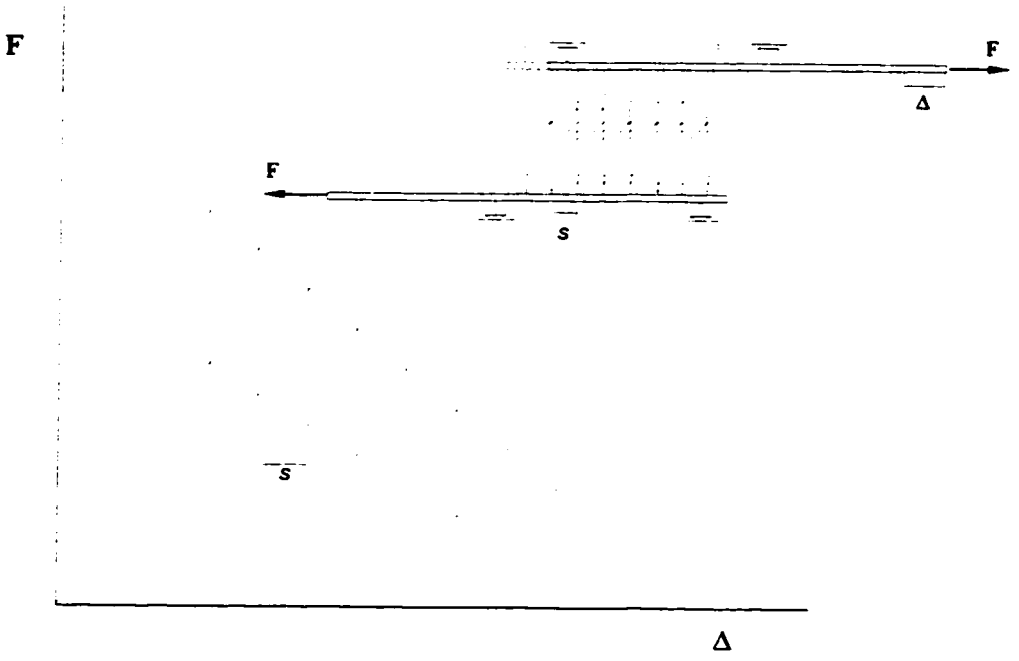

Figure 3.12: Brush Mechanics. Example of a structure with stable but negative slope force-length relation. (from Epstein 1994).

The linear, constant parameter model presented above can be modified to account for this fact by introducing a damping coefficient that varies with the square of the contraction velocity, such as:

$$c = c_o + \varepsilon \cdot \dot{x}^2 \tag{3.20}$$

for which Eq. 3.4 and 3.5 transform to:

$$F = f(t, L_o) + \frac{EA}{L_o} x + (1 + \frac{EA}{kL_o})\,(c_o + \varepsilon \cdot \dot{x}^2)\,\dot{x} \tag{3.21}$$

$$L = L_o + x + \frac{c_o + \varepsilon \cdot \dot{x}^2}{k} \dot{x} \tag{3.22}$$

A close-form solution of Eq. 3.21 and 3.22 is not possible, but assuming that ε is a small quantity a perturbation method[3] can be used to get an approximate solution. The solution to the non-linear problem can be expressed in terms of the solution to the linear problem plus corrective terms that depend on the small, parameter ε. The term $\varepsilon \cdot \dot{x}^2$ can be considered as a small perturbation of the linear equation. Retaining only the linear terms in ε, the perturbed solution can be written as:

$$x = x_o + \varepsilon \cdot x_1 \tag{3.23}$$

where x_1 is a correction to the solution, x_o being the solution to the linear problem. Using the following notation: $\Delta = F - f(t, L_o)$; $\xi = \frac{EA}{L_o}$; $\psi = (1 + \frac{EA}{kL_o})$; $\gamma = \frac{\xi}{\psi \cdot c_o}$, the solution to Eq. 3.4 can be expressed as:

$$x_o = \frac{\Delta}{\xi}\left(1 - e^{-\gamma t}\right); \quad \dot{x}_o = \frac{\Delta}{\psi \cdot c_o} e^{-\gamma t} \tag{3.24}$$

Substituting 3.24 into 3.23 and the result into 3.21:

$$\xi \cdot x_1 + \psi \cdot c_o \cdot \dot{x}_1 + \psi \cdot \dot{x}_o^3 = 0 \tag{3.25}$$

where the validity of 3.4 and the approximation $\dot{x}^3 \approx \dot{x}_o^3$ were assumed. Solving Eq. 3.25 we obtain:

$$\begin{aligned} x &= \frac{\Delta}{\xi}\left(1 - e^{-\gamma t}\right) + \frac{\varepsilon}{2\xi}\left(\frac{\Delta}{\psi \cdot c_o}\right)^3 \left(e^{-3\gamma t} - e^{-\gamma t}\right) \\ \dot{x} &= \frac{\Delta}{\xi}\gamma\, e^{-\gamma t} + \frac{\varepsilon}{2\xi}\left(\frac{\Delta}{\psi \cdot c_o}\right)^3 \left(-3e^{-3\gamma t} + \gamma e^{-\gamma t}\right) \end{aligned} \tag{3.26}$$

Replacing 3.25 and $\dot{x}^3 \approx \dot{x}_o^3$ in Eq. 3.21 we arrive at:

---

[3] See chapter on perturbation methods in Butkov, 1968.

$$L - L_o = \frac{\Delta}{\xi} + \left(\frac{c_o}{k}\gamma - 1\right)\cdot\left(\frac{\Delta}{\xi} + \frac{\varepsilon}{2\xi}\left(\frac{\Delta}{\psi \cdot c_o}\right)^3\right)\cdot e^{-\gamma t} + \\ + \frac{\varepsilon}{2\xi}\left(\frac{\Delta}{\psi \cdot c_o}\right)^3\left(1 - 3\frac{c_o}{k}\gamma + \frac{\varepsilon}{k}\right)\cdot e^{-3\gamma t} \tag{3.27}$$

$$\left.\frac{d(L - L_o)}{dt}\right|_{t=0} = -\gamma\left(\frac{c_o}{k}\gamma - 1\right)\cdot\left(\frac{\Delta}{\xi} + \frac{\varepsilon}{2\xi}\left(\frac{\Delta}{\psi \cdot c_o}\right)^3\right) - \\ -3\gamma\frac{\varepsilon}{2\xi}\left(\frac{\Delta}{\psi \cdot c_o}\right)^3\left(1 - 3\frac{c_o}{k}\gamma + \frac{\varepsilon}{k}\right) \tag{3.28}$$

Eq 3.28 clearly shows that the force-velocity curve for the non-linear model can be approximated by a third-degree polynomial on the force difference.

3.4 Discussion

Aside from the inclusion of the elastic rack element, there is a fundamental difference between the model presented here and Hill's two-component model: Hill's model has the characteristic force-velocity relation built into the description of the contractile element, while here, the characteristic equation arises from the combined action of the elements external to the contractile element. From the analysis, it is clear that such an objective cannot be attained with a linear, i.e. constant parameter, model. Despite this deficiency, our model captures some features of skeletal muscle, such as force depression (enhancement) after shortening (lengthening), which is not contained in traditional Hill-type models, as well as the instantaneous response of shortening (lengthening) muscle. An examination of the current model reveals that the key element which accounts for the history-dependent effects of muscle force is the elastic rack. The rack acts as a parallel spring that is recruited only when the muscle is activated. Edman

and Tsuchiya (1996) arrived at a similar conclusion in an experimental way, i.e. that there must be some elastic structure in muscle which is recruited upon activation. The objective of this part of the work was not to uncover what structure in muscle (if any) should be responsible for producing this elastic effect upon activation, but to develop a simple representation that can be used in entire muscle models.

Another fundamental issue which we wanted to address was whether viscoelasticity should be ruled out as a model for muscle behaviour. An analysis of the response of the present model is sufficient to discard linear viscoelasticity; however, more complex forms of viscoelasticity cannot be discarded at present.

Phenomenological models have the appeal of remaining simple even when used in complex systems, and they fill the gap between the molecular level and the entire system level at which most experiments on muscle are performed. There is no intent here to uncover the mechanism by which muscle contracts. The elastic rack, linear spring, damper, and contractile elements are fictitious representations that help in the derivation of a differential equation. Moreover, the equation is the model regardless of how it was obtained. It was not the objective of this work to find a model that represents the muscle under a wide variety of working conditions, but only to bring attention to the fact that there are simple models that are able to represent many aspects of muscle mechanics accurately.

3.5 Interaction Between Muscle Stimulation and Movement

We want to conclude this chapter on entire muscle modelling with some considerations on the important issue of muscle stimulation. It is through the electrical stimulation of muscle by the nervous system that the delivery of mechanical work is

controlled. There are two basic ways by which the nervous system can control the force produced by a muscle; one is by varying the number of fibres[4] producing force at any given time and the other is by varying the frequency at which the stimulation pulses are delivered. In modelling the entire muscle, the first modality of controlling the force does not offer much difficulty; in unipennate muscles a scaling factor multiplying the force in the contractile element, with due regard to the angle of pinnation, is the only addition one needs to effect to the model. Even if the muscle is multipennate, the force can be resolved in components parallel to the fibres and each component can be scaled accordingly to the number of active motor units and added vectorially. However, with the second modality, i.e., the control of the stimulus-pulse frequency, things are not so easy due to the non-commutative nature of the process of stimulation and stretching (or shortening).

Before going into the mathematics of the problem, we simplify its description by using a different measure of stimulation than the electrical activity of nerves. Because of the complex mechanisms involved, it is not easy to relate directly the electrical stimulation on the nerve endings to the force output in a fibre. In simple terms, the variation of the electrical field on the sarcolemma triggers the release into the intracellular space of the Ca++ stored in the sarcoplasmic reticulum. Once the Ca++ is released, not only diffusive forces, but also the internal geometry of the cell (Kargacin 1994), the calcium pump and the changing affinity for calcium of actin filament due cooperativity effects (Zhou and Phillips, 1994), act to determine the rates of binding and detachment of cross-bridges, which transduce the chemical energy of ATP into mechanical work. We will loosely talk about 'activation' as a measure of muscle contractile activity; for example, in an isometric contraction we can associate the activity with the stimulation

---

[4] To be precise, we must say the number of motor units, since each motor nerve inervates a number of fibers and stimuli go simultaneously to all the fibers in the motor unit.

frequency, the higher the frequency: the more isometric force the muscle is able to exert until a frequency is reached for which further increases do not affect significantly the force outcome. The idea is to extend the concept of activation as a description of the contractile state of the muscle regardless of the output force. In this way, if a contracting muscle is stretched or allowed to contract, we will say that the activation does not change as long as the stimulus does not change. Without further consideration to the mechanisms involved in the transduction of electrical pulses into number of bound cross-bridges, we can define the activation as an internal variable that enters the list of constitutive parameters. This variable has a value 0 for the relaxed state and a value $\rightarrow\infty$ for the fully tetanized state[5]. Intermediate values of activation need not be linearly related to the stimulus frequency nor to the Ca++ concentration, but we assume that it is possible to quantify the activation as a function of either one. In a sense, our definition of activation is not different than that commonly used in biomechanics, except that in our case it is not directly applied as a scaling factor for the force produced in the contractile element. To understand why it is not possible to apply the activation as a scaling factor, consider the outcome of the following two experiments; a) an isometrically contracting muscle that is fully activated is shortened by a certain distance, thus reducing the force, b) the same muscle is passively stretched to the final length reached in experiment a), where it is stimulated in such a way that its isometric force is equal to the force reached after shortening in experiment a) (point P in Fig 3.13).

---

[5]To define the activation as a function that asymptotically tends to one for stimulus of magnitude infinity will helps to simplify the mathematics.

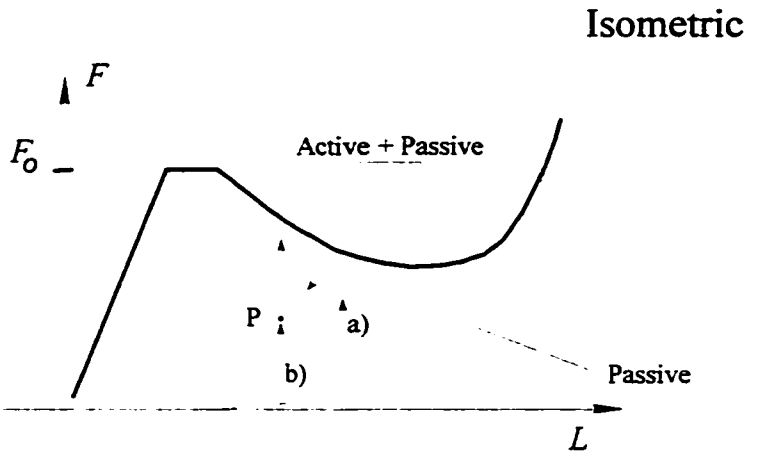

Figure 3.13: Shortening from fully active state and activation from resting state to reach the same F-L point.

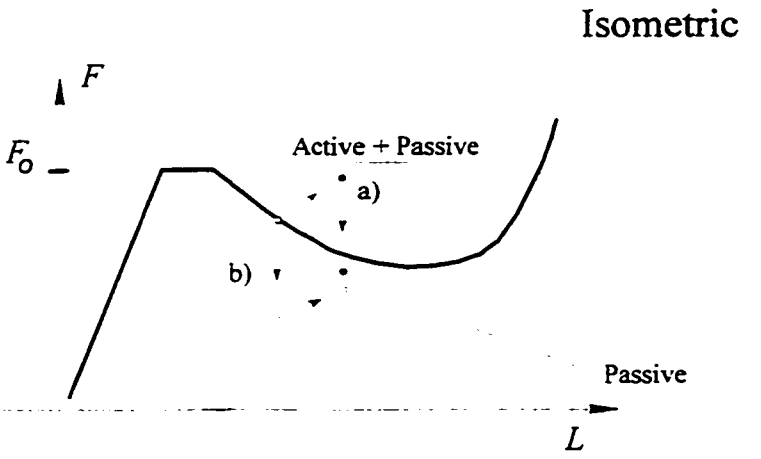

Figure 3.14: Stretching and reduction of stimulus from fully active state compared to reduction of the activation and stretching .

In both experiments, by definition, the same point in the force-length plane is reached, however, the 'state' of the muscle is different depending on the path followed to reach point P. The state is different in the sense that if the path labeled a) was followed, at point P the muscle is fully activated and an increase in the stimulus frequency will not

increase the force. On the other hand, if the path labeled b) was followed to reach point P, the muscle still has the potential to increase the force if an increase in the stimulus frequency is provided.

Consider also what happens when a tetanized muscle is given a stretching followed by a reduction in activation, as shown by the path labeled a) in Fig 3.14, and compare it to what happens when the same two operations are applied in reverse order (path labeled b) in Fig 3.14). In general the points in the force-length plane reached by the two processes will be different because the force-length properties of muscle change when the stimulus frequency history change (Roszek et al., 1994, Roszek, 1996).

From the preceding analysis we can conclude that not only the activation acts as a state variable, but also that in order to have a complete description of the contractile state of a muscle, it is necessary also to include the order in which changes in stimuli and changes in length were given to the muscle. To model a change in the contractile state of a muscle, we assume that it is made up of and arbitrarily ordered sequence of the following two elementary operations:

(i) change in activation at a constant length;

(ii) change in length at a constant activation.

In this analysis we are ignoring the effects of the velocity at which the changes in length proceed, considering that changes occur only between isometric states, that is, assuming that after a transient period the force reaches a constant value that depends only on the state. The passive response of the muscle is represented with the function $f(L)$ and the collection of fully activated states obtained at constant length by $g(L).f(L)$ and $g(L)$ are represented in Figures 3.13 and 3.14 by the curves labeled 'Passive' and 'Active + Passive', respectively. The outcome of the two elementary operations can be calculated using the following formulas due to M. Epstein, 1996:

$$\hat{F} = e^{-k\hat{a}} \cdot f(L) + (1 - e^{-k\hat{a}}) \frac{g(L)\, F}{e^{-k\hat{a}} \cdot f(L) + (1 - e^{-k\hat{a}}) \cdot g(L)} \tag{3.29}$$

for a change in activation, and,

$$\hat{F} = F + e^{-k\hat{a}} \cdot (f(\hat{L}) - f(L)) + (1 - e^{-k\hat{a}}) \cdot E(\hat{L} - L) \tag{3.30}$$

for a change in length. In these expression, the hat over the variable represents the new value, k is a time constant that can be a function of the type of muscle and the activation, and E is a stiffness constant which in general is a function of a and L.

Equations 3.29 and 3.30 have some interesting properties such as the non-linear summation of activation effects, i.e., the application of two different activations at constant length will give a different result than the application of the sum of activations from the resting state. Memory effects are also included in the formulation; for instance, the formulae will distinguish between the states of two identical points in the force-length plane if they were reached following different paths, and if further changes are applied, the two identical points will move differently in the force-length plane. The setting of the activation to 0, resets the muscle to the virgin state and the memory of past changes is lost.

So far we have described a possible theoretical approach to the modelling of the non-commutativity effect in muscle. Unfortunately there are not many experiments performed that address the issue of history-dependence of muscle properties. Herzog and Leonard have published in 1997 the result of two experiments in which the length and the activation of an *in-vivo* preparation of cat soleus are varied. In one of the experiments the length of the muscle is shortened at the same time that the frequency of the stimulation is reduced to a fraction of the maximal frequency, following the shortening the stimulation is restored to the maximal value and the force trace is recorded. From the results it is apparent that, after restoring the stimulation, the force returns to the isometric value

corresponding to the final length only when the stimulation is reduced to zero. When the stimulation frequency is reduced to a value different from zero, the force returns to a lesser value than the isometric value corresponding to the final length, the smaller the reduction in stimulation, the lower is the isometric force reached after restoration. This behaviour seems to be at odds with the mathematical model proposed, although it is fair to say that the experiment does not exactly fit into the theoretical framework because in it the stimulus and the length are changed simultaneously. In their manuscript, Herzog and Leonard used the results of this experiment to support the hypothesis that it is the stress in the muscle during shortening that inhibits the contractile machinery to recover the force after shortening. This hypothesis contradicts the commonly held notion that the non-uniformities in sarcomere length along the fibre are responsible for the force depression after shortening. It is known that non-uniformities in sarcomere length are always present in experimental set ups, however, it is still unclear what is (if any) the relative importance of the stress inhibition and sarcomere length non-uniformity in the force depression/enhancement. From the point of view of continuum mechanics, the stress history cannot be *a priori* deleted from the list of constitutive variables that determine the changes in internal energy produced by the chemical reactions. Going to the molecular level it is easy to understand why if we consider that the macromolecules forming the myofilaments are deformable, and therefore that the rates of reaction depending on the formation of stereo-specific links can be hindered by strain.

Here we want to raise the points that need to be investigated further. One way to do that is to develop experimental protocols to probe the hypotheses advanced so far. To conclude this chapter we present here the results of some exploratory experiments suggested by the theoretical analysis presented above. The experiments described below, were conducted by Herzog and Leonard, 1997b.

3.6.1 Non-Commutativity Between Shortening And Stretching

The first test case was designed to assess the commutativity between active shortening and stretching. An *in vivo* preparation of cat soleus muscle is isometrically activated and when it reaches a steady isometric force it is actively shortened 4 mm at a rate of 4 mm/s. After a delay dt, it is actively stretched back to the initial length at the same rate. The force is measured throughout the cycle. Figure 3.15 shows the resulting force and length traces for three different values of dt, from 0 to 1 s.

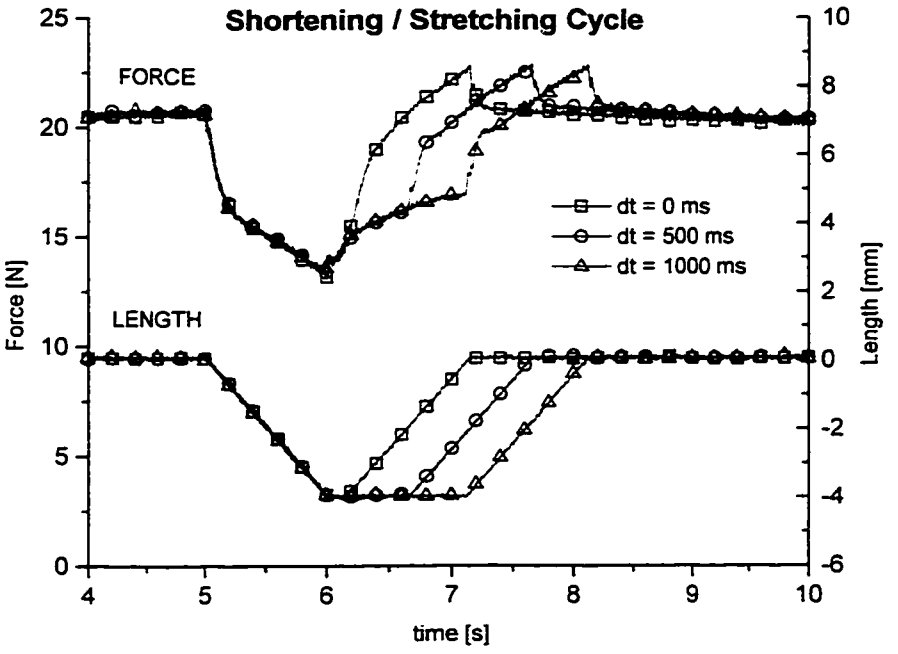

Figure 3.15: Active Shortening followed by Stretching of *in vivo* cat soleus.

It is apparent from the graph that the force returns to its isometric value independently of the value of the delay. Additionally, the force follows the same path on the recovery phases for all cases. If the order of the experiment is reversed, that is, if the

stretch is applied first followed by a shortening to the initial length, the force does not recover the isometric value but a value that is 15% lower, as shown in Figure 3.16. This asymmetry in the response of muscle can be attributed to the presence of a mechanism of inhibition to the formation of new cross-bridges after stretching that is not present (or not as important) during shortening.

A second test case was tried to see the influence of a reduction in activation. In this case the isometrically contracting muscle is subjected to an active shortening, followed by a reduction of the activation frequency from 30 Hz to 7.5 Hz during a variable period of time, and a stretching back to the initial length after that the frequency of the activation was restored to 30 Hz. The same experiment is repeated reversing the order of the shortening and the stretching with the results depicted in Figures 3.17 and 3.18.

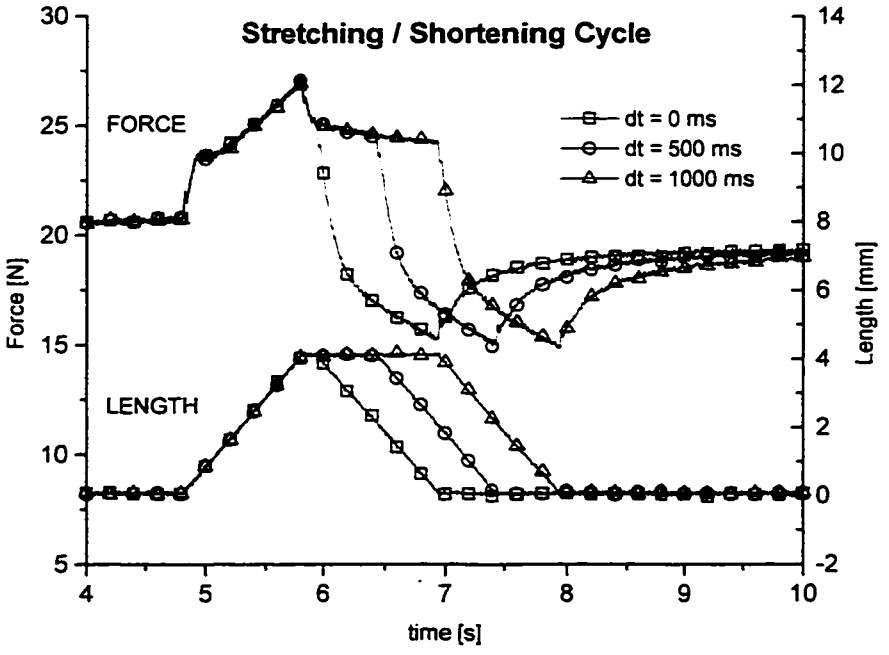

Figure 3.16: Active Stretching followed by Shortening of *in vivo* cat soleus.

As in the first test case, the order in which the shortening and the stretching are applied determines the final value of the force to be slightly enhanced (Fig 3.17) or considerably depressed (Fig 3.18) with respect to the isometric level. To our knowledge, there is no muscle model able to represent the experimental behaviour described by these two test cases. A fair amount of experimental and theoretical work is needed to elucidate whether this type of behaviour can be attributed to non-uniformities in the sarcomere lengths or to a mechanism of inhibition of new cross-bridges formation due to stress. In our opinion, the latter is the more plausible explanation of this and similar phenomena.

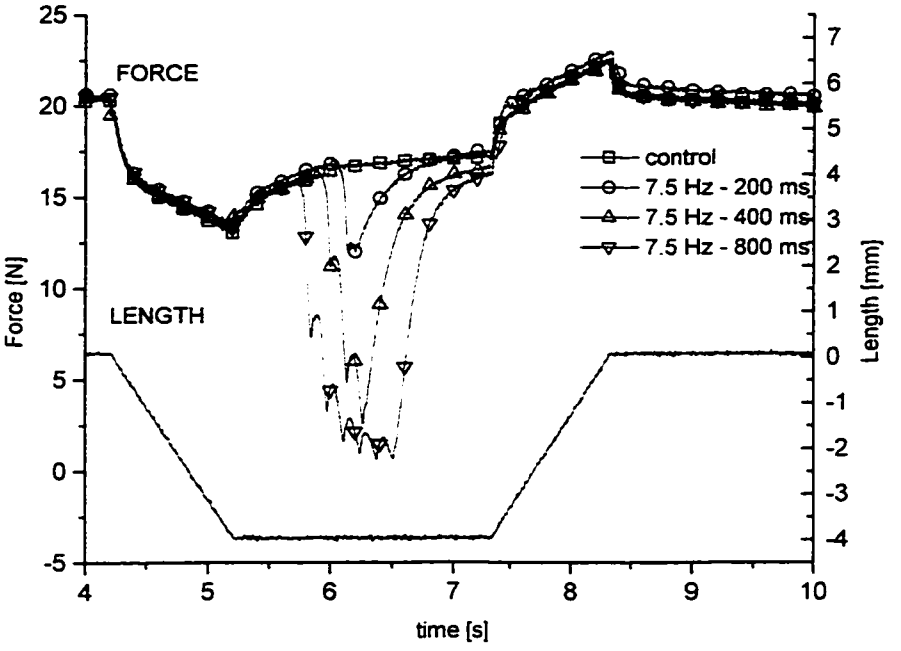

Figure 3.17: Active Shortening followed by reduction of the activation and Stretching of *in vivo* cat soleus.

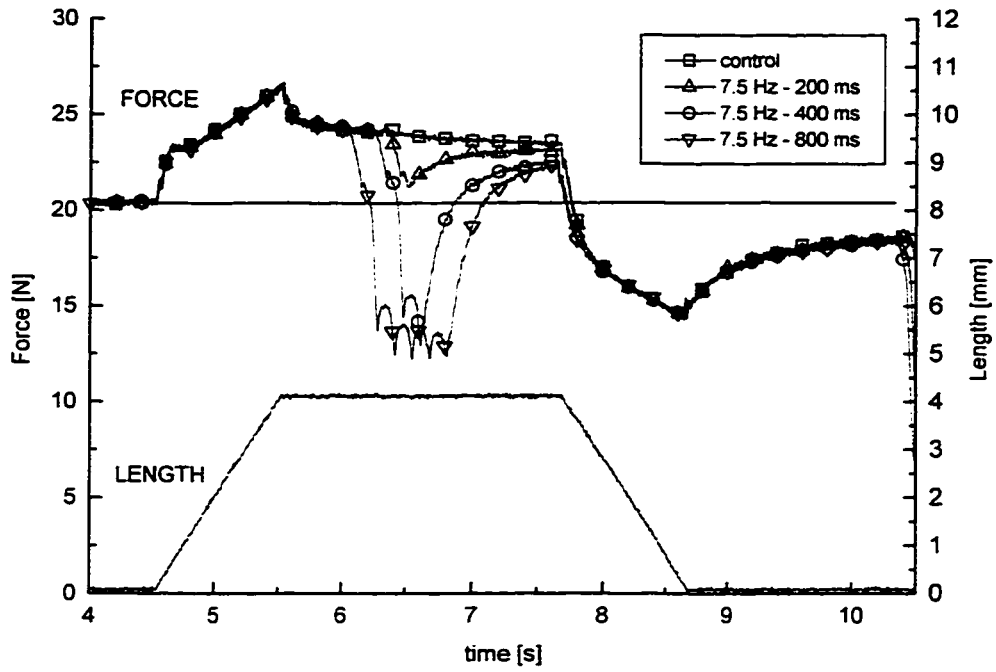

Figure 3.18: Active Stretching followed by reduction of the activation and Shortening of *in vivo* cat soleus.

IV

Mechanics and Thermodynamics

In chapters II and III we presented simple, one-dimensional mechanical models of muscle. Although useful to extract some general conclusions, they are very limited in scope. The limitations are not only because their spatial dimensionallity, but also due to the limited physics and chemistry considered. Continuum mechanics, with its formalism based upon a strong axiomatic set, gives the framework to construct models that are general enough to consider all possible interactions and, at the same time, mechanically correct. The intention here is to introduce those theoretical constructions that could be used as the basis for development of more complete models of muscle in the future. We shall emphasize here that the mechanics and the thermodynamics for the general case of a deformable body are well known; what is not known in the particular case of muscle mechanics are the constitutive equations. Continuum mechanics alone is not able to give the constitutive equations; they will be found only through careful experimentation and by using theories dealing with events happening at the molecular level, however, continuum mechanics will tell us what to search for.

This chapter presents a brief review of the general continuum mechanics and thermodynamics that can be applied to the study of muscle. We will follow here the treatment given by Truesdell (1969), Wang and Truesdell (1973), Bowen (1976) and Eringen (1980), describing briefly the fundamental laws and going into some detail regarding the theory of chemically reacting mixtures.

4.1 Continuum Mechanics

We identify a deformable, spatial body with an oriented, three-dimensional differentiable manifold which can be covered by a global coordinate chart. The elements of $\mathcal{B}$ are called *body-points*, **X**. Any open submanifold of $\mathcal{B}$ is also a body called a *subbody* of $\mathcal{B}$. In a given frame of reference, the *configuration* of $\mathcal{B}$ at instant t is a map $\kappa_t:\mathcal{B} \to \mathcal{E}^3$, where $\mathcal{E}^3$ is a Cartesian co-ordinate system on a 3-dimensional oriented manifold called the *instantaneous space*. It is convenient to introduce the concept of *reference configuration* of the body $\mathcal{B}$ that is simply a particular configuration $\kappa_0:\mathcal{B} \to \mathcal{E}^3$ of the body, which is deemed convenient to take as reference.

The *motion* of a body is a one parameter family of diffeomorphisms $\chi_t:\mathcal{B} \to \mathcal{E}^3, t \in \mathcal{R}$. Normally, the parameter is the time t. If we name with **x** the spatial position at time t of the point identified with the body-point **X**, then $\mathbf{x} = \chi_t(\mathbf{X},t)$ represents a motion.

The *velocity* and *acceleration* of a particle are defined, respectively, as the first and second time derivative of the motion **x**:

$$\dot{\mathbf{x}} = \frac{\partial}{\partial t}\chi_t(\mathbf{X},t), \qquad \ddot{\mathbf{x}} = \frac{\partial^2}{\partial t^2}\chi_t(\mathbf{X},t) \tag{4.1}$$

Consider the configuration κ at time t. There exists a diffeomorphism $\zeta_{0,t} \equiv \kappa_t \circ \kappa_0^{-1}:\kappa(\mathcal{B}) \to \kappa_t(\mathcal{B})$ called the *deformation*, that maps the position of body points from the reference configuration to the current configuration.

The *deformation gradient* is the tensor defined by the gradient of the motion at the reference point X:

$$\mathbf{F} = \frac{\partial \chi}{\partial \mathbf{X}}(\mathbf{X}, t) \qquad \text{or} \qquad d\mathbf{x} = \mathbf{F}\, d\mathbf{X} \tag{4.2}$$

that is, the deformation gradient, **F**, maps a line element in the reference configuration to the corresponding line element in the deformed configuration. We will use the symbol $\frac{d}{dt}(\cdot)$ or a superimposed dot to indicate the material time derivative, that is the time derivative calculated following the material particle.

Let *M*, the *mass*, be defined as a non-negative measure defined over all measurable subsets of the body. *M* is invariant under motion and it is assumed that *M* is an absolutely continuous function of volume in space and therefore a non-negative *mass-density* ρ exists everywhere in the body. The *Principle of Conservation of Mass* establishes that the total mass of the body does not change during the motion. This principle may be expressed by:

$$\frac{d}{dt}\int_{\mathcal{B}} \rho \cdot dV \tag{4.3}$$

where *dV* is the differential of volume in the reference configuration. If the mass-density and velocity fields are sufficiently smooth, the conservation of mass can be written in its local form:

$$\dot{\rho} + \rho \cdot \operatorname{div} \dot{\mathbf{x}} = 0 \tag{4.4}$$

The *linear momentum* **m** and the *rotational momentum* $\mathbf{r}_{\mathbf{x}_0}$ respect to a fixed position $\mathbf{x}_0$, of $\mathcal{B}$ in its present configuration are defined by:

$$\mathbf{m} = \int_{\mathcal{B}} \dot{\mathbf{x}}\, dM \quad \text{and} \quad \mathbf{r}_{\mathbf{x}_0} = \int_{\mathcal{B}} (\mathbf{x} - \mathbf{x}_0) \wedge \dot{\mathbf{x}}\, dM \tag{4.5}$$

respectively, where *dM* is the differential of mass.

According to *Euler's laws* of mechanics, for every body the time rates of change of linear momentum and angular momentum are, respectively, equal to the *total force* f and the *total torque* t acting upon the body. The total force f is assumed to be the sum of two special kinds: an absolutely continuous function of mass called the *total body force* $\mathrm{f_b}$, and an absolutely continuous function of surface called the *total contact force* $\mathrm{f_c}$. The body force is usually the resultant of an external field, e.g., gravitational and/or electromagnetic, whose intensity per unit mass is given by **b**. Contact forces represent the action of neighbouring parts of material upon one another or *traction* and is denoted by **t**. A theorem by Cauchy established that the traction is delivered linearly through the outer unit normal to the surface in consideration, **n**, by the *stress tensor* **T**:

$$\mathbf{t} = \mathbf{T}\mathbf{n} \tag{4.6}$$

The balance of linear momentum can then be written as:

$$\frac{\mathrm{d}}{\mathrm{d}t}\int_{\mathcal{B}} \dot{\mathbf{x}}\rho\, dV = \int_{\mathcal{B}} \mathbf{b}\rho\, dV + \int_{\partial\mathcal{B}} \mathbf{T}\mathbf{n}\, dA \tag{4.7}$$

where dA is the differential of surface in the reference configuration. Eq. (4.7) can be expressed in local form, if fields are smooth enough, as:

$$\rho\ddot{\mathbf{x}} = \mathrm{div}\,\mathbf{T} + \rho\mathbf{b} \tag{4.8}$$

which is usually known as Cauchy's first law of motion. For the case in which all torques are moment of forces, the conservation of angular momentum implies that:

$$\mathbf{T} = \mathbf{T}^{\mathsf{T}} \tag{4.9}$$

also known as Cauchy's second law of motion.

The *kinetic energy*, K, is defined by:

$$K = \tfrac{1}{2}\int_{\mathcal{B}} \dot{\mathbf{x}}^2 \, dM \tag{4.10}$$

while the *power*, P, is the rate of working of all forces acting on the body:

$$P = \int_{\mathcal{B}} \mathbf{b}\cdot\dot{\mathbf{x}}\, dV + \int_{\partial\mathcal{B}} \mathbf{T}\mathbf{n}\cdot\dot{\mathbf{x}}\, dA \tag{4.11}$$

Stokes proved that the net working W, that is, the power not used up in producing motion is given by $W = \int_{\mathcal{B}} w\, dV = P - K$, where the scalar w, the net working per unit volume, is called the *stress power* and is defined by:

$$w = \mathbf{T}\cdot\operatorname{grad}\dot{\mathbf{x}}, \tag{4.12}$$

where the dot indicating the inner product in the vector space of second-order tensors, i.e., $\mathbf{A}\cdot\mathbf{B} = \operatorname{tr}(\mathbf{A}\mathbf{B}^{\mathrm{T}})$. On the basis of the purely mechanical principles established so far, we can start to construct a thermodynamical theory compatible with continuum mechanics. To that end we introduce the principle of *balance of energy* also called first law of thermodynamics:

$$\dot{U} = W + Q \tag{4.13}$$

where U is the internal energy and Q is the heating, that takes into account the effects of non-mechanical sources on the total energy of the body. Note that Q must have units of power and must be an additive function of the mass[1]. Similarly to what was done previously for the total force, the heating Q is assumed to be the sum of two kinds of heating: the *body heating* Q_b, assumed to be a continuous function of the mass with volume density s, and the *contact heating* Q_c, a continuous function of the surface area

---

[1] In a certain way the conservation of energy acknowledges the notion that doing work may change the energy level of a body, that heating may effect work and that there is an equivalence between the two.

with surface density q. The internal energy U is assumed to be an additive, continuous function of the mass with volume density ε called the *specific internal energy*. Cauchy's theorem is also valid for the contact heating, therefore a *heating flux vector* $\mathbf{h}$ can be defined by:

$$q = \mathbf{h} \cdot \mathbf{n}, \tag{4.14}$$

The balance of energy principle can now be written as:

$$\frac{\mathrm{d}}{\mathrm{d}t}\int_{\mathcal{B}} \varepsilon \rho dV = \int_{\mathcal{B}} w dV + \int_{\partial \mathcal{B}} \mathbf{h} \cdot \mathbf{n}\, dA + \int_{\mathcal{B}} s \rho dV, \tag{4.15}$$

which for sufficiently smooth fields reduces to:

$$\rho \dot{\varepsilon} = w + \operatorname{div} \mathrm{h} + \rho s \tag{4.16}$$

We introduce here the concept of *absolute temperature* θ by assigning a positive-valued field $\theta = \theta(\mathbf{x}, t) > 0$ defined over the present configuration of $\mathcal{B}$. The temperature is a measure of how hot a point in the body is and can be measured with a thermometer or thermocouple.

In the relationships between mechanical and thermal quantities established so far, there is no restriction to the conversion of heat in work and vice versa, that is, the balance of energy does not forbid a process where all the heating is converted to mechanical work in a reversible manner or where heat flows to a hotter body from a colder one. Natural processes are irreversible[2] and this irreversibility can be represented by assigning an *a priori* least upper bound Q^* for the heating Q. For a homogeneous system, namely, a

---

[2] We will accept this as an axiom without further considerations to the philosophical reasons or implications.

body that can be sufficiently described by functions of time only, the *axiom of irreversibility* or *second law of thermodynamics* will read:

$$Q \le Q^*, \text{or, } \dot{U} - W \le Q^* \tag{4.17}$$

In order to render this principle in a more familiar form, and to make it useful, we define a new quantity $\underset{\sim}{\mathbb{E}}$ called *entropy*. For a process lasting from t_0 to t the entropy is given by:

$$\underset{\sim}{\mathbb{E}}(t,t_0) = \int_{t_0}^{t} \frac{Q^*}{\theta}\, dt, \tag{4.18}$$

which is definite for every process because $\theta > 0$ everywhere. Considering now an non-homogeneous process, as with other extensive properties we assume that there is a corresponding volumetric density η or *specific entropy* such that $\underset{\sim}{\mathbb{E}} = \int_{\mathcal{B}} \eta\, dM$. Entropy is introduced so as to represent gross dissipation, and although η locally can be a negative quantity, the total entropy can only increase. The dissipation principle can be formulated as:

$$\frac{\mathrm{d}}{\mathrm{d}t}\underset{\sim}{\mathbb{E}} \ge \int_{\partial\mathcal{B}} \frac{q}{\theta}\, dA + \int_{\mathcal{B}} \frac{s}{\theta}\, dV, \tag{4.19}$$

known as the *Claussius-Duhem* inequality. The application to particular cases of this last principle provide additional restrictions on the constitutive equations, such as the restriction that a the viscosity coefficient of a fluid cannot be negative, for example.

4.2 Constitutive Equations

The conservation principles used to derive the equations in 4.1 gives a system with more unknowns than equations. Except for some trivial situations, like in the case of rigid

body, motions in absence of heat conduction, additional equations must be supplied to make the problem determinate. The necessity to complement the system of equations derived from kinematic and mechanical principles can be understood as a way to introduce different material behaviours into the continuum mechanics formulation. So far nothing was assumed about how different materials will behave under the application of an external field. For example, a solid block made of steel will deform slightly under a given pressure, while a solid block of rubber will deform much more under the same stress. Moreover, consider the case of a solid body, which preserves its shape when subject to a gravitational field, and compare it to a liquid that will adapt to its container. Continuum mechanics equations should be applicable to all possible materials, provided that proper functions describing the particularities of the material are known. These functions are known as constitutive equations. The variables in terms of which they are expressed are known as constitutive variables. There is no systematic way to choose constitutive variables nor to derive constitutive equations. A constitutive theory is used to represent a number of physical phenomena relevant to the particular material under particular conditions, by equations relating variables which represent an ideal material (or ideal behaviour). For example, Elasticity theory represents only the behaviour of certain materials in a given range of stress, The behaviour of the same material outside of this range must be represented by another theory, e.g. plasticity theory.

Constitutive equations shall conform to the following basic principles or axioms

1. *Axiom of Equiprescence*: All constitutive functionals should include the same list of independent variables *a-priori*.

2. *Axiom of Determinism*: The value of the constitutive functions at a material point of the body is determined by the history of the motion and temperature of all material points of the body.

3. *Axiom of Objectivity or Frame Indifference*: constitutive equations must be form invariant with respect to rigid motions of the frame of reference

4. *Axiom of Local Action or Neighbourhood*: The values of the independent variables at distant material points do not affect appreciably the values of the dependent variables at the point x.

5. *Axiom of Dissipation*: All constitutive relations are such as to satisfy the dissipation inequality (such as the Clausius-Duhem inequality) for all arguments in their domains.

4.3 Mixture Theory

Whenever two or more substances sharing the same physical space are interacting mechanically and chemically, the description of the mechanics of continua presented so far is not able to describe the thermomechanical state of each separate component. The mixture theory presented below aims to represent the phenomena of diffusion, dissociation, combination and chemical reaction in the broadest sense.

The philosophy behind the mathematical construction of the mixture theory can be summarized in the following three principles:

1. All properties of the mixture must be consequences of the properties of its constituents.

2. The motion of a constituent can be described as the motion of the constituent in isolation provided the actions of the other constituents upon it are properly taken into account.

3. The motion of the mixture is governed by the same equations as is a single body.

We will distinguish the quantities associated with each constituent with the word *peculiar* and a small letter written below them, thus $\underset{a}{\rho}$ will denote the peculiar mass density of the a constituent, for instance. As the motion of each constituent has its own kinematics, we need to define material derivatives with respect to the constituents. We will use a backward prime to denote the time derivative when $\underset{a}{\mathbf{X}}$ is held constant. Therefore the velocity of the constituent a is defined as:

$$\underset{a}{\mathbf{x}}' \equiv \frac{\partial}{\partial t}\underset{a}{\mathbf{x}}\left(\underset{a}{\mathbf{X}}, t\right) \tag{4.20}$$

and the acceleration as:

$$\underset{a}{\mathbf{x}}'' \equiv \frac{\partial^2}{\partial t^2}\underset{a}{\mathbf{x}}\left(\underset{a}{\mathbf{X}}, t\right) \tag{4.21}$$

We consider only those points $\mathbf{x}$ in space which are simultaneously occupied by one particle of each constituent. The total mass density of the mixture is defined by:

$$\rho \equiv \sum_{a=1}^{\pi} \underset{a}{\rho} \tag{4.22}$$

The concentration or mass fraction of the constituent a is the dimensionless ratio:

$$\underset{a}{c} \equiv \frac{\underset{a}{\rho}}{\rho}, \tag{4.23}$$

therefore,

$$\sum_{a=1}^{\pi} \underset{a}{c} = 1 \tag{4.24}$$

For the mixture, regarded as a single body, we can define the velocity as:

$$\dot{\mathbf{x}} \equiv \sum_{a=1}^{\pi} \underset{a}{c}\,\underset{a}{\mathbf{x}}' \tag{4.25}$$

As in the case of a simple body, each constituent is acted upon by actions at a distance like the body force $\underset{a}{\mathbf{b}}$ and the body heating $\underset{a}{s}$, and by contact actions represented by the stress $\underset{a}{\mathbf{T}}$ and the heating flux $\underset{a}{\mathbf{h}}$. The inner parts of the resultant actions on the mixture are the sums:

$$\mathbf{b}_I = \sum_a c_a \mathbf{b}_a, \quad s_I = \sum_a c_a s_a, \quad \mathbf{T}_I = \sum_a \mathbf{T}_a, \quad \mathbf{h}_I = \sum_a \mathbf{h}_a \tag{4.26}$$

In the same way we define the internal parts of the internal energy and entropy of the mixture such that, in a given region, they are the sums of the internal energy and entropy of the constituent bodies occupying the same region, or:

$$\varepsilon_I = \sum_a c_a \varepsilon_a, \quad \eta = \sum_a c_a \eta_a \tag{4.27}$$

The relative motion of the constituents and the transfer of mass, momentum and energy produced by physical transfers and chemical reactions are not taken into account by these inner parts. The correct definition for the stress, body force, internal heating, heating flux and internal energy are to be deduced from the application of the third principle mentioned above. First, the equations of motion for the mixture must be formulated in terms of the constituents. That can be achieved by applying the following conservation laws to the growth of mass, $\hat{\underset{a}{c}}$, the growth of linear momentum, $\hat{\underset{a}{\mathbf{m}}}$, the growth of rotational momentum, $\hat{\underset{a}{\mathbf{M}}}$, and the growth of energy, $\hat{\underset{a}{e}}$:

$$\sum_a \hat{c}_a = 0, \quad \sum_a \hat{\mathbf{m}}_a = 0, \quad \sum_a \hat{\mathbf{M}}_a = 0, \quad \sum_a \hat{e}_a = 0, \tag{4.28}$$

Assuming that all fields are sufficiently smooth, as we did for the case of a single body, the conservation laws can be expressed in their local forms:

$$\rho \hat{\underset{a}{c}} = \dot{\rho}_a + \rho_a \operatorname{div} \dot{\mathbf{x}}_a \tag{4.29}$$

$$\rho \hat{\underset{a}{\mathbf{m}}} = \rho c_a \dot{\mathbf{x}}_a + \hat{\rho \mathbf{x}}_a - \operatorname{div} \mathbf{T}_a - \rho_a \mathbf{b}_a \tag{4.30}$$

$$\rho \bar{\mathbf{M}}_a = \mathbf{T}_a - \mathbf{T}_a^T \tag{4.31}$$

$$\rho \bar{e}_a = \rho \bar{\mathbf{m}}_a \cdot \dot{\mathbf{x}}_a + \rho \bar{c}_a \left(\varepsilon_a - \frac{1}{2} \dot{x}_a^2 \right) + \rho \bar{\varepsilon}_a - \mathrm{tr}(\mathbf{T}_a^T \mathbf{grad} \dot{\mathbf{x}}_a) - \mathbf{div} \mathbf{h}_a - \rho s_a \tag{4.32}$$

The mixture considered as a single body in motion cannot distinguish whether it is formed by only one component or if it is heterogeneous, therefore by properly defining mixture variables the conservation laws should have the same form as those for a single component. Assuming that the velocity of the mixture is given by $\dot{\mathbf{x}}$ and defining the diffusion velocity of the a constituent as $\mathbf{u}_a \equiv \dot{\mathbf{x}}_a - \dot{\mathbf{x}}$, the appropriate definitions are as follows:

stress, $$\mathbf{T} = \mathbf{T}_I - \sum \rho_a \mathbf{u}_a \otimes \mathbf{u}_a, \tag{4.33}$$

total body force, $$\mathbf{b} = \sum c_a \mathbf{b}_a, \tag{4.34}$$

internal energy, $$\varepsilon = \varepsilon_I + \frac{1}{2} \sum c_a u_a^2, \tag{4.35}$$

total heating flux, $$\mathbf{h} = \mathbf{h}_I + \sum \left[\mathbf{T}_a^T \mathbf{u}_a - \rho_a (\varepsilon_a + \frac{1}{2} u_a^2) \mathbf{u}_a \right], \tag{4.36}$$

and total heating supply, $$s = s_I + \sum c_a \mathbf{b}_a \cdot \mathbf{u}_a. \tag{4.37}$$

As in the case of single bodies, a dissipation axiom is added to the conservation laws. In order to do that it is necessary to calculate the contribution of changes in entropy and relative motion of each constituent to the growth in entropy of the mixture. Measures of *coldness*, defined by $\vartheta_a = \frac{1}{\theta_a}$, and entropy, η_a, are assigned to each constituent. The growth of entropy $\bar{\eta}_a$ of the constituent a can be defined through an equation of balance such as:

$$\rho \dot{\eta}_a = \rho \bar{c}_a \eta_a + \rho_a \dot{\eta}_a - \operatorname{div}(\vartheta_a \mathbf{h}_a) - \vartheta_a \rho_a s_a \tag{4.38}$$

Summing on a we obtain:

$$\rho \dot{\eta} = \rho \sum_a \dot{\eta}_a + \operatorname{div} \sum \left(\vartheta_a \mathbf{h}_a - \rho_a \eta_a \mathbf{u}_a \right) + \sum \vartheta_a \rho_a s_a \tag{4.39}$$

As we consider the entropy of each constituent to reflect exchanges and transfers between constituents rather than true processes of creation or annihilation, there is no restriction imposed to the values of $\dot{\eta}_a$. However the total growth of entropy for the mixture must remain non-negative, that is:

$$\sum \dot{\eta}_a \geq 0 \tag{4.40}$$

is the axiom of dissipation. Using 2.39, 2.40 can be written as:

$$\rho \dot{\eta} \geq \operatorname{div} \phi + \rho \sigma \tag{4.41}$$

where:

$$\phi = \sum \left(\vartheta_a \mathbf{h}_a - \rho_a \eta_a \mathbf{u}_a \right), \tag{4.42}$$

$$\sigma = \sum \vartheta_a c_a s_a \tag{4.43}$$

Introducing the free energy of the a-th constituent as:

$$\psi_a = \varepsilon_a - \theta_a \eta_a, \tag{4.44}$$

the dissipation axiom for mixtures (4.40) can be written in its reduced form:

$$\sum \left\{ \underset{a}{\vartheta} \left[-\underset{a}{\dot{e}} + \underset{a}{\dot{\mathbf{m}}} \cdot \underset{a}{\mathbf{x}} + \underset{a}{\dot{c}} \left(\underset{a}{\psi} - \frac{1}{2} \underset{a}{x}^2 \right) \right] + \underset{a}{c} \left(\underset{a}{\vartheta} \underset{a}{\dot{\psi}} - \underset{a}{\eta} \underset{a}{\dot{\vartheta}} / \underset{a}{\vartheta} \right) \right.$$
$$\left. - \frac{1}{\rho} \left[\underset{a}{\vartheta} \operatorname{tr} \left(\underset{a}{\mathbf{T}}^{\mathsf{T}} \cdot \operatorname{grad} \underset{a}{\mathbf{x}} \right) - \underset{a}{\eta} \cdot \operatorname{grad} \underset{a}{\vartheta} \right] \right\} \leq 0 \qquad (4.45)$$

4.4 Mixture of Chemically Reacting Bodies

In a mixture, the total mass preservation, $\sum \underset{a}{\hat{c}} = 0$ is a very general statement for the exchange of mass among constituents. If chemical reactions are taking place between the constituents, they combine and dissociate only in definite proportions according to the laws of chemical reactions. These laws can be explained by saying that the substances consist of molecules and that each molecule is formed by a whole number of atoms, each class of atoms having a fixed atomic weight. The molecular weight of a substance is the sum of the weights of the atoms in each molecule. During the reactions, molecules are destroyed and created but atoms remain constant in number and nature. Here the terms 'atom' and 'molecule' are being used in a broad sense. In a particular case a real molecule can be considered as an atom as long as it remains an indestructible entity through the reaction process. In this way we see that in the framework of mixture theory, chemical reactions restrict the number of possible transfers allowed by the total mass preservation law. The algebraic form of chemical laws have also important geometrical implications for the continuum theories.

Let the κ atomic substances with atomic weights $a^{\alpha}, \alpha = 1,2,...,\kappa$, be capable of combining to form ζ molecular substances. The molecular weight of these substances will be given by:

$$m^b = \sum_{\alpha=1}^{\zeta} t_\alpha^b a^\alpha, \tag{4.46}$$

where t_α^b is the number of moles of the α^{th} atomic substance in one mole of the a^{th} molecular substance, a non-negative integer supposed to be given *a priori*, together with a^α, by the laws of chemical kinetics. The permanence of atomic substances asserts that:

$$\sum_{\alpha=1}^{\zeta} \frac{t_\alpha^b}{m^a} \dot{\underset{a}{c}} = 0, \quad \alpha = 1,2,...,\kappa \tag{4.47}$$

Solving the system in equation 4.47 for the concentration growths we obtain:

$$\dot{\underset{a}{c}} = \rho m^a \sum_{\alpha=1}^{\zeta-\Re} P_a^\alpha j_\alpha = 0 \tag{4.48}$$

where $\Re \leq \min(\zeta - \kappa)$ is the rank of the matrix $[t_\alpha^b]$, $[P_a^\alpha]$ is any $\zeta \times (\zeta - \Re)$ matrix of rank $\zeta - \Re$ that obeys the condition

$$\sum_{a=1}^{\zeta} t_\alpha^a P_a^\nu = 0 \tag{4.49}$$

for $\nu = 1,2,...,\zeta - \Re, \alpha = 1,2,...,\kappa$ and is called the stoichiometric matrix and the $\zeta - \Re$ quantities j_α are called the reaction rates. In other words, 4.48 is not more than the application of a theorem that states that a system of κ homogeneous linear equations in ζ unknowns has $\kappa - \Re$ linearly independent solutions. Multiplying 4.49 by m^α and summing on α, we obtain,

$$\sum_{a=1}^{\kappa} P_a^\alpha m^a = 0 \tag{4.50}$$

that can be recognized as the condition that the $\kappa - \Re$ reaction equations are balanced[3]. As the stoichiometry matrix is not unique, the set of $\kappa - \Re$ reaction equations is not

---

[3] Now the motivation to call P_a^α the stoichiometry matrix becomes clear.

unique, but the number $\kappa - \Re$ is unique and represents the number of linearly independent chemical reactions possible in a given mixture. For a given mixture, reaction equations are assumed in advance , therefore the coefficients of the stoichiometric matrix can be read off from them. Chemists usually regard certain constituents of a given reaction as products and the remaining as reactants. They can be distinguished in 4.49 by taking positive coefficients for the reactants and negative coefficients for the products. For each chemical reaction there is a quantity j_α, the reaction rate of the α^{th} reaction, which is also not unique. To see the rationale behind this name, let us rewrite 4.29 in terms of the mean motion and the velocity of diffusion $\underset{a}{\mathbf{u}}$;

$$\rho \dot{\underset{a}{c}} = -\operatorname{div}\left(\rho \underset{a}{c} \underset{a}{\mathbf{u}}\right) + \rho \hat{\underset{a}{c}}, \tag{4.51}$$

for the special case in which there is no diffusion, the first term in the right hand side of 4.51 is zero. Integrating the resulting equation one obtains:

$$\sum_{a=1}^{\zeta} t_\alpha^a \left(\frac{\underset{a}{c}}{m^\alpha} - \frac{\underset{a0}{c}}{m^\alpha} \right) = 0 \tag{4.52}$$

where $\underset{a0}{c}$ is the concentration of the α^{th} constituent at some reference time. The system of equations in 4.52 can be inverted to yield:

$$\underset{a}{c} - \underset{a0}{c} = m^a \sum_{\alpha=1}^{\zeta-\Re} P_a^\alpha \xi_\alpha , \tag{4.53}$$

where ξ_α is the extent of the α^{th} reaction. By using 4.51 without the diffusive term and 4.48 it follows that:

$$\rho \dot{\underset{a}{c}} = \rho m^a \sum_{\alpha=1}^{\zeta-\Re} P_a^\alpha j_\alpha = \rho m^a \sum_{\alpha=1}^{\zeta-\Re} P_a^\alpha \dot{\xi}_\alpha \tag{4.54}$$

Thus, because $[P_a^\alpha]$ has rank $\zeta - \Re$ means that:

$$j_\nu = \dot{\xi}_\nu, \quad \nu = 1,2,\ldots,\zeta - \Re, \tag{4.55}$$

That is, in a non-diffusing mixture, the reaction rate is the time rate of change of any corresponding extent of reaction. In chemistry, these relations are always expressed in terms of components corresponding to a particular choice of independent reactions.

A *thermokinetic process* for the mixture is the set of fields:

$$\underset{a}{\mathbf{x}}(\underset{a}{\mathbf{X}},t), \qquad \underset{a}{\theta}(\mathbf{x},t), \quad a = 1,2,\ldots,\pi \tag{4.56}$$

defined for all points in the bodies constituting the mixture when $-\infty < t < k$ for some k. For a region in which a given thermokinetic process is occurring, a *calordynamic process* is a set of field of two kinds, those defined for each body:

$$\underset{a}{\mathbf{T}}(\mathbf{x},t), \ \underset{a}{\mathbf{h}}(\mathbf{x},t), \ \underset{a}{\varepsilon}(\mathbf{x},t), \ \underset{a}{\eta}(\mathbf{x},t), \ \underset{a}{\mathbf{b}}(\mathbf{x},t), \ \underset{a}{s}(\mathbf{x},t), \tag{4.57}$$

and those describing reactions and exchanges in the mixture:

$$\underset{a}{\hat{c}}(\mathbf{x},t), \ \underset{a}{\hat{\mathbf{m}}}(\mathbf{x},t), \ \underset{a}{\hat{\mathbf{M}}}(\mathbf{x},t), \ \underset{a}{\hat{e}}(\mathbf{x},t) \tag{4.58}$$

provided they are subject to the general axioms 4.28. The general constitutive axiom can be expressed[4] as: For each a, the seven fields

$$\underset{a}{\mathbf{T}}, \ \underset{a}{\mathbf{h}}, \ \underset{a}{\psi}, \ \underset{a}{\eta}, \ \underset{a}{\hat{c}}, \ \underset{a}{\hat{\mathbf{m}}}, \ \underset{a}{\hat{e}}, \tag{4.59}$$

are determined at $\underset{a}{\mathbf{X}}$ by the history of an arbitrary thermokinetic process in a neighborhood of $\underset{b}{\mathbf{X}}$ presently occupying the same place as $\underset{a}{\mathbf{X}}$, in such a way that

---

[4]This axiom is known as the *effective principle of thermodynamic determinism.*

$\tilde{c}_a = \overset{\sim}{\mathbf{m}}_a = \tilde{e}_a = 0$, $\sum_a \mathbf{T}_a$ is a symmetric tensor and the reduced dissipation inequality (4.45) is satisfied identically.

To apply the balance equations, we need to supply the constitutive relations, that is, the functional relations that represent the response of the bodies under study. For example, a mixture whose mechanical response is that of an elastic material but is capable of reacting chemically, conducting heat and transferring energy between constituents can be defined by the set of functionals (Bowen, 1979):

$$\begin{aligned} \mathbf{T} &= \overline{\mathbf{T}}(\mathbf{F}, \theta, \text{grad}\,\theta, \xi) \\ \mathbf{h} &= \overline{\mathbf{h}}(\mathbf{F}, \theta, \text{grad}\,\theta, \xi) \\ \eta &= \overline{\eta}(\mathbf{F}, \theta, \text{grad}\,\theta, \xi) \\ \varepsilon &= \overline{\varepsilon}(\mathbf{F}, \theta, \text{grad}\,\theta, \xi) \\ \dot{\xi} &= \overline{\dot{\xi}}(\mathbf{F}, \theta, \text{grad}\,\theta, \xi), \end{aligned} \tag{4.60}$$

for each constituent. Because of the equipresence axiom, the same list of independent variables appear in all functionals. To model different physical phenomena, the list of independent variables will change accordingly, for example, if viscous effects are to be included as part of the material response, $\dot{\mathbf{F}}$ must be added to the list of independent variables.

4.5 Comments on the Application of Mixture Theories to Muscle.

The theory of chemically reacting mixtures presented has the advantage of being developed from a rigorous framework based on first principles and axioms generally accepted in continuum mechanics. It is also a general theory with very few restrictions to its range of application, however, it was never applied to solve problems in biomechanics,

perhaps due to its difficulty. The application of continuum thermodynamics or mixture theories to problems in muscle mechanics is limited by the fact that the functional forms of the necessary constitutive equations are unknown. It is not clear how to relate the rates of chemical reactions to the thermomechanical variables such as strain, strain rate and stress. The general theory itself gives little help to find these relations, it can only be used to find the restrictions imposed by the thermodynamics of the chemical reactions onto the value of certain parameters.

It is worthwhile however, to explore how mixture theory could be applied to model muscle. We can assume that the muscle is a mixture formed by at least[5] four 'atomic' components, myosin (M), actin (A), ADP and Pi that forms 'molecular' substances such as actomyosin (AM), ATP, AM*ATP, AM*ADP, etc. Suppose also that A, M and all substances in which they enter are elastic solids[6], that ATP, ADP and Pi are solutions subjected only to diffusion and chemical forces. The formalism described in previous sections can be applied to the interchanges of mass and energy between components. In this case the force will be the resultant of the stress between A and M, and the velocity given by the time derivative of their relative motion. An important simplification can be obtained by assuming that all the constituents in the mixture are at the same temperature, that is $\underset{1}{\theta} = \underset{2}{\theta} = ... = \theta$. For for this case only one energy balance equation is required and the terms in $\underset{a}{\tilde{e}}$ are dropped from the equations. Still, the resulting theory will be more complex than any muscle model developed so far: however, because all the possible effects of thermomechanical variables on the chemistry (and vice versa) are already considered by the conservation equations, it will be possible to treat more general cases.

---

[5] The list can be extended to include other components such as Ca++ if activation is to be modeled as part of the problem, for example.

4.5.1 Non-Equilibrium Thermodynamics.

More traditional thermodynamical theories of mixtures are often used in muscle mechanics. The so-called irreversible or non-equilibrium thermodynamics (Prigogine, 1967, Hill, 1989) is a less rigorous, although easier to apply approach. Those theories are based in what is known as Onsager relations and they assume that there is a linear relation between thermodynamical forces and fluxes. One of the fundamental problems is that there are no strict and general rules to determine which quantities are to be considered as forces and which are to be considered as fluxes. The relation between forces and fluxes is linear, and additionally, it is required that the coefficients of the matrix relating fluxes to forces be symmetric. The entropy, or dissipation is calculated using a quadratic form. Hill, 1989, described the application of this type of theories to a three states cross-bridge model of muscle.

4.5.2 Other Approaches Worth Exploring.

The standard chemical kinetics framework for enzymatic reactions assumes that the reactions occurs in homogeneous, dilute solutions. This assumption results in an expression for the rate at which the elemental process occurs that can be written as a

---

[6] In view of what was discussed in chapter III, a viscoelastic solid maybe is more appropriate.

constant, the rate constant, times a product of the concentration factors. The concentration in each factor is raised to a positive integer value called the kinetic order of the reaction with respect to the corresponding metabolite. These integers also represent the number of molecules of each type that enter the reaction. However it is clear from the experimental evidence that the elementary chemical kinetics is different from a conventional rate law when the reactions are limited by diffusion or dimensionally restricted. Under such conditions, the rate constants given by conventional rate laws change with time. For example, in a bimolecular reaction with two molecules of a single substrate reacting to form a product, the rate will be proportional to the concentration of the substrate to the second power, if the reaction occurs in a diluted, homogeneous, solution. If the reaction occurs under dimensionally restricted conditions, the constant rate will decrease with time. Savageau (1995) proposed that in such cases the rate law can be replaced by a power law with constant rate and increased kinetic order, not necessarily of integer value. The increased kinetic order results in a behaviour with increased cooperativity and a fractional order of the rate. The *in vitro* experiments used to determine the reaction rates between actin and myosin, are usually performed in perfect dilution conditions. In the muscle, this is not the case given the highly ordered structural arrangement of molecules. For reactions restricted to a one-dimensional channel, the power-law based kinetic order of a bimolecular reaction is 3, a 50% difference with respect to that predicted by mass-action law. In a similar direction, a totally different approach that has enormous potential is the one based on cellular automata. Zhou and Phillips, 1994, used cellular automata to address the problem of Ca++ binding to the actin filament taking into account the regulatory presence of tropomyosin and troponin. Cellular automata can be used to track the interaction between molecules in cases in which there are a finite number of them and they have a certain spatial distribution. One of the typical applications of cellular automata is the modelling of chemical reactions and diffusion, where it can be shown that

cellular automata converge to the differential equations[7] representing the phenomena. Cellular automata and related approaches, such as geometrical automata (Forcinito, 1993, Forcinito and Epstein, 1995), have also shown their potential to address complex kinematics problems such as the stability of sand piles or the dynamic segregation of granular materials. They should be considered as viable alternative tools to address problems related to cross-bridge or inter-sarcomere dynamics.

---

[7] A wealth of applications of cellular automata to similar problems can be found on Doolen, 1991.

V

Conclusions and Recommendations

The variety of subjects addressed in this dissertation may leave in the reader the impression of a lack of direction or focus in the study of the phenomena at hand. Instead it should be understood as reflecting the ample variety of mechanisms put to work with every muscle contraction. As the behaviour of muscle has many aspects, we decided to use the analytical tools most appropriate for each one of them. However, the principal objective, to understand muscle contraction and to model it with the greatest possible generality, was never left out of sight.

5.1 Conclusions.

- With a simple, discrete model of interaction between thick and thin filament it was shown that the stiffness of a sarcomere and the number of cross-links between filaments are not directly related when the filaments are compliant. This conclusion can have important implications in the design and interpretation of experiments, in particular, for those cases when very small preparations are used (e.g., a few sarcomeres long), or when there is a small overlap between filaments, or when the activation is submaximal. The model presented in chapter II retains the static characteristics of a sarcomere and, in the limit, the properties of a continuum model previously published (Ford et al. 1981). We also found a corrective factor that makes the continuum model match the results from the

discrete one for the case of a uniform distribution of links. It was also shown that the effects on the effective stiffness per cross-link of neighbouring filaments of a three-dimensional mesh of interdigitating filaments are small, if physiologically relevant parameters are used.

Although in the case of evenly distributed cross-links, the corrected continuum and the discrete approach will give practically the same results, only the discrete model can readily handle cases with an uneven distribution of cross-links or with filaments with variable stiffness along its length.

- Phenomena such as force depression after shortening or force enhancement after stretching can be modelled using the simple rheological model introduced in chapter III. The introduction of an elastic rack with an activation dependent switching mechanism and the reinterpretation of the contractile element, give to this model its ability to 'memorize' the length at which it was activated. Another particularity of the model is that the force-velocity characteristic of the model is a consequence of the interaction between the elements explicit in the model, and not an intrinsic property of the contractile element, as in the case of standard Hill type models.

- A series of exploratory experiments performed *in vivo*, suggest that the temporal order in which changes in length and changes in activation are imposed upon muscle is important and it must be considered in the modelling. A possible way to handle this non-commutativity between operations was suggested. Experimental results contradict some of the theoretical results, therefore alternative ways to handle non-commutative operations on muscle need to be developed.

- Continuum theories of chemically reacting mixtures can be used to advance the development of theoretical models of muscle. To do so will involve a lot of theoretical work as well as many new experiments aimed at determining the influence of thermomechanical parameters on chemical reactions.

5.2 Recommendations for Future Work

We said in the introduction that caution must be used when conclusions are to be extrapolated from the microscopic to the macroscopic realm and vice versa. The careful study of muscle models from the point of view of theoretical mechanics has an important role to play in the advancement of biomechanics and physiology. The complexity of the phenomena at hand are so formidable that even with sophisticated experimental techniques it is very difficult to obtain results whose interpretation is beyond debate. In our view it is very unlikely that a simple model will be found to describe all the variety of behaviours that muscle, and living tissue in general, exhibit. The probabilities of finding a universal, microscopic mechanism driving muscle contraction are more certain, although as in the case of plasticity in metals, even when the microscopic mechanism is conceptually known, it is very difficult to devise mathematical models of constitutive relations that can encompass all possible outcomes.

We have shown here that it is possible to answer some pressing questions, such as what is the influence of filament compliance, by using simple mechanical models. Also, that simple mechanical models can extend the range of application of phenomenological models to handle behaviours previously thought to correspond to some sort of memory function. But in spite of the relative success of this type of models, we advocate for a complete, rational model based on firmly established axioms of mechanics. In our view the two possible ways to achieve that global model are either to use some derivative of the continuum theory of chemically reacting substances or to use a totally discrete approach such as cellular automata. Some guidelines for the former were already discussed at the end of Chapter IV. The latter can be approached in two ways: 1) a lattice-gas automata representing the differential equations of a chemically reacting mixture developed by formulating the proper rules for the interaction of the particles, in a similar

way to that used by Firsch et al., 1986 for the Navier-Stokes equations, or 2) an *ad hoc* set of rules for the interaction of molecules (or ensembles of molecules) in a similar fashion as the one presented by Zhou and Phillips, 1995, for the Ca++ binding to the actin filaments, or the one presented by Forcinito, 1993, and Forcinito and Epstein, 1995, for studying the stability of piles of granular materials.

Bibliography

Abbott, BC, Aubert, XM, (1952) The force Exerted by Active Striated Muscle During and After Change of Length. *Journal of Physiology.* **117**, 77-86.

Allinger, TL, (1995) Stability and the Descending Limb of the Force-Length Relation in Mouse Skeletal Muscle - A Theoretical and Experimental Examination. PhD Dissertation, Dept. of Mechanical Engineering, The University of Calgary.

Bagni, ME, Cecchi, G, Schoenberg, M, (1988) A Model of Force Production that Explains the Lag Between Cross-Bridge Attachment and Force After Electrical Stimulation of Striated Muscle, *Biophys J.*, **54**, 1105-1114.

Bobet, J, Stein, RB, (1996) A Simple Model Reproduces Behaviour of Isometric Muscle, *Proceedings. IX Biennial Conference of the Canadian Society for Biomechanics,* Vancouver.

Bowen, RM, (1976) Theory of Mixtures, in *Continuum Physics. Vol. III*, Eringen, AC, Editor, Academic Press, New York.

Bowen, RM, (1979) A theory of Constrained Mixtures with Multiple Temperatures, *Archive for Rational Mechanics and Analysis*, **70**, 235-250.

Butkov, E, (1968), *Mathematical Physics*, Addison-Wesley Publishing Company, Reading, Massachusetts.

Cantino, M, Squire, J, (1986) Resting Myosin Cross-bridge Configuration in Frog Muscle Thick Filaments. *The Journal of Cell Biology* **102**, 610-618.

Cole, GK, van den Bogert, AJ, Herzog, W, Gerritsen, KGM, (1996) Modelling of Force Production in Skeletal Muscle Undergoing Stretch, *Journal of Biomechanics* **29**, 1091-1104.

Cooke, R, White, H, Pate, E, (1994) A Model of the Release of Myosin Heads from Actin in Rapidly Contracting Muscle Fibers *Biophysical Journal* **66**, 778-788

Doolen, GD, editor (1991), *Lattice Gas Methods for PDE's, Theory applications and Hardware*, Noth-Holland.

Edman, KAP (1979) The Velocity of Unloaded Shortening and Its Relation to Sarcomere Length and Isometric Force in Vertebrate Muscle Fibres, *Journal Physiology* **291**, 143-159.

Edman, KAP (1986) Double-Hyperbolic Nature of The Force-Velocity Relation in Frog Skeletal Muscle, *Molecular Mechanisms of Muscle Contraction (Sugi, Pollack, eds.)* **226**, 643-652.

Edman, KAP, Reggiani, (1983) Length-Tension-Velocity Relationships Studied in Short Consecutive Segments of Intact Muscle Fibres of the Frog, *Contractile Mechanism of Muscle. Mechanics, Energetics and Molecular Models (Pollack, Sugi. eds.) Plenum. New York* Vol. II 495-510.

Edman, KAP, Tsuchiya, T, (1996) Strain of Passive Elements During Force Enhancement by Stretch in Frog Muscle Fibres, *Journal of Physiology*, **490.1**, 191-205.

Epstein, M, (1994) *Brush Mechanics* (personal communication).

Epstein, M, (1996) *A vindication of the force-length relation* (personal communication).

Erickson, HP, (1997) Stretching Single Protein Molecules: Titin Is a Weird Spring, *Science*, **276**, 1090-1092.

Eringen, AC, (1980) *Mechanics of Continua (Second Edition)*, Robert E. Krieger Publishing Co., Huntington, New York.

Finer, JT, Simmons RM, Spudich JA (1994) Single Myosin Molecule Mechanics: Piconewton Forces and nanometre steps *Nature* **368**, 113-119.

Firsch, U, Hasslacher, B, Pomeau, Y, (1986) Lattice-Gas Automata for the Navier-Stokes Equation, *Physical Review Letters*, **56**,14 1505-1508

Forcinito, M, (1993), *Geometrical Approach to Problems on Granular Materials*, MSc thesis, Dept. of Mechanical Engineering, University of Calgary.

Forcinito, M, Herzog, W, (1994) A Model of the Mechanics and Energetics of Muscular Contractions: Considerations on a Half Sarcomere, *Proceedings of the VIII Biennial Conference and Symposium of the Canadian Society for Biomechanics, Calgary.*

Forcinito, M, Epstein, M, (1995) Granular Media Model with Internal Structure, *Physica D* **81** 305-313.

Forcinito, M, Epstein, M, Herzog, W, (1996) Mechanical Considerations on Sarcomere Stiffness, *Proceedings of the IX Biennial Conference and Symposium of the Canadian Society for Biomechanics, Vancouver.*

Forcinito, M, Epstein, M, Herzog, W, (1997a) Theoretical Considerations on Myofibril Stiffness, *Biophys J.*, **72**, 1278-1286.

Forcinito, M, Epstein, M, Herzog, W, (1997b) Discrete Correction to the Continuous Formula for the Stiffness of a Sarcomere, *Proceeding of the XVI Canadian Congress of Applied Mechanics*, Quebec.

Forcinito, M, Epstein, M, Herzog, W, (in press) A Numerical Study of the Stiffness of a Sarcomere, *J. of Electromyography and Kinesiology.*

Ford, LE, Huxley AF, Simmons RM, (1977) Tension Responses to Sudden Length Change in Stimulated Frog Muscle Fibres Near Slack Length *J. Physiol* **269**, 441-515.

Ford, LE, Huxley AF, Simmons, RM (1981) The Relation between Stiffness and Filament Overlap in stimulated Frog Muscle Fibres, *J. Physiol.* **311,** 219-249.

Fung, Y, (1993) *Biomechanics, Mechanical Properties of Living Tissue, 2nd Edition* Springer-Verlag, New York.

Gasser, HS, Hill, AV, (1924) The Dynamics of Muscular Contraction, *Proceedings of the Royal Society,* **B96**, 398-437.

Goldman, YE, Huxley, AF, (1994) Actin Compliance: Are You Pulling My Chain?, *Biophys. J.* **67,** 2131-2136.

Gordon, AM, Huxley, AF, Julian, FJ, (1966) The Variation in Isometric Tension with Sarcomere Length in Vertebrate Muscle Fibres, *Journal Physiology* **184**, 170-192.

Granzier, HLM, Pollack, GH, (1989) Effect of Active Pre-Shortening on Isometric and Isotonic Performance of Single Muscle Fibres. *Journal of Physiology.* **415**, 299-327.

Hardt (1978) Ph.D. Thesis, Massachusetts Institute of Technology.

Harrington, WF, (1979) On the origin of the contractile force in skeletal muscle. *Proceedings of the National Academy of Sciences USA* **76**, 5066-5070.

Herzog, W, Kamal, S, Clarke, HD, (1992) Myofilament Lengths of Cat Skeletal Muscle: Theoretical Considerations and Functional Implications, *Journal of Biomechanics* **25**, 945-948.

Herzog, W, Leonard, TR, (1997) Depression of Cat Soleus Forces Following Isokinetic Shortening, *Journal of Biomechanics* **30**, 865-872.

Herzog, W, Leonard, T, (1997b) *In vivo experiments on cat soleus muscle* (personal communication).

Higuchi, H, Yanagida T, Goldman, Y, (1995). Compliance of Thin Filament in Skinned Fibers of Rabbit Skeletal Muscle, *Biophys. J.* **69,** 1000-1010.

Hill, TL, (1989) *Free Energy Transduction and Biochemical Cycle Kinetics*, Springer-Verlag New York Inc.

Hill, AV, (1938) The Heat of Shortening and the Dynamic Constants of Muscle, *Proc Royal Society (London)* **126**, 136-195.

Huxley, AF, (1957) Muscle Structure and Theories of Contraction, *Progress in Biophysics. Chem.* 255-318.

Huxley, AF, Niedergerke, R., (1954) Structural Changes in Muscle During Contraction, *Nature*, **173**, 971-973

Huxley, AF, Simmons RM, (1971) Proposed Mechanism of Force Generation in Striated Muscle, *Nature, London* 233-533-538.

Huxley, AF, Simmons, RM, (1972) Mechanical Transients and the Origin of Muscular Force, Cold Spring Harbor Symposium on *Quant. Biol.* **37**, 669-680.

Huxley, HE, Hanson, J, (1954) Structural Changes in Muscle During Contraction, *Nature*, **173**, 973-976

Huxley, HE, Stewart, A, Sosa, H, Irving, T, (1994). X-ray Diffraction Measurements of Extensibility of Actin and Myosin Filaments in Contracting Muscle. *Byophys. J.* **67**, 2411-2421.

Julian, FJ, Sollins, KR, Sollins, MR, (1974) A Model for the Transient and Steady-State Mechanical Behavior of Contracting Muscle, *Biophysical Journal*, **14**, 547-562.

Kargacin, GJ, (1994) Calcium Signaling in restricted Diffusion Spaces, *Biophysical Journal* **67**, 262-272

Kawai, M, Wray, JS, Zhao, Y, (1993) The Effect of Lattice Spacing change on Cross-bridge Kinetics in Chemically Skinned Rabbit Psoas Muscle Fibers, *Biophys. J.* **64**, 187-196

Kellermayer, MSZ, Smith, SB, Granzier, HL, Bustamante, C, (1997) Foldin-Unfolding Transitions in Single Titin Molecules Characterized with Laser Tweezers, *Science*, **276**, 1112-1116

Kojima, H, Ishijima, A, Yanagida, T, (1994) Direct measurement of stiffness of single actin filaments with and without tropomyosin by *in vitro* nanomanipulation, *Proc. Natl. Acad. Sci. USA*, **91**, 12962-12966.

Lombardi, V, Piazzesi, G, (1990) Contractile Response During Steady Lengthening of Stimulated Frog Muscle Fibers, *J. Physiol* **37**, 669-680.

Maréchal, G, Plaghki, L, (1979) The Deficit of the Isometric Tetanic Tension Redeveloped after a Release of Frog Muscle at a Constant Velocity. *Journal of General Physiology*. **73**, 453-467.

Mijailovich S, Fredberg J, Butler J, (1996) On the Theory of Muscle Contraction: Filament Extensibility and the Development of Isometric Force and Stiffness. *Biophysical Journal* **71**, 1475-1484.

Müller, I, Villagio, P, (1977) A Model for an Elasto-Plastic Body, *Arch. Rat Mech. Anal.*, **65**, 25-46.

Nishizaka, T, Miyata, H, Yoshikawa, H, Ishiwata S, Kinosita, K, (1995) Unbinding of a single motor molecule of muscle measured using optical tweezers, *Nature* **377**,251-254.

Podolsky, RJ, (1960) Kinetics of Muscular Contraction: the Approach to the Steady State, *Nature* **188**, 666-668.

Pollack, GH, (1990) *Muscles & Molecules, Uncovering the Principles of Biological Motion*, Ebner & Sons Publishers, Seattle.

Pollack, GH, (1995) Muscle Contraction Mechanism: are Alternative Engines Gathering Steam?, *Cardiovascular Research* **29**, 737-746.

Prigogine, I, (1967) *Introduction to Thermodynamics of Irreversible Process (Third Edition)*, Interscience Publishers, New York.

Rayment, I, Rypniewski, WR, Schmidt-Bäse, K, Smith, R, Tomchick, DR, Benning, D, Winkelmann, DA, Wesenberg, G, Holden, HM, (1993) Three Dimensional Structure of Myosin Subfragment-1: A Molecular Motor, *Science* **261,** 50-58

Rayment, I, Holden, HM, Whittaker, M, Yohn, CB, Lorenz, M, Holmes, KC, Milligan, RA, (1993b) Structure of the Actin-Myosin Complex and its Implications for Muscle Contraction, *Science* **261,** 58-65.

Rief, M, Gautel, M, Oesterhelt, F, Fernandez, JM, Gaub, HE, (1997) Reversible Unfolding of Individual Titin Immunoglobulin Domains by AFM, *Science*, **276,** 1109-1112.

Roszek, B, Baan, GC, Huijing, PA, (1994) Decreasing stimulation frequency-dependent length-force characteristics of rat muscle. *Journal of Applied Physiology*, **77,** 2115-2124.

Roszek, B, (1996) Effects of submaximal activation on skeletal muscle properties: Length-force characteristics of fully recruited rat muscle, Ph.D. Thesis, Vrije Universiteit Amsterdam.

Savageau, MA, (1995) Michaelis-Menten Mechanism Reconsidered: Implication of Fractal Kinetics, *Journal of Theoretical Biology*, **176,** 115-124.

Squire, J, (1981) *The Structural Basis of Muscular Contraction*, Plenum Press, New York.

Squire, JM, editor (1990) *Molecular Mechanisms in Muscular Contraction*, CRC Press, Inc., Boca Raton.

Sugi, H, Tsuchiya, T, (1988) Stiffness Changes During Enhancement and Deficit of Isometric Force by Slow Length Changes in Frog Skeletal Muscle Fibres. *Journal of Physiology* **407** 215-229.

Truesdell, C, (1969) *Rational Thermodynamics*, Mc Graw-Hill, New York.

Truskinovksy, L, Zanzotto, G, (1996) Ericksen's Bar Revisited: Energy Wiggles, *J. Mech. Phys. Solids,* **44**,1371-1408.

Wakabayashi, K, Sugimoto, Y, Tanaka, H, Ueno, Y, Takezawa, Y, Amemiya, Y, (1994) X-ray Diffraction Evidence for the Extensibility of Actin and Myosin Filaments During Muscle Contraction. *Biophys. J.* **67**, 2422-2435.

Wang, CC, Truesdell, C, (1973) *Introduction to Rational Elasticity*, Noordhoff International Publishing, Leyden.

Woledge, RC, Curtin, NA, Homsher, E, (1985) *Energetic Aspects of Muscle Contraction*, Academic Press, London.

Xu, S, Brenner, B, Yu, LC, (1993) State-dependent Radial Elasticity of attached Cross-bridges in Single Skinned Fibres of Rabbit Psoas Muscle, *Journal of Physiology.* **465**, 749-765.

Zahalak, GI, (1990) Modeling Muscle Mechanics (and Energetics), *Multiple Muscle Systems: Biomechanics and Movement Organization. (.M. Winters & Yoo eds.)* Springer-Verlag NY.

Zahalak, GI, Ma, SP, (1990) Muscle Activation and Contraction: Constitutive Relations Based Directly on Cross-Bridge Kinetics, *J. of Biomechanical Engineering ASME Trans.* **112,** 52-62.

Zahalak, GI, Motabarzadeh, I, (1997) A Re-examination of Calcium Activation in the Huxley Cross-Bridge Model, *J. of Biomechanical Engineering ASME Trans.* **119,** 20-29.

Zhou, G, Phillips, GN, (1994) A Cellular Automaton Model for the Regulatory Behavior of Muscle Thin Filaments, *Biophysical Journal* **67**, 11-28

Appendix A

The equation of Ford et al. (1981) revisited

Our departure point is the generic panel of the ladder structure which we now recast following the notation shown in Fig A.1, where a and b are the stiffness of the filaments and cross-bridges respectively, h is the panel width, $u(x)$ and $v(x)$ are the displacements of the points corresponding to the lower filament and upper filament respectively. For simplicity, we consider the case in which both filaments have the same properties.

We intend to pass to the limit as the panel width goes to zero while keeping the stiffness properties unaltered. It is clear that the stiffness of the filaments is inversely proportional to the panel width, that is $a = \sigma / h$ where σ is the characteristic stiffness per unit length. The generic equilibrium equations for the upper and lower nodes are respectively

$$a(u_i - u_{i+1}) + a(u_i - u_{i-1}) + b(u_i - v_i) = 0 \tag{A.1}$$

$$a(v_i - v_{i+1}) + a(v_i - v_{i-1}) + b(v_i - u_i) = 0 \tag{A.2}$$

which can be recast as

$$-\frac{\sigma}{h^2}(u_{i-1} - 2u_i + u_{i-1}) + \frac{b}{h}(u_i - v_i) = 0 \tag{A.3}$$

$$-\frac{\sigma}{h^2}(v_{i-1} - 2v_i + v_{i-1}) + \frac{b}{h}(v_i - u_i) = 0. \tag{A.4}$$

Denoting $\eta = b/h$, the cross-bridge stiffness per unit length, and passing to the limit as $h \to 0$ while keeping σ and η constant, we obtain the ordinary differential equations:

$$-\sigma u'' + \eta(u - v) = 0 \tag{A.5}$$

$$-\sigma v'' + \eta(v - u) = 0 \tag{A.6}$$

The boundary conditions are (with the notation on Fig B2):

$$x = 0 \rightarrow u' = 0; \quad v = 0 \tag{A.7}$$

$$x = L \rightarrow u' = 0; \quad v' = F/\sigma \tag{A.8}$$

The boundary conditions of force was obtained from a passage to the limit at the last panel.

Subtracting equations (B3a) from (B3b) we obtain: $\sigma \vartheta'' = 2\eta\vartheta$ for the distortion field $\vartheta = u - v$ which is equivalent to equation [A.3] in the paper by Ford et al. (1981).

The complete solution of the system, with due account of the boundary conditions, can be expressed as:

$$u(x) = \frac{F\left[\left(1+e^{-\gamma L}\right)e^{\gamma x} + \left(1+e^{\gamma L}\right)e^{-\gamma x}\right]}{2\gamma\sigma\left(e^{\gamma L} - e^{-\gamma L}\right)} + \frac{Fx}{2\sigma} + \frac{F\left(2+e^{\gamma L}+e^{-\gamma L}\right)}{2\gamma\sigma\left(e^{\gamma L} - e^{-\gamma L}\right)} \tag{A.9}$$

$$v(x) = -\frac{F\left[\left(1+e^{-\gamma L}\right)e^{\gamma x} + \left(1+e^{\gamma L}\right)e^{-\gamma x}\right]}{2\gamma\sigma\left(e^{\gamma L} - e^{-\gamma L}\right)} + \frac{Fx}{2\sigma} + \frac{F\left(2+e^{\gamma L}+e^{-\gamma L}\right)}{2\gamma\sigma\left(e^{\gamma L} - e^{-\gamma L}\right)} \tag{A.10}$$

where $\gamma = (2\eta/\sigma)^{1/2}$, is identical to the quantity μ defined by Ford et al.

The stiffness of the structure can be calculated as the ratio between the force applied to the free end and the displacement of that node. Replacing x with L in the above expressions, the total stiffness can be expressed as:

$$k_{cl} = \frac{F}{u(L)} = \frac{\sigma}{\frac{L}{2} + \frac{2 + e^{\gamma L} + e^{-\gamma L}}{\gamma\left(e^{\gamma L} - e^{-\gamma L}\right)}} = \frac{\sigma}{\frac{L}{2} + \frac{\coth(\gamma L/2)}{\gamma}} \qquad \text{(A.11)}$$

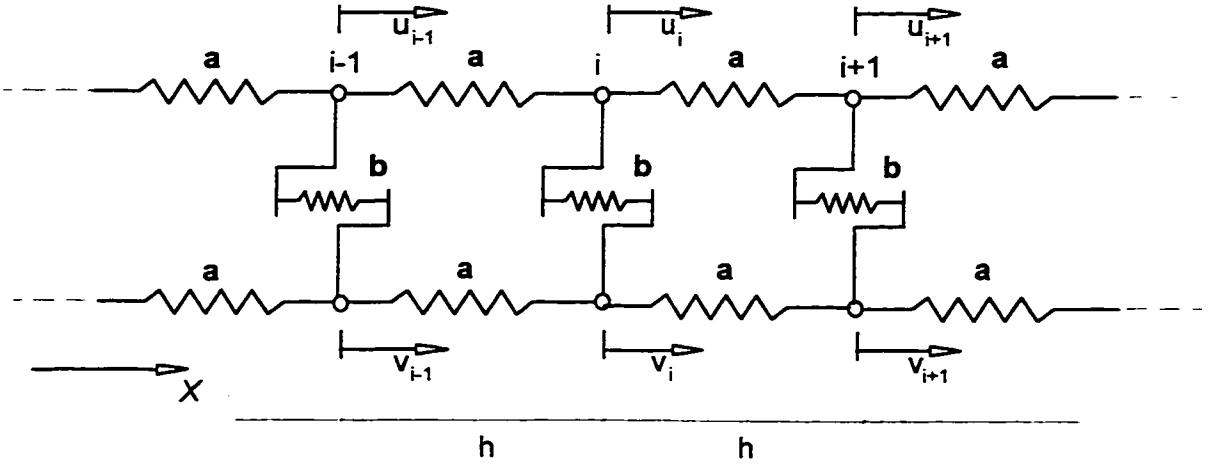

Figure A.1: Ladder structure with infinite panels.

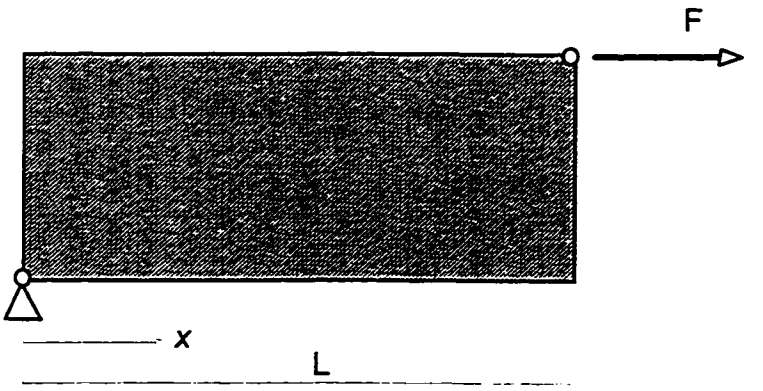

Figure A.2: Coordinate system definition for boundary conditions.

INDEX

A

acceleration, 99

actin, 5, 17

activation, 8

ADP, 18

angle of pinnation, 88

ATP, 5, 18, 21, 61

  hydrolysis, 22

B

balance of energy, 102

C

calcium pump, 18, 89

calordynamic process, 114

Cauchy, 101

  first law of motion, 102

  second law of motion, 102

cellular automata, 5, 119

Claussius-Duhem inequality, 104

concentration, 108

configuration, 99

Constitutive Equations, 105

Continuum Mechanics

  generalities, 99

contractile element, 64, 68

cooperativity, 4

Cross Bridge, Theory, 19

cross-bridge, 20

cross-bridge theory, 19

D

deformation, 100

deformation gradient, 100

diffusion velocity, 109

E

elastic rack, 68, 81

Euler's laws, 101

extent of reaction, 114

F

F-actin, 18

first law of thermodynamics, 102

force depression, 65, 74, 76

force enhancement, 65, 74, 76

force stroke, 4

force-length

  negative slope, 82

force-length relation, 67

force-velocity, 62, 75

G

G-actin, 18

H

helix-coil transition, 20

Hill type models, 60
Hill's muscle model, 3
Hill-type model, 72
Huxley's Cross-bridge theory, 3
Huxley's cross-bridge theory, 4
I
independent force generators, 20
K
kinetic order, 119
kinetic order of reactions, 6
M
M-band, 16
metabolic energy, 8
Mixture of Chemically Reacting Bodies, 111
Mixture Theory, 106
Application to Muscle., 116
molecular weight, 111
motion, 99
Myofibrils, 13
myofibrils, 7
myofilaments, 2
myosin
head, 3
myosin filaments, 17
N
non-equilibrium thermodynamics, 118
Non-Equilibrium Thermodynamics., 118
O
Onsager relations, 118
optical tweezers, 4
P
phenomenological model of muscle, 67
power law, 119
Principle of Conservation of Mass, 100
Pseudo Rheological Muscle Models, 61
R
rack element, 70
rate law, 119
reaction rate, 114
reference configuration, 99
S
sarcolemma, 13, 88
Sarcomere
structure, 15
sarcomere, 15
stiffness, 7

sarcoplasmic reticulum, 14, 18, 89
second law of thermodynamics, 104
series elastic element, 64
sliding filament
  model, 16
speed of contraction, 76
stereospecific
  attachement, 22
stoichiometric matrix, 113
T
T-tubules, 15
thermokinetic process, 114
Thick filament, 17
Thin filament, 17
thin filament, 17
tilting head, 19
titin, 15
titin filaments, 7
tropomyosin, 17
troponin, 5, 17
twitch, 81
V
velocity, 99
W
weakly coupled models, 6
Z
Z-discs, 7, 14

IMAGE EVALUATION
TEST TARGET (QA-3)

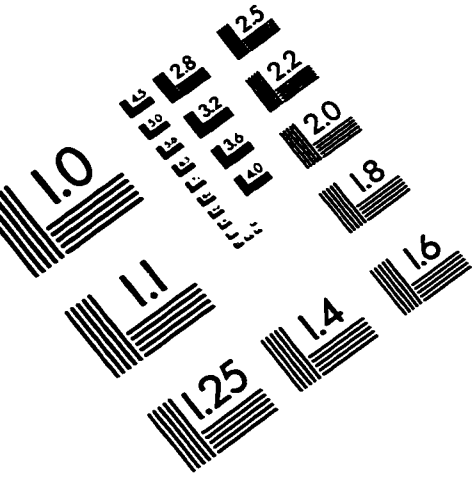

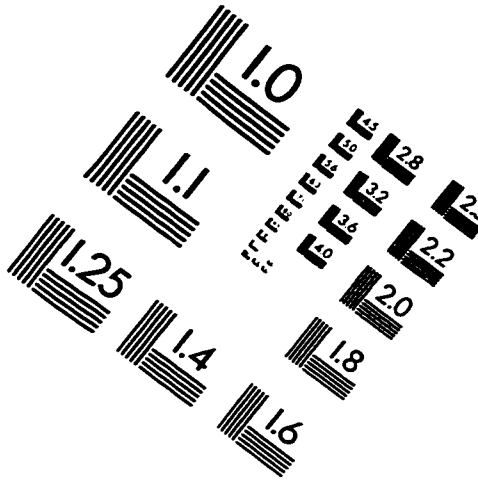

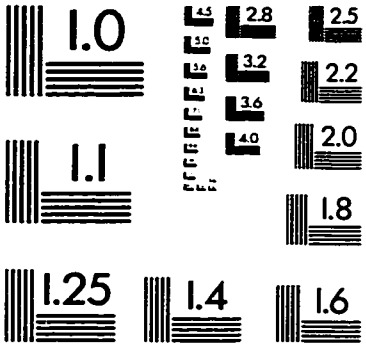

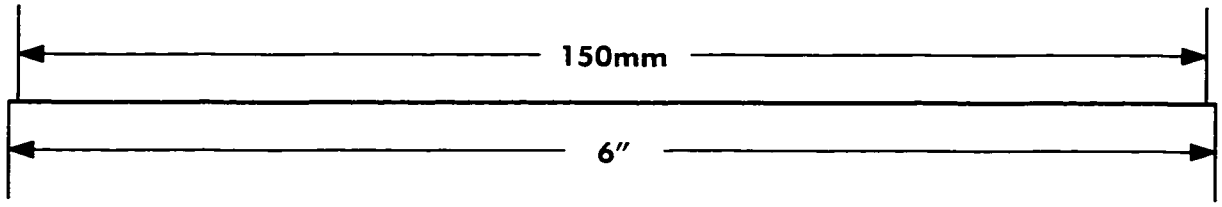

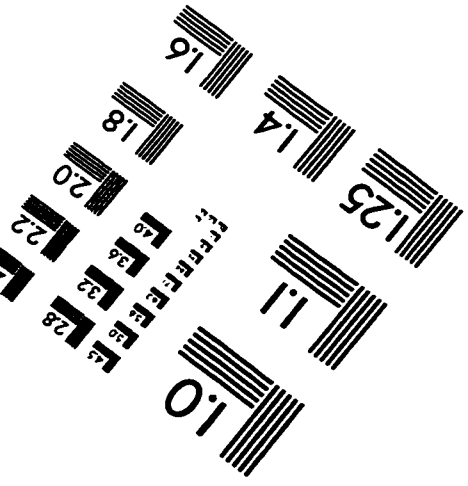

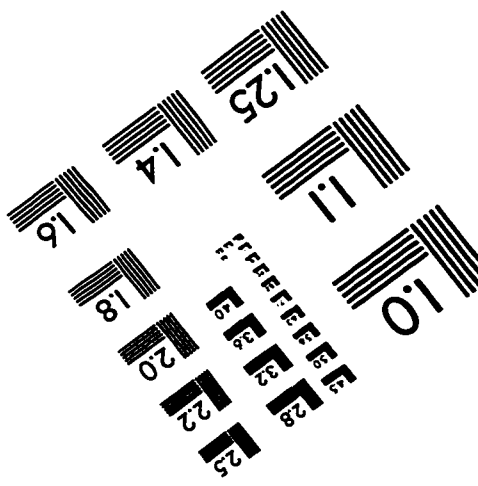

APPLIED IMAGE, Inc
1653 East Main Street
Rochester, NY 14609 USA
Phone: 716/482-0300
Fax: 716/288-5989